Energy, Mines and Resources Canada

Énergie, Mines et Ressources Canada

CANMET

Canada Centre for Mineral and Energy Technology

Centre canadien de la technologie des minéraux et de l'énergie

Mining Research Laboratories

Laboratoires de recherche minière

Canada

STRENGTH DETERMINATIONS OF LUCIEN C. BÉLIVEAU MINE ROCKS

B. Gorski

MRL 90-113(TR)

DATE: Oct. 1990

CLIENT: Cambior Inc.

This document is the property of the Canada Centre for Mineral and Energy Technology (CANMET)

Ce document est la propriété du Centre canadien de la technologie des minéraux et de l'énergie (CANMET)

MICROMEDIA

115pp

91-01035/

STRENGTH DETERMINATIONS OF LUCIEN C. BÉLIVEAU MINE ROCKS

by

B. Gorski*

ABSTRACT

Laboratory tests were conducted on drill cores originating from diamond drilling activity at Lucien C. Béliveau Mine, located in Val d'Or, Quebec. The results of strength and deformation properties of 46 test specimens are presented in this report.

---

*Rock Mechanics & Development Technologist, Canadian Mine Technology Laboratory
Mining Research Laboratories, CANMET, Energy, Mines and Resources Canada, Ottawa, Canada

Keywords:

Brazilian tensile strength, multi-stage triaxial test, uniaxial compressive strength, axial displacement control, post-failure, residual strength, confinement pressure, peak strain, modulus of elasticity, Poisson's ratio, Hoek and Brown failure criteria

DÉTERMINATION DE LA RÉSISTANCE DES ROCHES PROVENANT DE LA MINE LUCIEN C. BÉLIVEAU

par

B. Gorski*

RÉSUMÉ

Des essais sur des échantillons de sondage provenant des activités de carottage au diamant à la mine Lucien C. Béliveau, située à Val d'Or (Québec), ont été menés en laboratoire. Les résultats relatifs aux propriétés de résistance et de déformation de 46 échantillons sont présentés dans ce rapport.

---

*Technicien de la mécanique des roches et du développement, Laboratoire canadien de technologie minière, Laboratoires de recherche minière, CANMET, Énergie, Mines et Ressources Canada, Ottawa, Canada

Mots clés :

essai de traction brézilien; essai triaxial multi-étagé; résistance uniaxiale à la compression; contrôle du déplacement axial; post-rupture; résistance résiduelle, pression de confinement; déformation maximale; module d'élasticité, rapport de Poisson; critères de rupture de Hock et Brown.

TABLE OF CONTENTS

		Page
	ABSTRACT	i
	RÈSUMÈ	ii
1.0	INTRODUCTION	1
2.0	TEST PROCEDURE	1
	SPECIMEN SELECTION	1
	SPECIMEN PREPARATION	1
	BRAZILIAN TEST	2
	CONVENTIONAL UNIAXIAL TEST	2
	MULTI-STAGE TRIAXIAL TEST	2
	DATA ACQUISITION/REDUCTION	2
3.0	TEST RESULTS	3
	TENSILE STRENGTH	3
	UNIAXIAL COMPRESSIVE STRENGTH	3
	ELASTIC CONSTANTS	3
	TRIAXIAL COMPRESSIVE STRENGTH	3
	HOEK AND BROWN M AND S MATERIAL CONSTANTS	4
4.0	OBSERVATIONS	4
5.0	REFERENCES	5

TABLES

No.		
1.	Specimen selection data	6
2.	Brazilian tensile strength	7
3.	Uniaxial compressive test results	8
4.	Multi-stage triaxial test results	9
5.	Geological Classification	10
6.	Hoek and Brown m and s material constants	11

FIGURES

No.

Fig. 1 Tuff specimens 12
Fig. 2 Diorite specimens 13
Fig. 3 Basalt specimens 14

APPENDICES

A Axial stress-strain curves of uniaxial tests 15
B Circumferential stress-strain curves of uniaxial tests 39
C Axial stress-strain curves of multi-stage tests 63
D Circumferential stress-strain curves of multi-stage tests 87

1. INTRODUCTION

MRL received from Cambior Incorporated, drill core samples originating from Lucien C. Béliveau Mine located in Val d'Or, Quebec. An MTS 815 Rock Mechanics Test System was used to conduct Brazilian, uniaxial and multi-stage triaxial tests. All tests were conducted using computer control on the MTS servo-hydraulic test system. The results of strength and deformation property tests are presented in this report.

2. TEST PROCEDURE

SPECIMEN SELECTION

Triaxial, uniaxial and Brazilian tests were conducted on rock specimens cut from each received core. Specimens have been identified according to the rock type received from the mine site, for example;

Example 90-1-3

90 - site location

1 - borehole number

3 - test number

The specimen location, test type, dimensions and density, δ, of each tested specimen, are listed in Table 1.

SPECIMEN PREPARATION

Rock core sample specimens selected for uniaxial and triaxial tests were prepared with length to diameter ratios of 2:1 to 2.5:1. Brazilian tensile strength specimens were prepared with length to diameter ratios of 1:2. All specimens were lapped to within specified MRL tolerances, oven dried, weighed and dimensioned. Prior to testing, planes of discontinuity, if any, or potential weaknesses were highlighted with ink. Specimen preparation was performed according to the procedures used at MRL [1,2].

BRAZILIAN TEST

Test specimens were loaded to failure using an MTS compression press. The test procedure conformed to ISRM suggested methods [4].

CONVENTIONAL UNIAXIAL TEST

Test specimens were loaded to failure uniaxially at a rate of 0.75 MPa/s.

MULTI - STAGE TRIAXIAL TEST

The specimen was brought to equilibrium, under load control mode, by the simultaneous application of axial load and confining pressure, at the rate of 0.75 MPa/s. After the desired confining pressure of the first stage was reached, the axial loading continued, at the rate of 0.75 MPa/s while the confining pressure was kept constant. When the specimen axial load was 60 kN greater than the equilibrium load, the axial load was then reduced by 20%. The control mode was then switched over to axial displacement control. The test was continued, at an axial displacement rate corresponding to an axial stress rate of 0.75 MPa/s until initial failure occurred, as detected by an axial load drop. The axial displacement rate was then stopped and then reduced by 33% of total axial displacement.

The desired confining pressure of the second stage was then applied and loading continued according to the same method just outlined for the first stage. The procedure was subsequently repeated for each predetermined increment of confining pressure. Confining pressures of 5, 10, 15 and 20 MPa were used.

The confining pressure of the last stage was held through the peak strength until the residual strength was visually established, as indicated by a plateau in the stess/strain curve recorded by the X-Y recorder. The specimen was then further axially displaced an additional 0.5 mm, while the confining pressure was linearly reduced to zero within a time period of 60 seconds. This last phase of the test was required for residual strength data.

DATA ACQUISITION/REDUCTION

Uniaxial and triaxial data were scanned and stored digitally on hard disk using a PDP 11/73 computer every 3 seconds. Analog signals from the load cell, circumferential extensometer, axial LVDTs, and confinement pressure were scanned. Real time plots of load versus axial displacement were obtained using a Kipp & Zonen X Y1 Y2 pen recorder wired to a MTS 448.85 controller.

The raw signals were reduced to engineering units and stored on hard disk for later recall. Measurements from axial LVDTs were corrected for end platen compression in the sensing gauge length. Reduced data were transferred to a VAX 750 computer for specimen material constant determinations. Hard copy plots of triaxial test results for report purposes were obtained using the DEC LVP16 pen plotter. A laser printer was used to provide hard copy plots of Mohr circle test results. The DEC LA50 printer was used to provide hard copies of reduced triaxial data for analyses.

3. TEST RESULTS

TENSILE STRENGTH

The tensile strength results, σ_t, obtained by Brazilian test, are listed in Table 2.

UNIAXIAL COMPRESSIVE STRENGTH

The peak strain values, ϵ_{peak}, listed in Table 3, were determined by readings from the axial strain gauges. The uniaxial compressive strength results, Q_u, are also listed in Table 3.

Appendices A and B provides stress-strain plots using signals from axial strain gauges and circumferential strain gauges mounted on specimen surfaces.

ELASTIC CONSTANTS

The modulus of elasticity (calculated at 0.5 Q_u), E, and the Poisson's ratio, ν, were established in each uniaxial compressive test case using load cell, and strain gauge data. The obtained results are listed in Table 3.

TRIAXIAL COMPRESSIVE STRENGTH

The triaxial compressive strengths of the selected specimens were determined at successive confining stages of: 5, 10, 15 and 20 MPa.

The stress-strain curve plots of the multi-stage triaxial tests are found in Appendices C and D. Axial strain measurements were made using LVDT units.

The results of the multi-stage tests are tabulated in Table 4.

HOEK AND BROWN M AND S MATERIAL CONSTANTS

Triaxial, uniaxial and Brazilian test results were used in the Hoek and Brown failure criteria to determine the failure envelope for each rock type. Table 6 contains the derived material constants, m and s. Figures 1 to 3 depict the Mohr circle plots for each of the rock types. The method of analyses is limited to triaxial strengths that exceed $3.4\sigma_3$.

4. OBSERVATIONS

The geological classification of different rock core units are listed in Table 5. For each rock type tested, triaxial strengths increased with increasing specimen density and decreased with the presence of existing planes of weakness. Specimens increased in triaxial strength with increasing confining pressure. The specimens behaved elastically prior to peak strength.

5. REFERENCES

1. Gorski, B. "The design and operation of a stiff triaxial assembly for post-failure rock property testing"; *Division Report MRP/MRL* 82-81(*TR*); CANMET, Energy, Mines and Resources Canada; 1982.

2. Gyenge, M. and Herget, G. "Pit slope Manual 3-2; Laboratory tests for design parameters"; *CANMET Report* 77-26; CANMET, Energy, Mines and Resources Canada; 1977.

3. Gorski, B. "A multi-use load system for rock testing";*Division Report M&ET/MRL* 86-25(*TR*); CANMET, Energy, Mines and Resources Canada; 1986.

4. Brown, E.T. "Rock characterization testing and monitoring"; *ISRM*; *Pergamon Press, London, England*; 211p; 1981.

Table 1 Specimen Selection Data

Sample Code	Depth (m)	Test Type	Length (cm)	Diameter (cm)	Density (Mg/m^3)
90-1-1	2.50	Uniaxial	11.23	5.56	2.57
90-1-2	2.63	Multi-stage	12.05	5.40	2.69
90-1-3	6.27	Uniaxial	9.67	4.74	2.76
90-1-4	6.38	Multi-stage	10.33	4.74	2.76
90-1-5	8.54	Uniaxial	10.22	4.74	2.80
90-1-6	8.68	Multi-stage	10.27	4.74	2.80
90-2-1	1.09	Uniaxial	9.99	4.74	2.75
90-2-2	1.20	Multi-stage	10.27	4.74	2.75
90-2-3	6.77	Uniaxial	10.36	4.74	2.77
90-2-4	6.95	Multi-stage	9.91	4.75	2.76
90-3-1	6.28	Uniaxial	9.88	4.75	2.81
90-3-2	6.39	Multi-stage	10.45	4.75	2.81
90-3-3	7.48	Uniaxial	10.50	4.75	2.93
90-3-4	7.59	Multi-stage	10.58	4.76	2.94
90-3-5	11.38	Uniaxial	10.49	4.75	2.77
90-3-6	11.48	Multi-stage	10.09	4.75	2.79
95-1-1	2.18	Uniaxial	10.42	4.74	2.79
95-1-2	2.67	Multi-stage	10.66	4.72	2.76
95-1-3	5.40	Uniaxial	10.57	4.73	2.84
95-1-4	5.53	Multi-stage	10.67	4.74	2.84
95-2-1	2.56	Uniaxial	10.66	4.70	2.83
95-2-2	2.98	Multi-stage	10.76	4.73	2.84
95-2-3	7.98	Uniaxial	10.95	4.75	2.89
95-2-4	8.13	Multi-stage	10.66	4.75	2.84
95-3-1	4.01	Uniaxial	10.28	4.74	2.77
95-3-2	4.12	Multi-stage	10.65	4.75	2.76
95-3-3	7.84	Uniaxial	10.46	4.74	2.76
95-3-4	7.95	Multi-stage	10.55	4.74	2.76
95-3-5	13.59	Uniaxial	10.52	4.75	2.89
95-3-6	13.70	Multi-stage	10.32	4.75	2.82
40-1-1	1.65	Uniaxial	11.29	4.71	2.75
40-1-2	1.88	Multi-stage	10.93	4.71	2.77
40-1-3	7.94	Uniaxial	11.43	4.75	2.86
40-1-4	8.06	Multi-stage	10.32	4.75	2.84
40-1-5	10.62	Uniaxial	10.58	4.75	2.78
40-1-6	10.72	Multi-stage	10.63	4.75	2.77
40-1-7	15.53	Uniaxial	11.22	4.75	2.79
40-1-8	15.64	Multi-stage	10.92	4.74	2.79
40-2-1	3.41	Uniaxial	10.87	4.75	2.72
40-2-2	3.52	Multi-stage	10.63	4.75	2.72
40-2-3	7.06	Uniaxial	10.65	4.75	2.82
40-2-4	7.17	Multi-stage	10.77	4.75	2.81
40-3-1	3.46	Uniaxial	10.78	4.75	2.79
40-3-2	3.57	Multi-stage	10.51	4.75	2.77
40-3-3	8.91	Uniaxial	10.93	4.75	2.80
40-3-4	9.02	Multi-stage	10.65	4.75	2.78

Table 2 Brazilian Tensile Strength

Sample Code	Depth (m)	Failure Load (kN)	σ_t (MPa)
90-1-2A	2.65	30.04	-11.71
90-1-2B	2.67	30.81	-12.92
90-1-4A	8.12	28.18	-17.61
90-1-4B	8.13	28.82	-16.13
95-2-1A	2.58	21.10	-11.88
95-2-1B	2.60	20.95	-11.77

Table 3 Uniaxial Compressive Test Results

Sample Code	Depth (m)	Q_u (MPa)	ε_{peak} (%)	E (GPa)	ν
90-1-1	2.50	85.78	0.14	68.28	0.35
90-1-3	6.27	104.51	0.16	67.97	0.43
90-1-5	8.54	158.54	0.32	61.93	0.32
90-2-1	1.09	109.85	0.17	67.70	0.41
90-2-3	6.77	130.64	0.24	65.40	0.35
90-3-1	6.28	143.01	0.22	68.96	0.42
90-3-3	7.48	287.61	0.42	85.62	0.37
90-3-5	11.38	149.73	0.24	67.67	0.34
95-1-1	2.18	136.75	0.24	62.77	0.34
95-1-3	5.40	140.43	0.23	69.37	0.42
95-2-1	2.56	104.71	0.18	63.04	0.32
95-2-3	7.98	93.03	0.14	62.81	0.44
95-3-1	4.01	148.43	0.20	76.75	0.32
95-3-3	7.84	137.89	0.20	71.60	0.33
95-3-5	13.59	192.47	0.32	77.46	0.34
40-1-1	1.65	148.80	0.25	68.46	0.33
40-1-3	7.94	104.77	0.18	66.80	0.25
40-1-5	10.62	115.75	0.19	72.04	0.30
40-1-7	15.53	148.45	0.30	69.65	0.24
40-2-1	3.41	165.68	0.28	72.50	0.27
40-2-3	7.06	172.92	0.32	70.58	0.41
40-3-1	3.46	162.39	0.24	74.37	0.32
40-3-3	8.91	216.88	0.34	76.06	0.34

Table 4 Multi-stage Triaxial Test Results

Sample Identification		σ_3=5.0 MPa		σ_3=10.0 MPa		σ_3=15.0 MPa		σ_3=20.0 MPa	
Sample Code	Depth (m)	σ_1 (MPa)	ε_{peak} (%)	σ_1 (MPa)	ε_{peak} (%)	σ_1 (MPa)	ε_{peak} (%)	σ_1 (MPa)	ε_{peak} (%)
90-1-2	2.63	118.31	0.19	136.13	0.22	146.05	0.24	163.88	0.31
90-1-4	6.38	130.87	0.25	137.87	0.27	155.69	0.32	176.45	0.41
90-1-6	8.68	153.44	0.28	160.38	0.30	169.22	0.33	178.93	0.37
90-2-2	1.20	111.23	0.22	(97.57)	(0.24)	(107.77)	(0.26)	(131.30)	(0.39)
90-2-4	6.95	161.37	0.32	(152.06)	(0.31)	190.51	0.39	195.85	0.46
90-3-2	6.39	160.07	0.48	—	—	—	—	—	—
90-3-4	7.59	285.22	0.45	337.28	0.54	381.79	0.63	424.05	0.80
90-3-6	11.48	—	—	156.20	0.26	161.20	0.28	175.16	0.34
95-1-2	2.67	146.74	0.26	168.00	0.31	184.38	0.35	(172.36)	(0.36)
95-1-4	5.53	127.71	0.22	156.13	0.27	175.71	0.31	206.38	0.44
95-2-2	2.98	(64.53)	(0.11)	120.92	0.21	127.51	0.23	136.18	0.27
95-2-4	8.14	96.03	0.18	103.61	0.20	110.17	0.22	121.20	0.26
95-3-2	4.12	148.87	0.22	166.45	0.26	179.03	0.28	191.78	0.34
95-3-4	7.95	135.12	0.20	176.25	0.21	(174.87)	(0.28)	194.05	0.46
95-3-6	13.70	169.22	0.27	200.27	0.33	219.25	0.37	245.81	0.51
40-1-2	1.88	128.05	0.22	(123.85)	(0.23)	(127.70)	(0.25)	(141.54)	(0.38)
40-1-4	8.06	127.82	0.25	130.76	0.27	142.31	0.32	(130.76)	(0.33)
40-1-6	10.72	123.92	0.21	138.89	0.24	159.72	0.29	169.53	0.34
40-1-8	15.64	156.21	0.29	168.82	0.32	178.50	0.35	(173.31)	(0.37)
40-2-2	3.52	162.58	0.27	178.95	0.33	180.85	0.35	(178.26)	(0.54)
40-2-4	7.17	193.89	0.35	212.52	0.40	223.73	0.44	(215.97)	(0.47)
40-3-2	3.57	178.14	0.29	190.53	0.31	250.25	0.45	266.08	0.53
40-3-4	9.02	200.16	0.28	(177.06)	(0.26)	(129.82)	(0.22)	(168.09)	(0.31)

Table 5 Geological Classification

Site Location	Borehole Number	Rock Type	Depth Interval (m)
90	1	Tuff	2.50-6.38
90	1	Diorite	8.54-8.68
90	2	Tuff	1.09-1.20
90	2	Diorite	6.77-6.95
90	3	Diorite	6.28-11.48
95	1	Diorite	2.18-2.67
95	1	Lamprophyre dyke	5.40-5.53
95	2	Basalt	2.56-8.13
95	3	Diorite	4.01-13.70
40	1	Diorite	1.65-1.88
40	1	Tuff	7.94-8.06
40	1	Diorite	10.62-15.64
40	2	Tuff	3.41-3.52
40	2	Diorite	7.06-7.17
40	3	Diorite	3.46-9.02

Table 6 Hoek and Brown m and s material constants

Rock Type	σ_t (MPa)	Q_u (MPa)	Q_c (MPa)	m	m_r	s	s_r	r^2	r_r^2
Tuff	-12.32	106.38	101.09	5.77	4.00	1.00	0.00	0.98	0.82
Diorite	-16.87	146.11	132.95	5.05	1.89	1.00	0.00	0.95	0.53
Basalt	-11.83	98.87	84.51	3.26	1.02	1.00	0.008	0.82	0.67

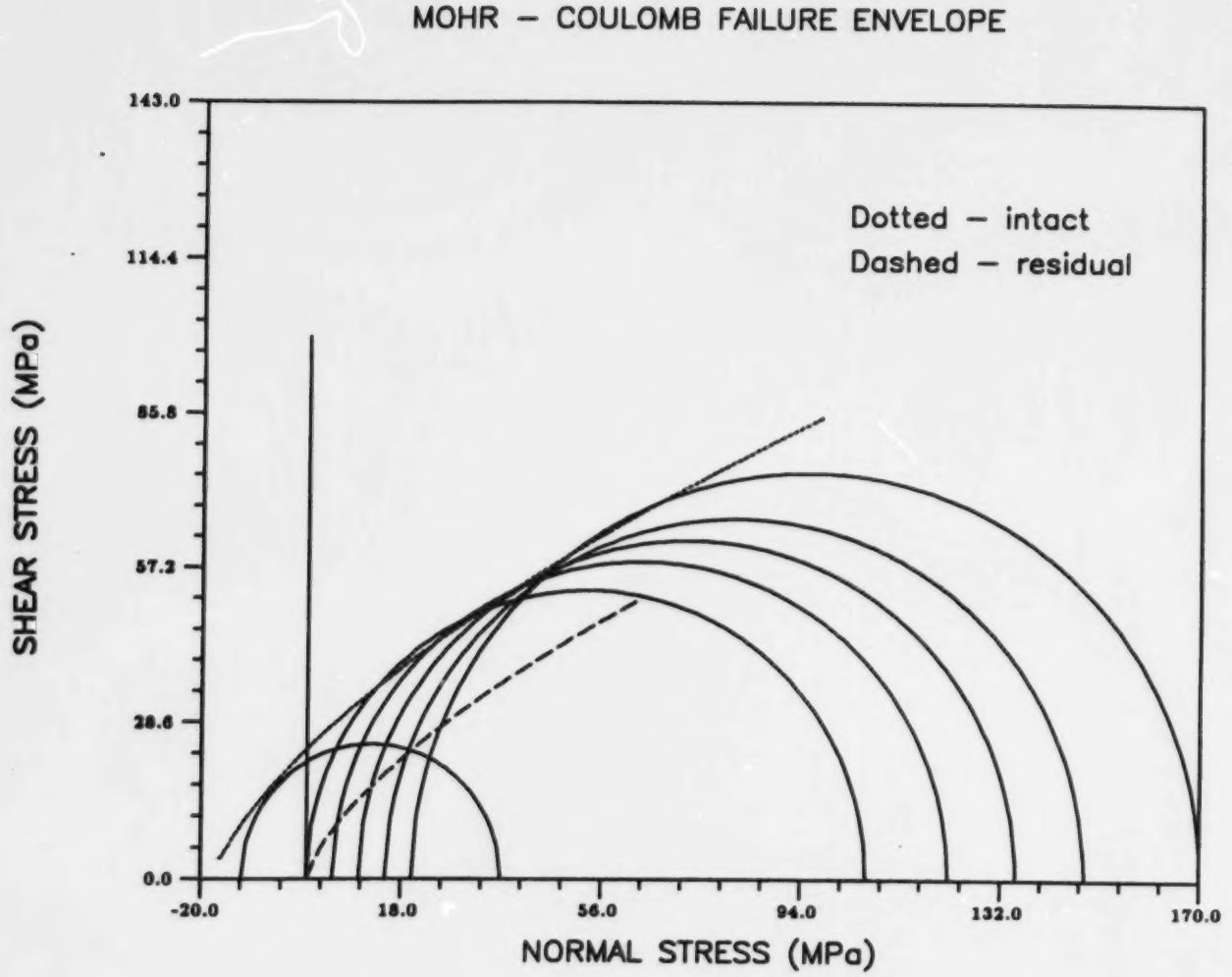

FIG. 1 TUFF SPECIMENS

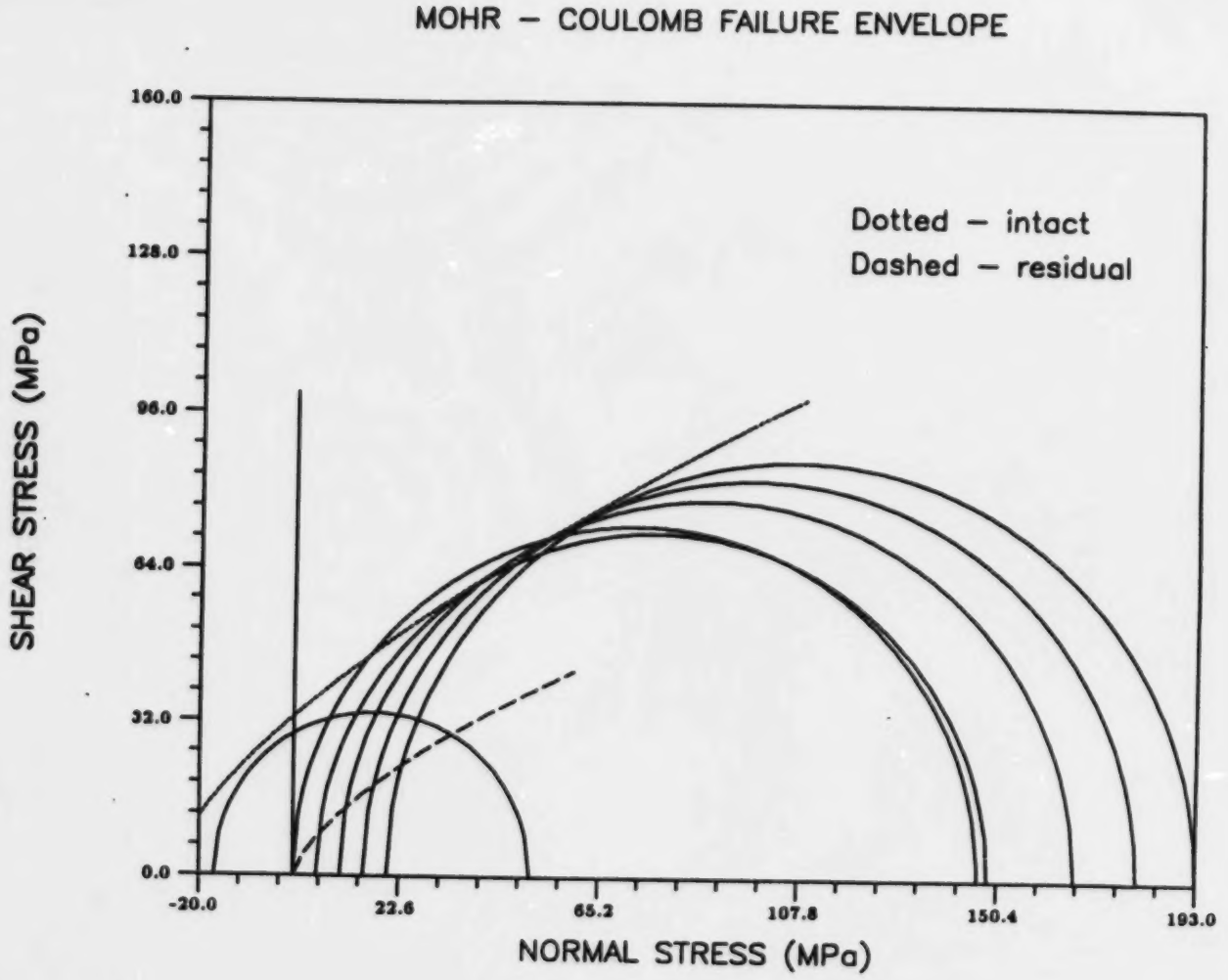

FIG. 2 DIORITE SPECIMENS

MOHR – COULOMB FAILURE ENVELOPE

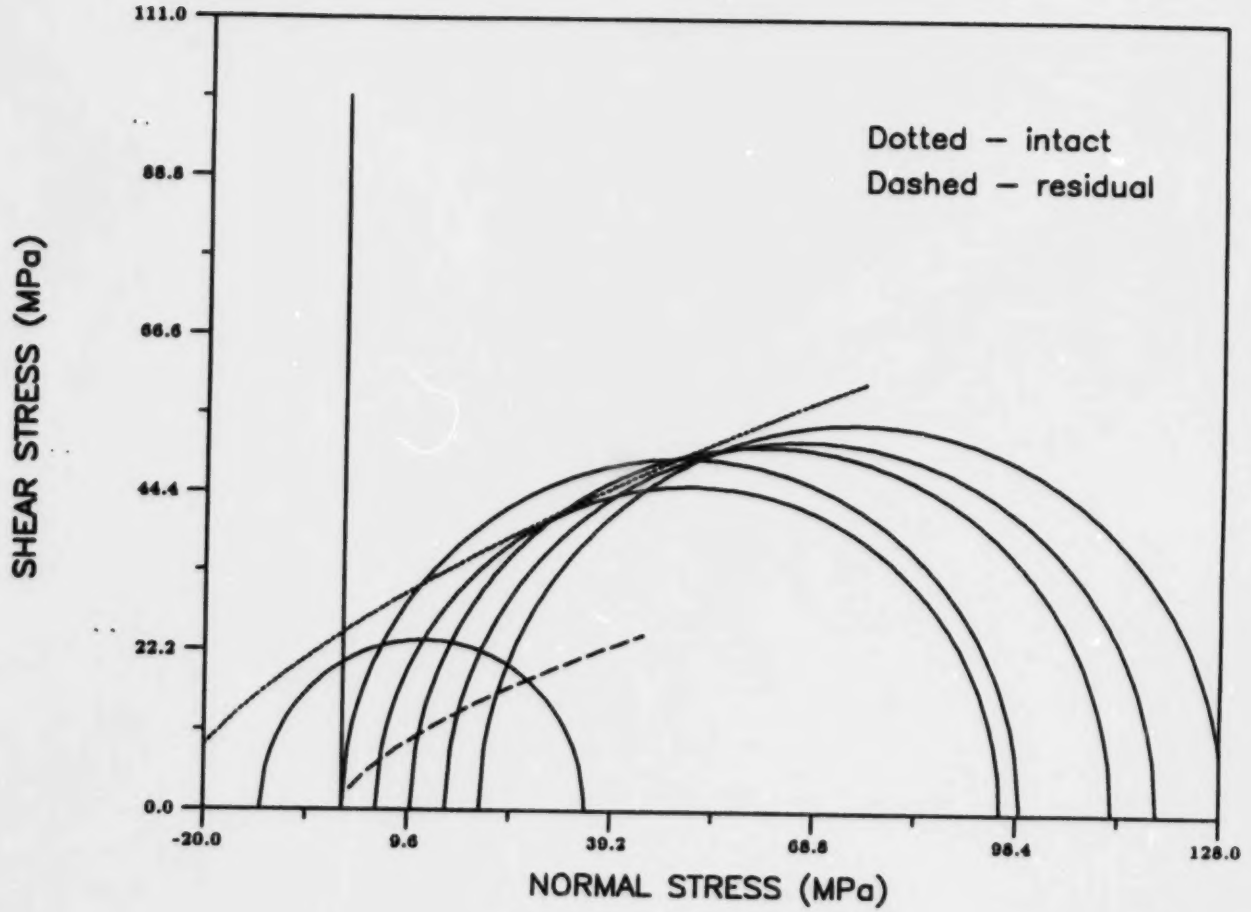

FIG. 3 BASALT SPECIMENS

APPENDIX A

AXIAL STRESS-STRAIN CURVES OF UNIAXIAL TESTS

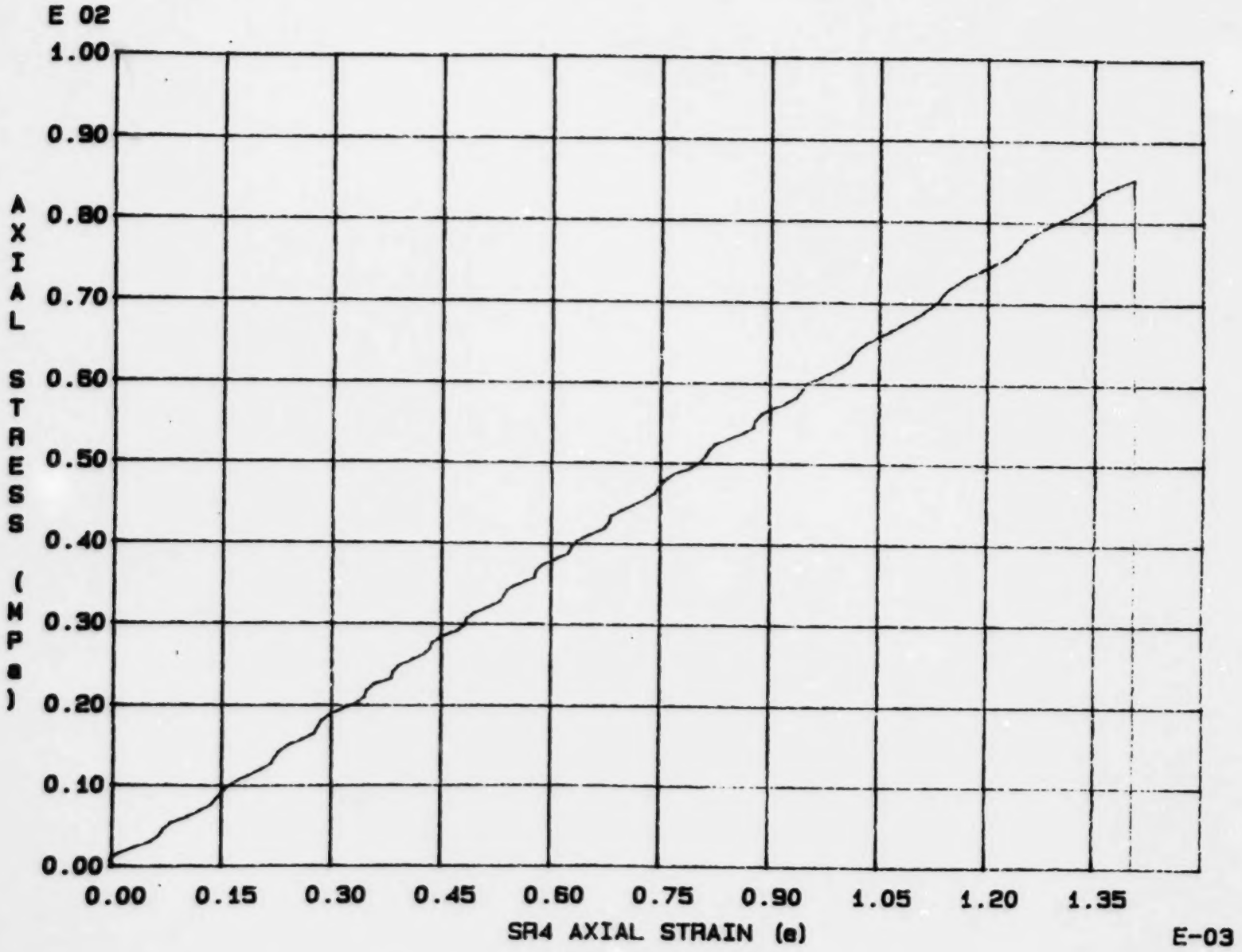

FIG. A-1 SPECIMEN 9011

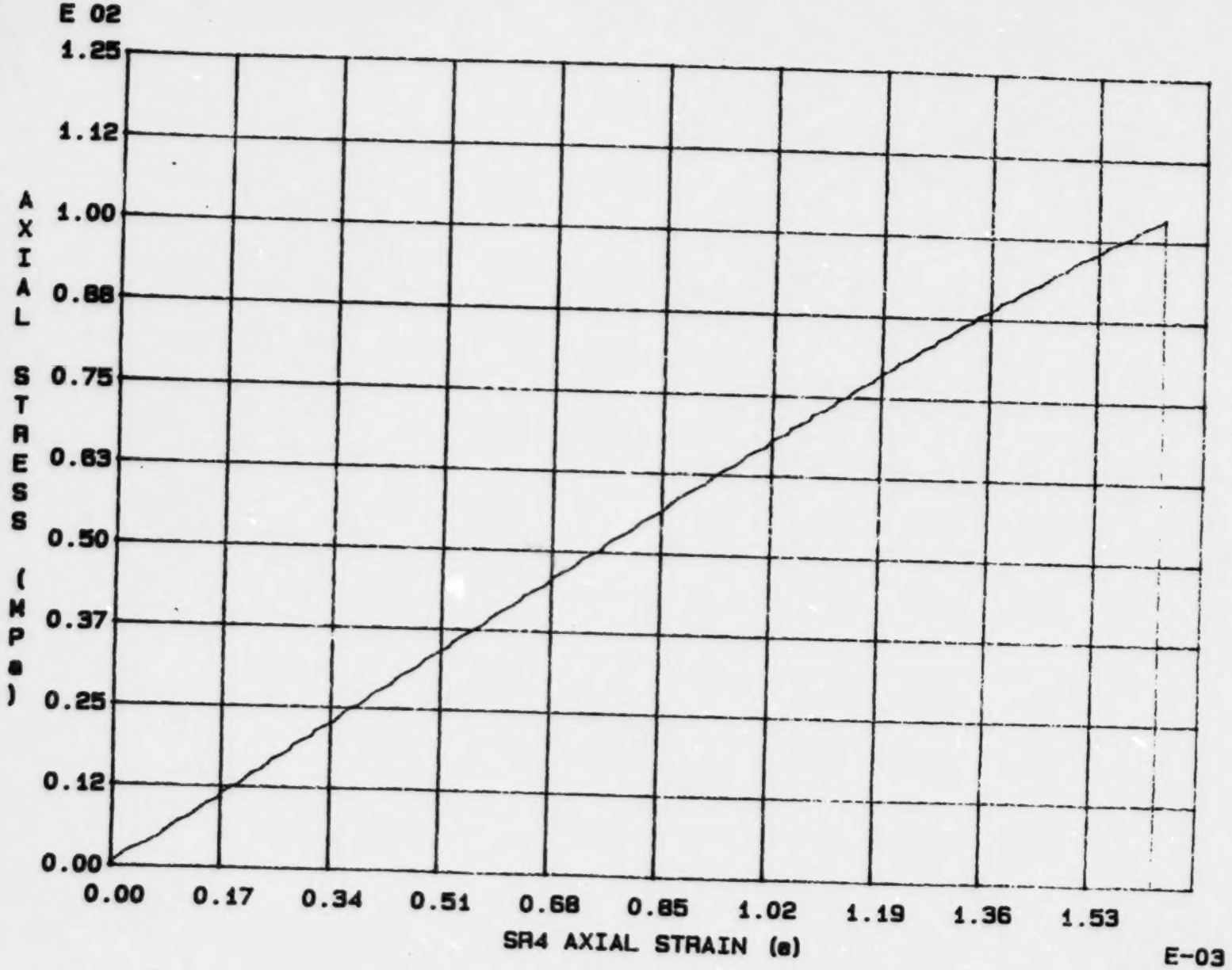

FIG. A-2 SPECIMEN 9013

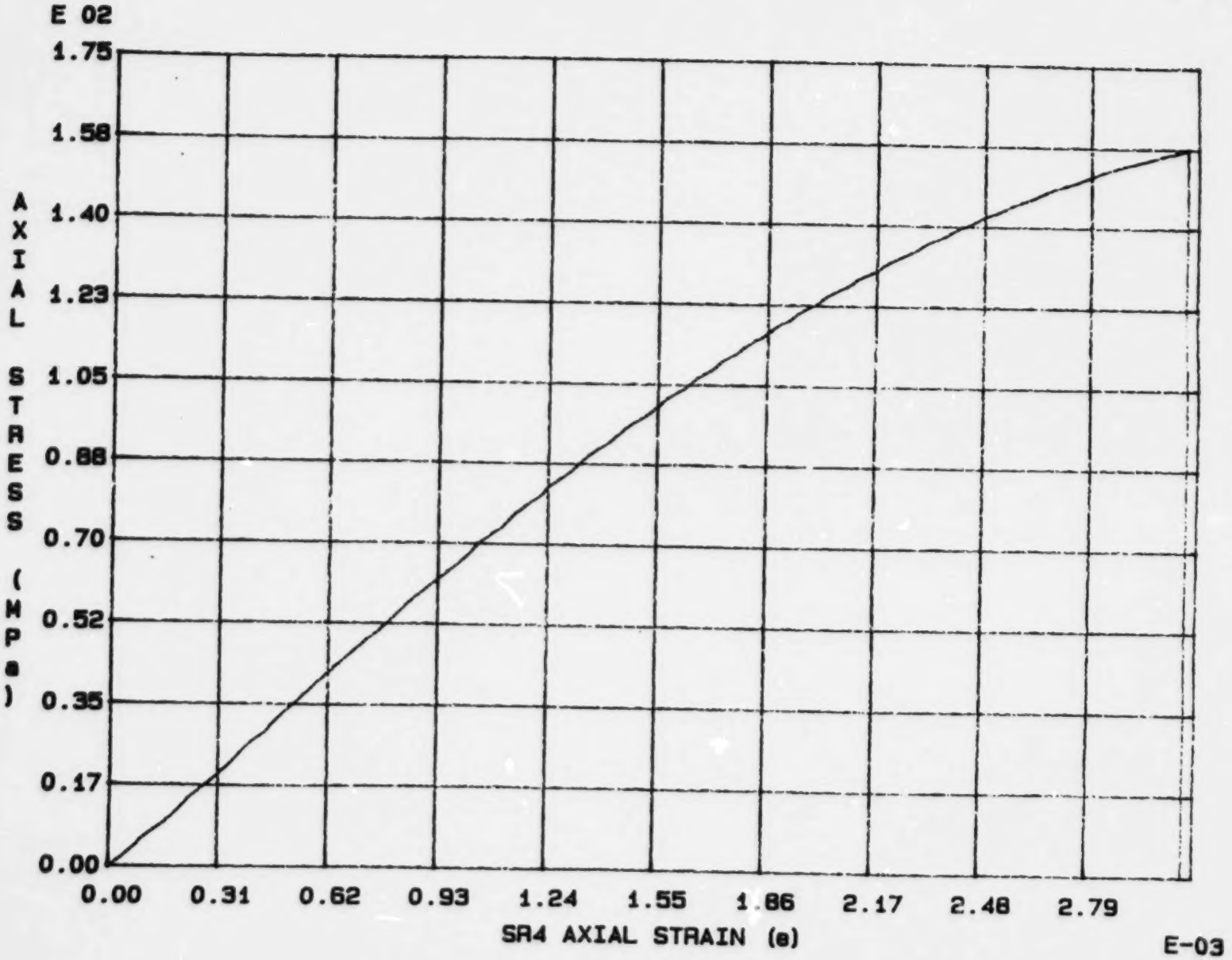

FIG. A-3 SPECIMEN 9015

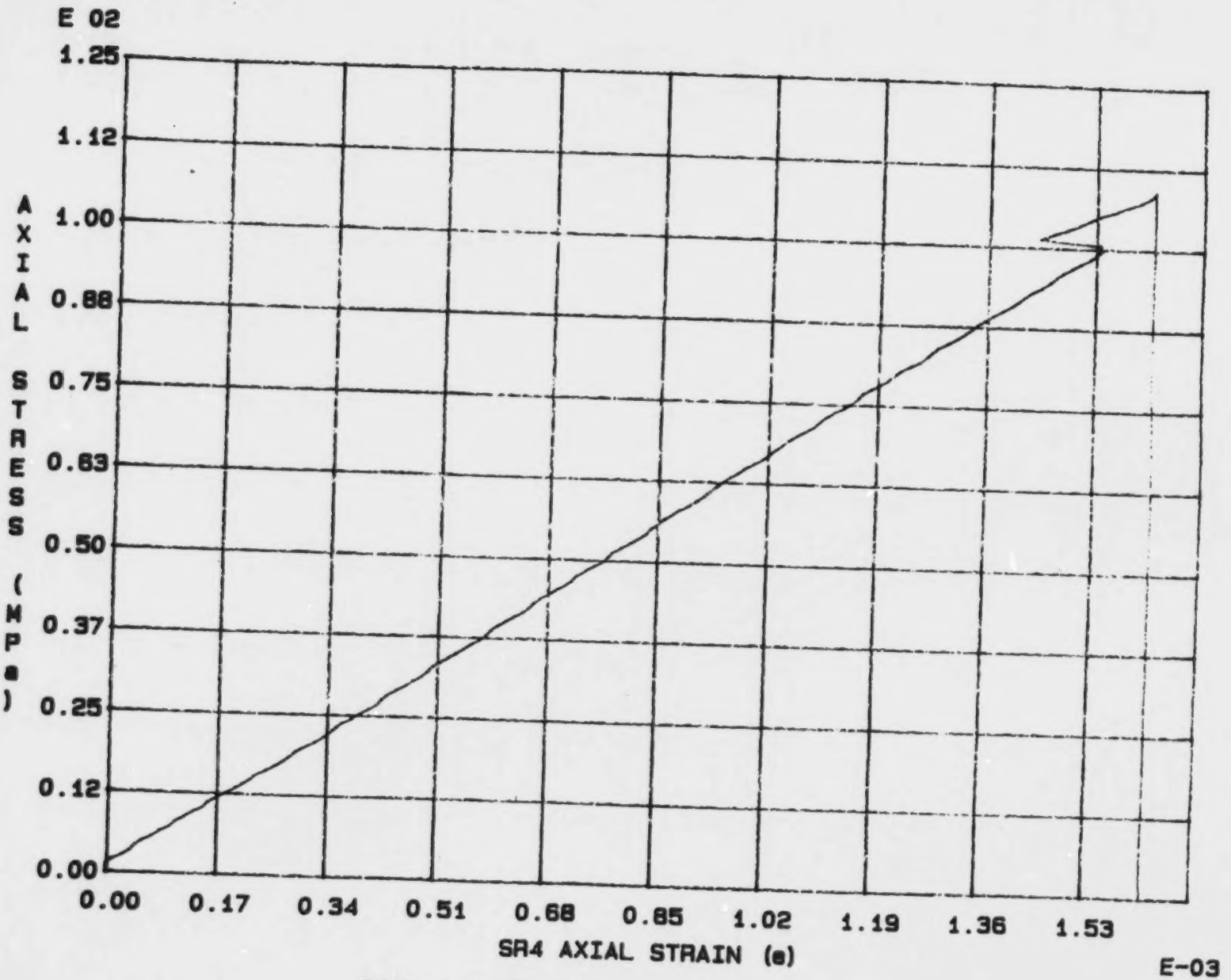

FIG. A-4 SPECIMEN 9021

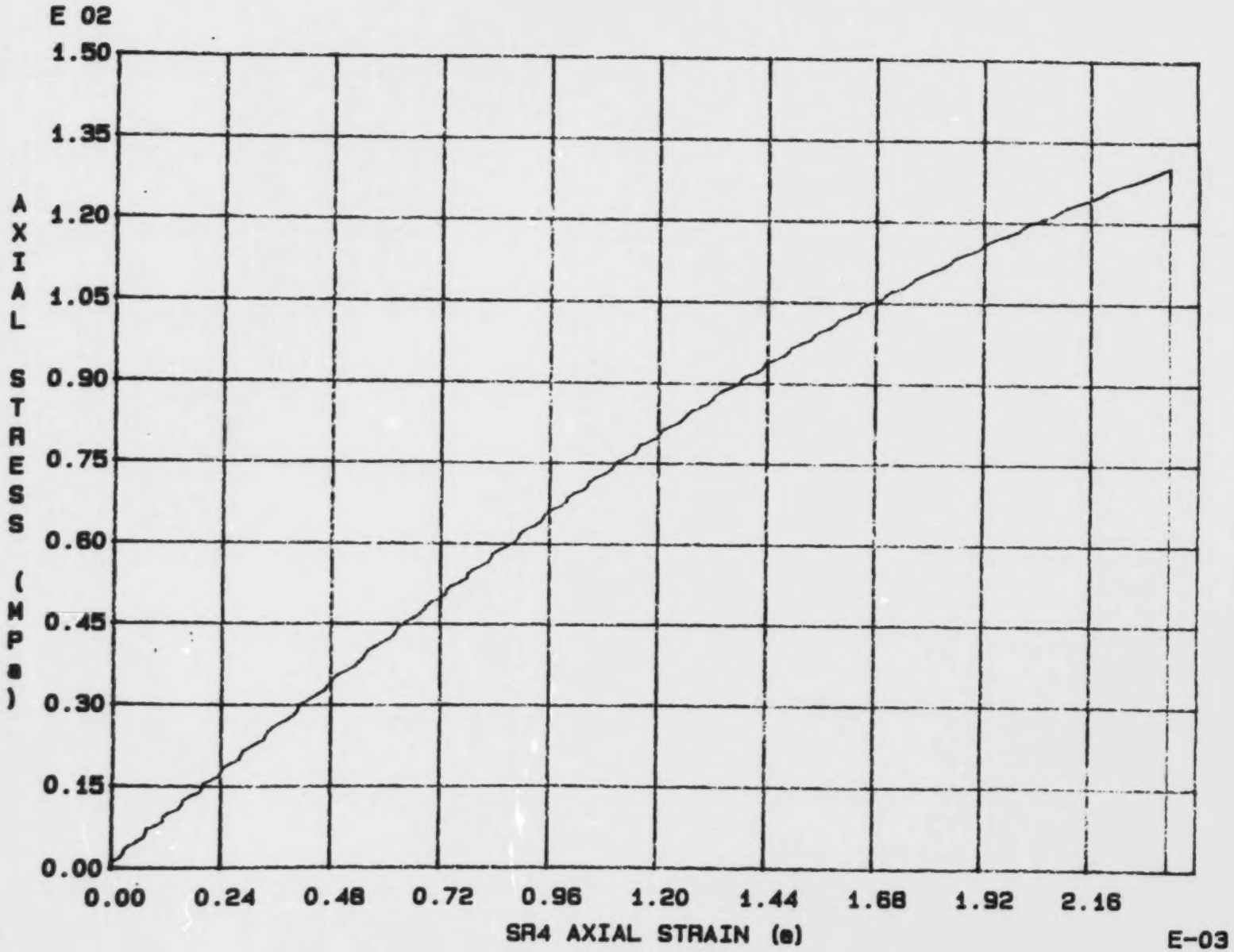

FIG. A-5 SPECIMEN 9023

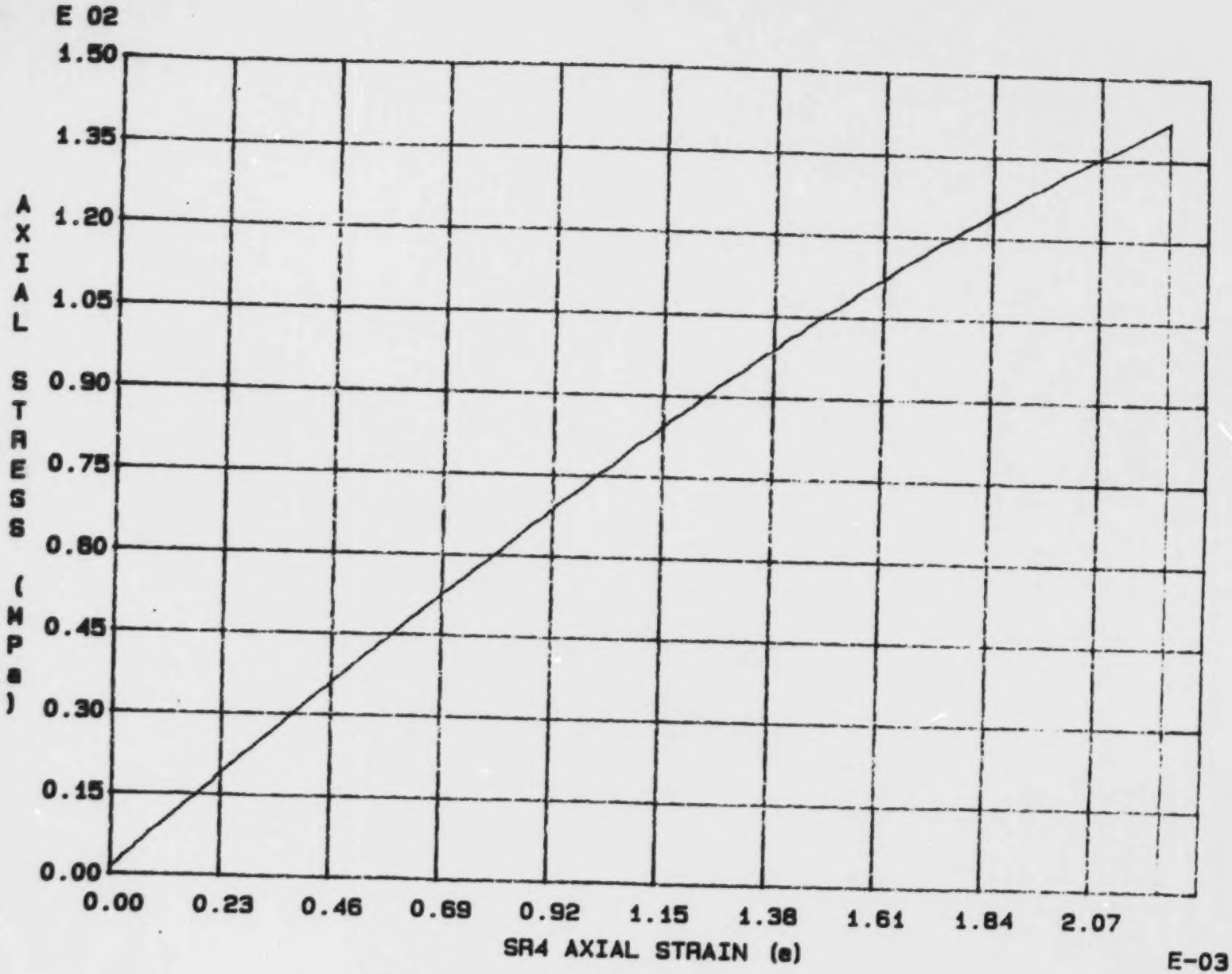

FIG. A-6 SPECIMEN 9031

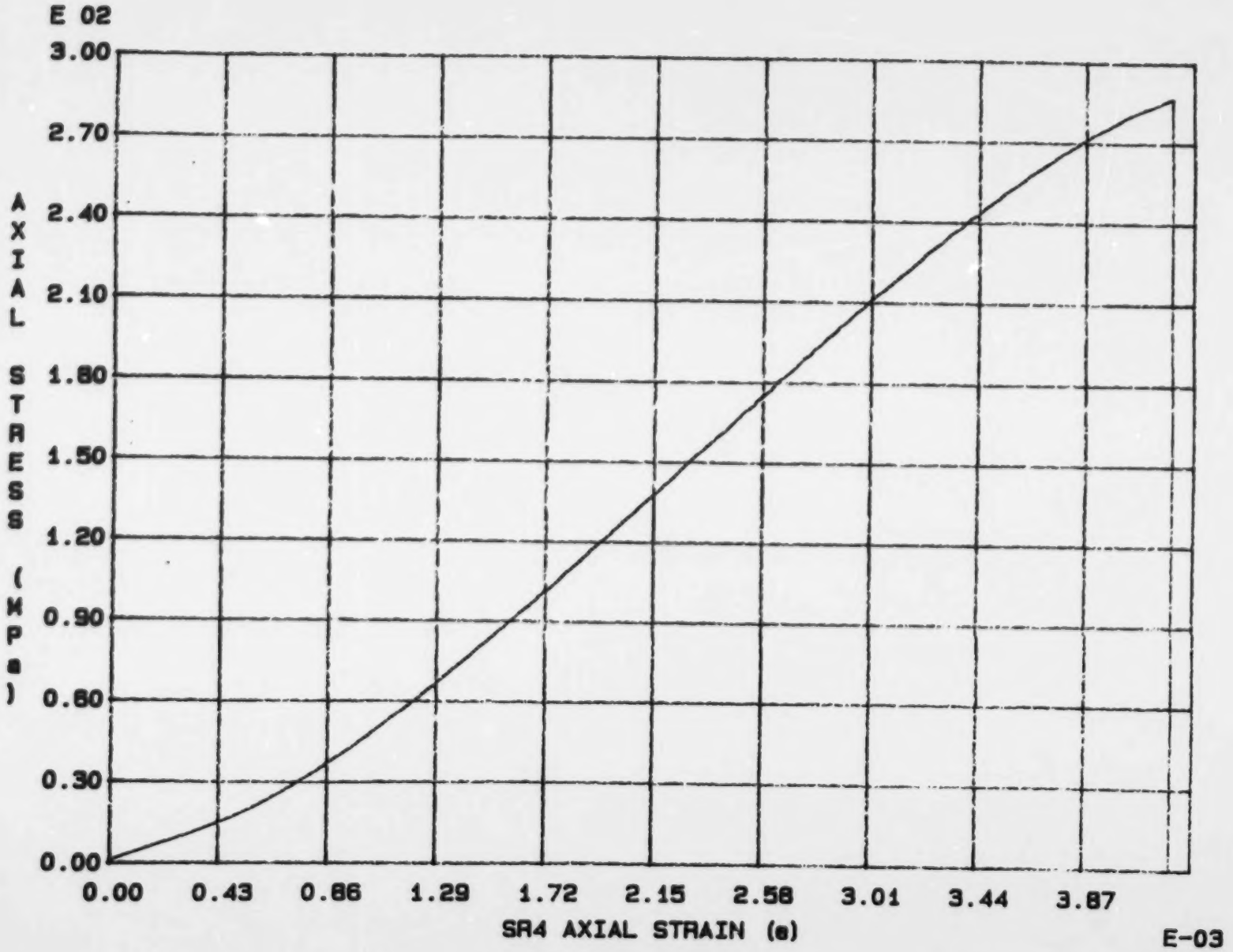

FIG. A-7 SPECIMEN 9033

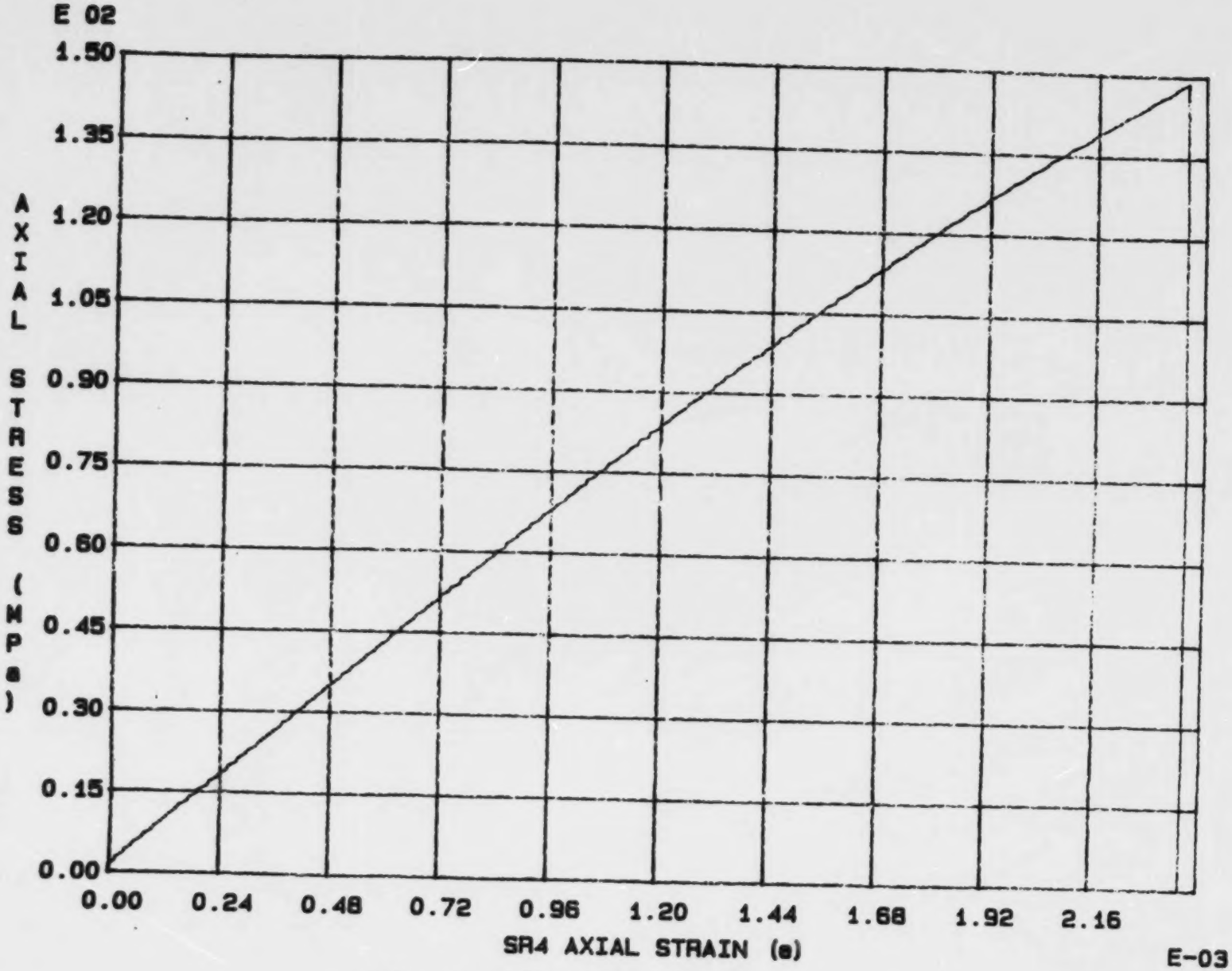

FIG. A-8 SPECIMEN 9035

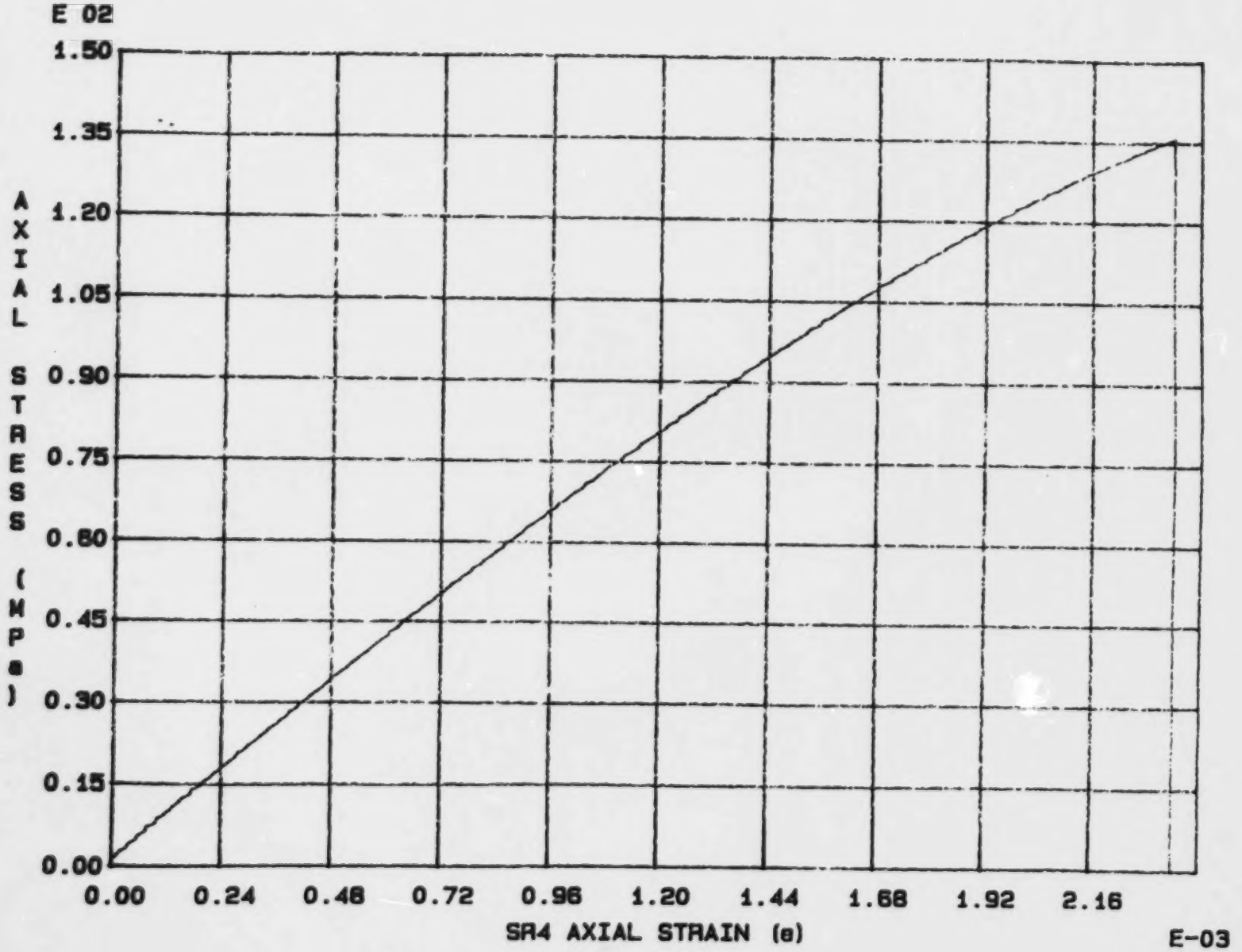

FIG. A-9 SPECIMEN 9511

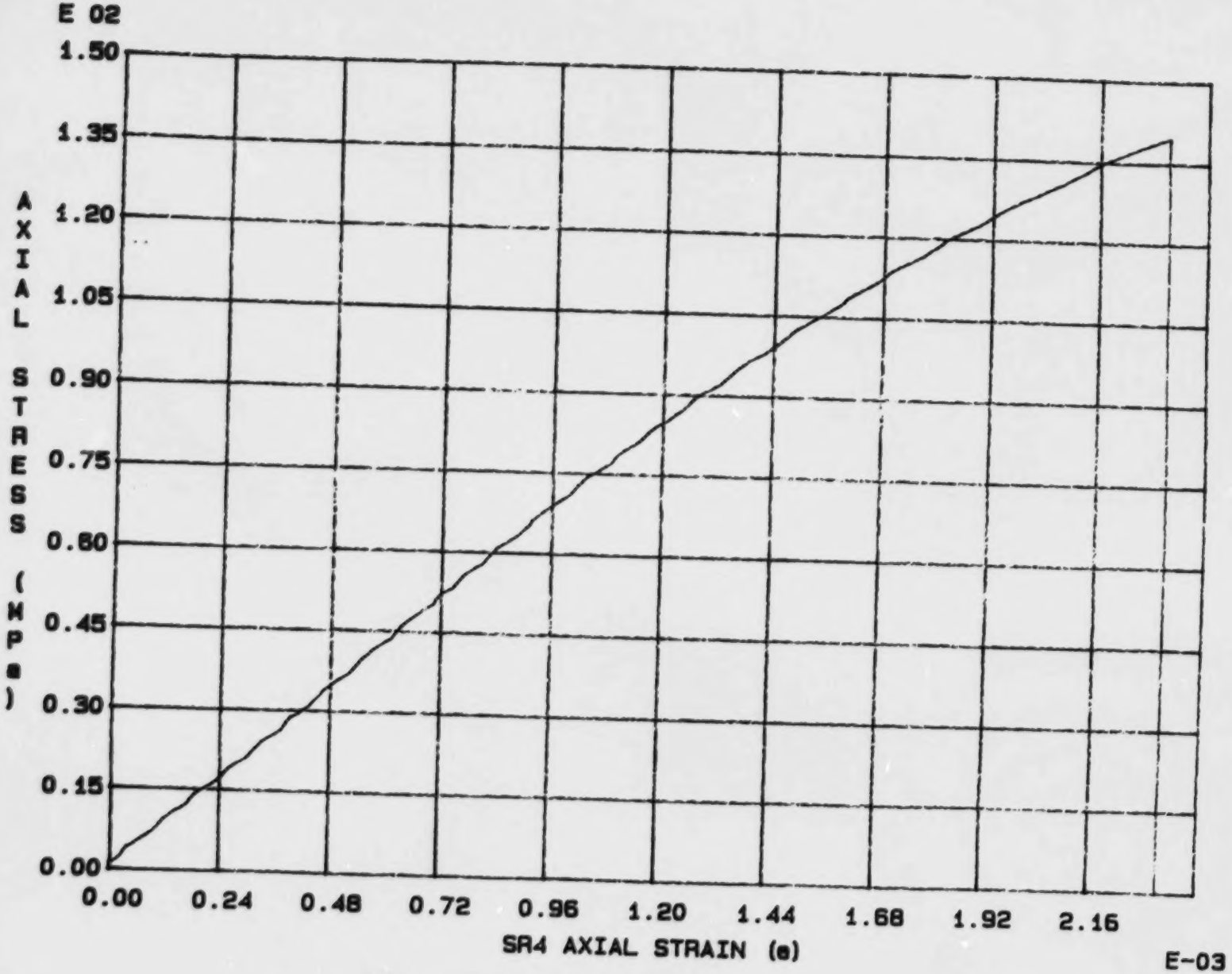

FIG. A-10 SPECIMEN 9513

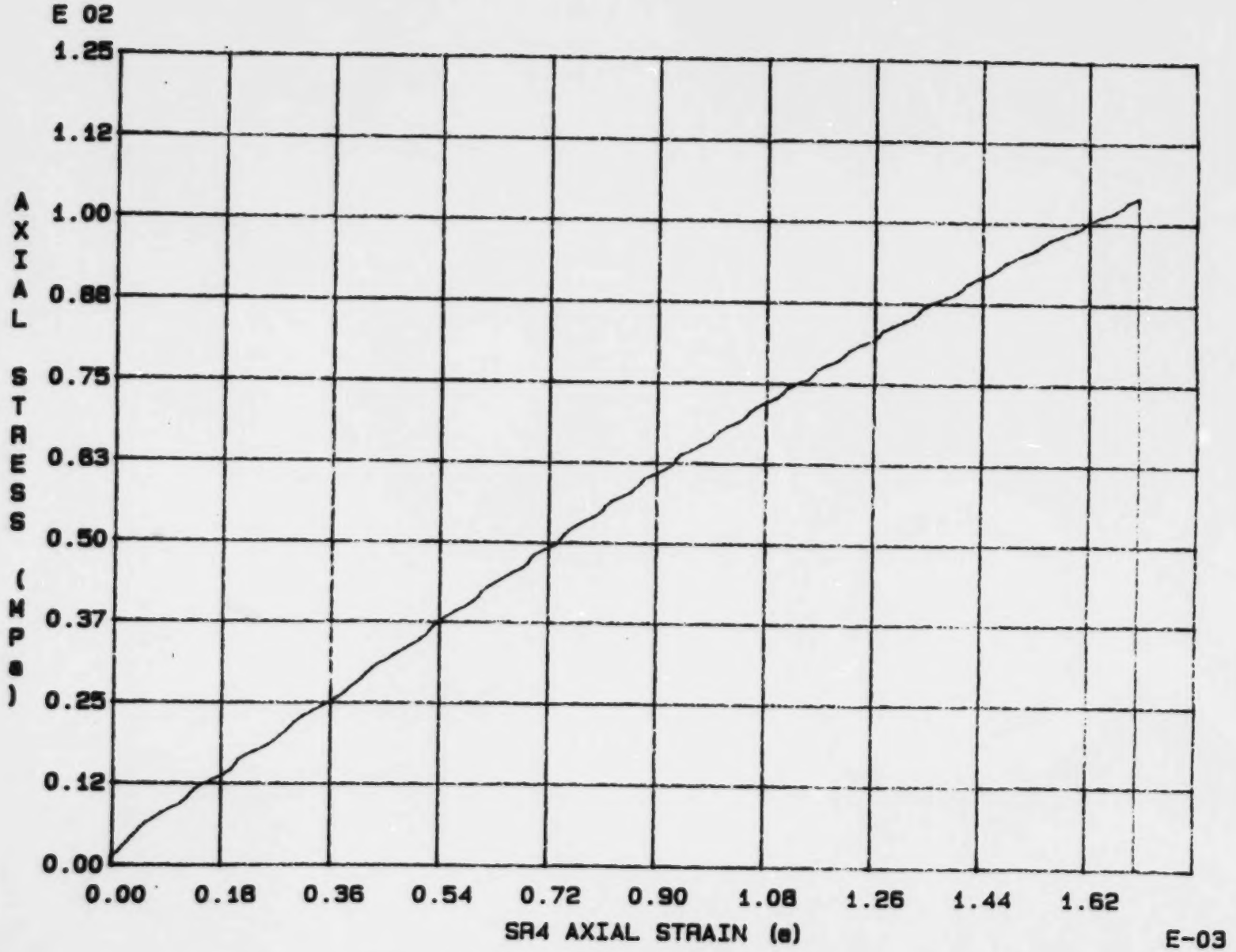

FIG. A-11 SPECIMEN 9521

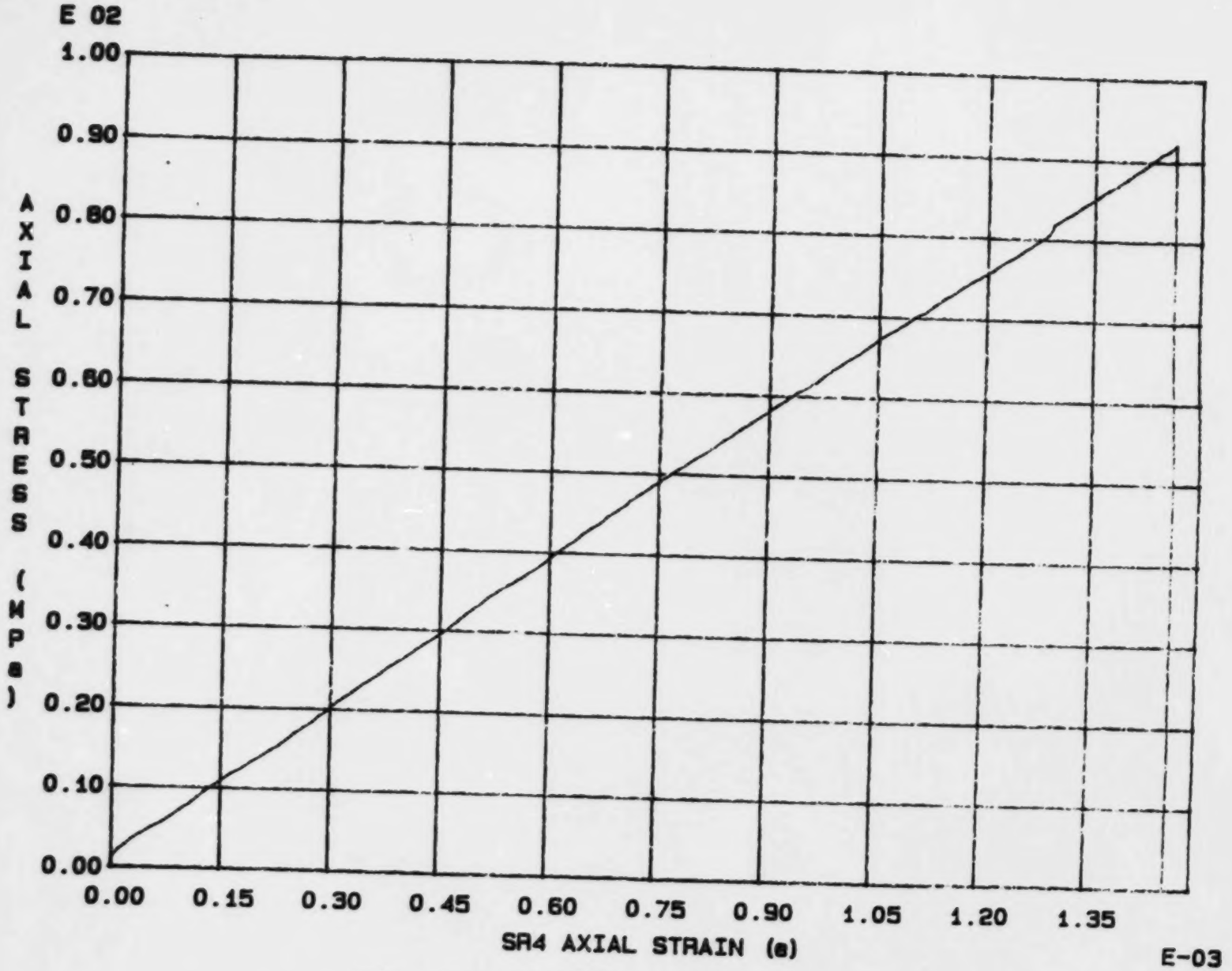

FIG. A-12 SPECIMEN 9523

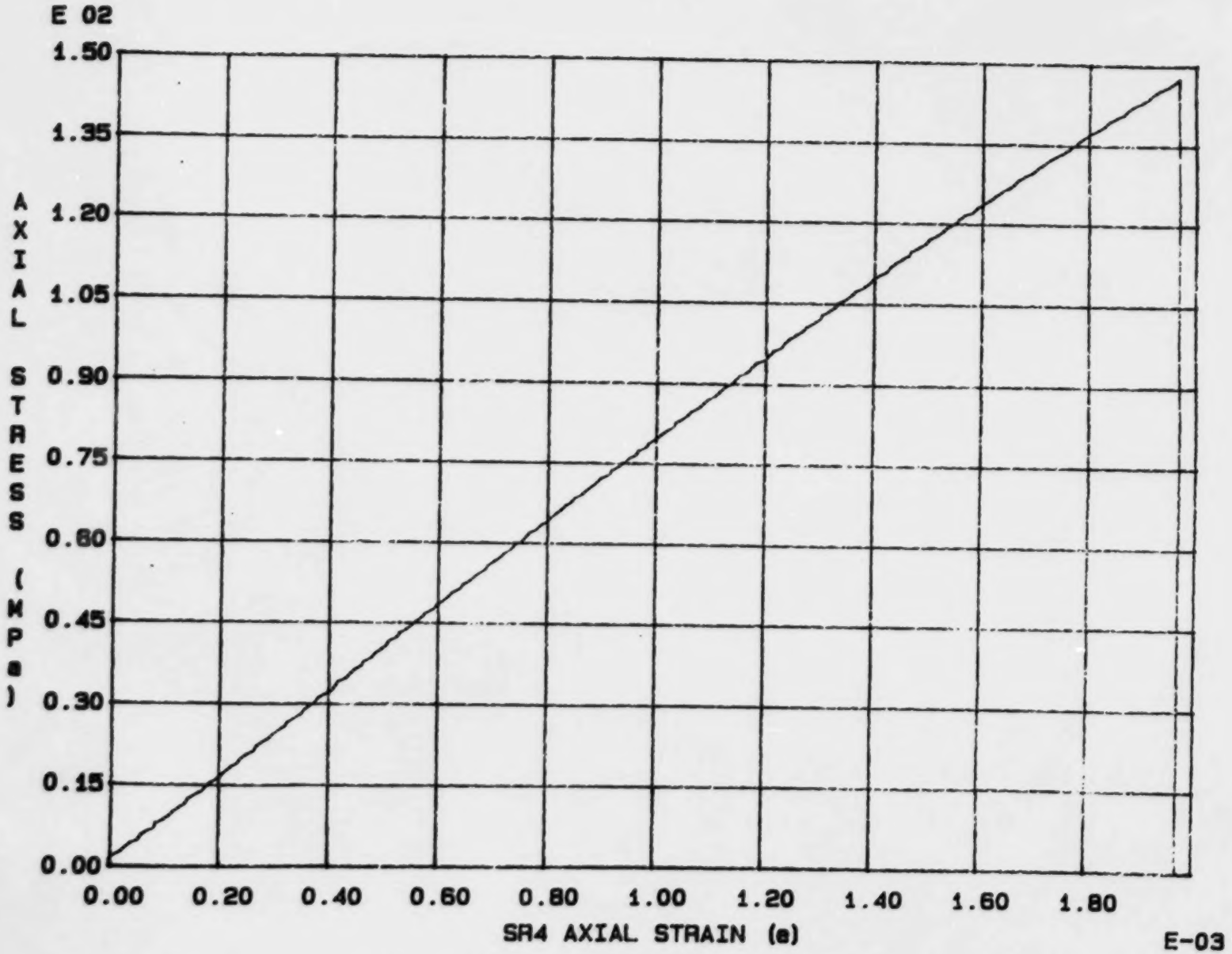

FIG. A-13 SPECIMEN 9531

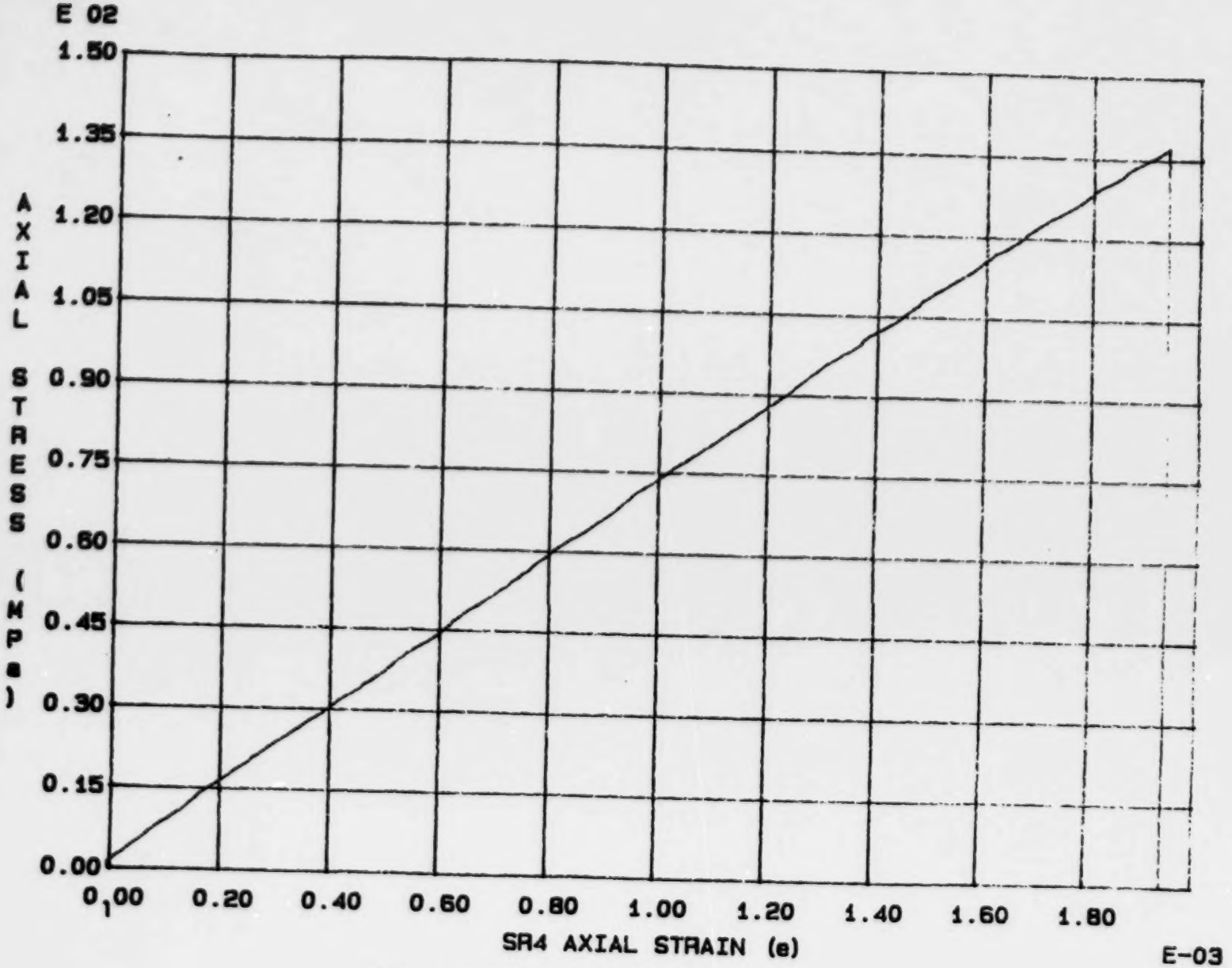

FIG. A-14 SPECIMEN 9533

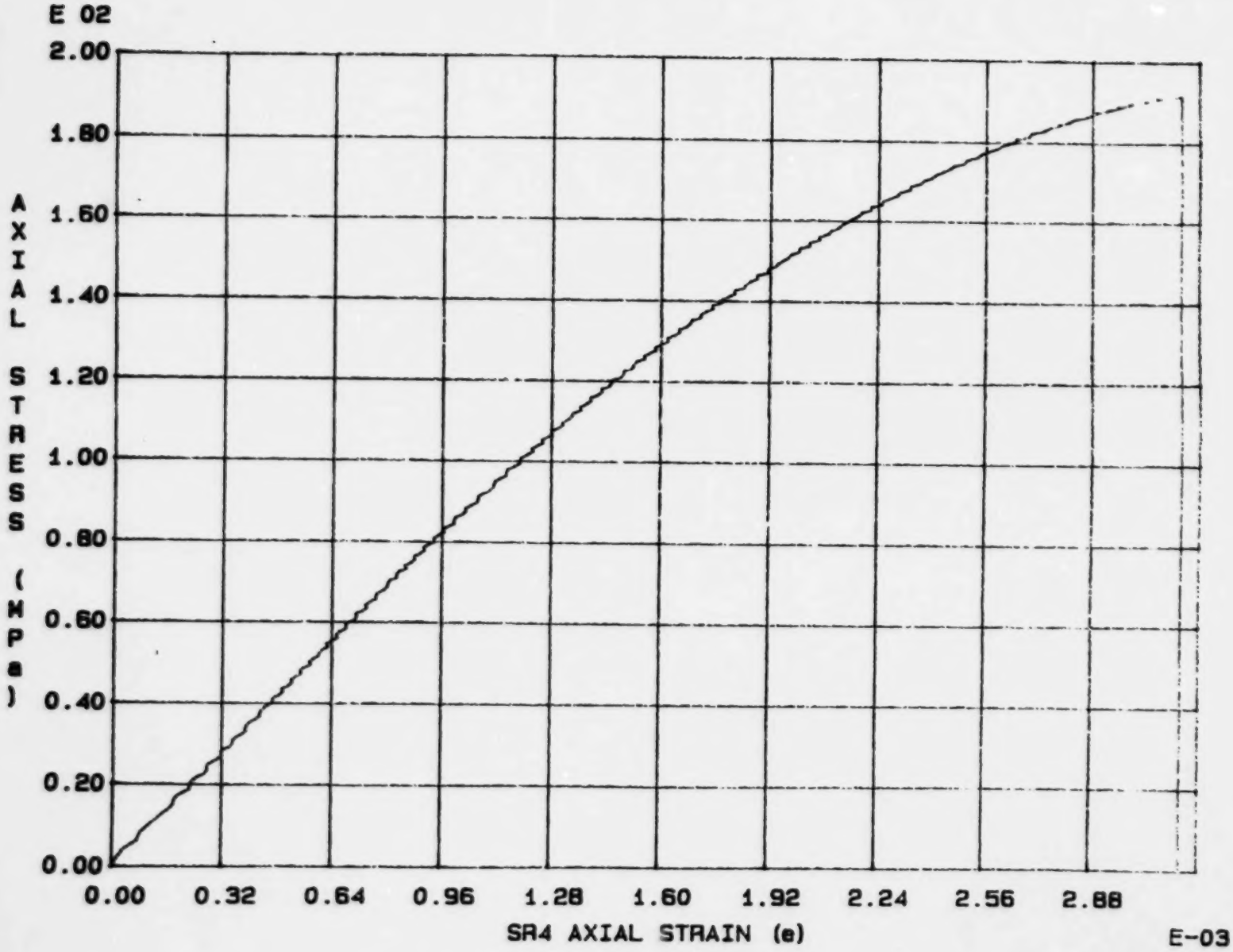

FIG. A-15 SPECIMEN 9535

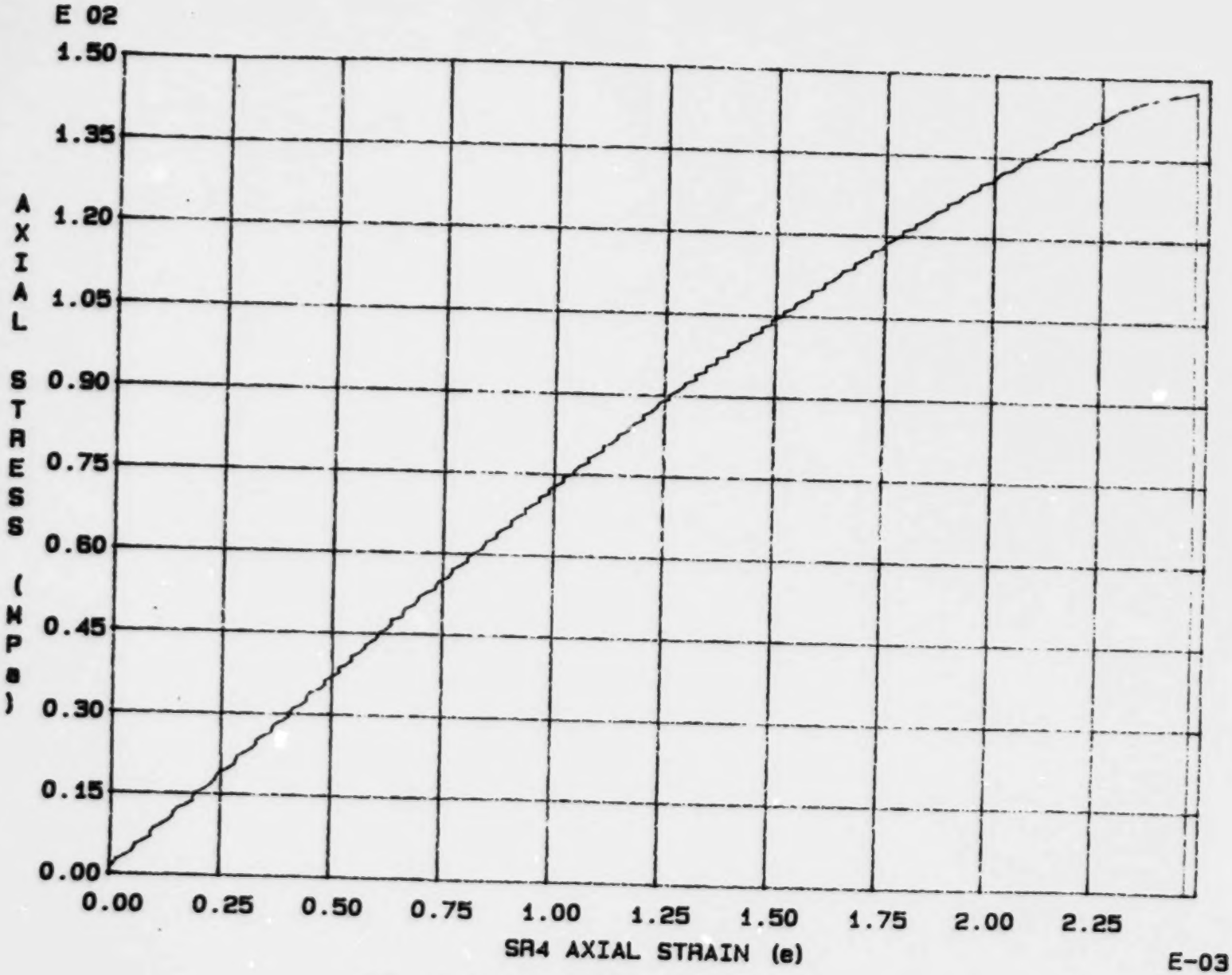

FIG. A-16 SPECIMEN 4011

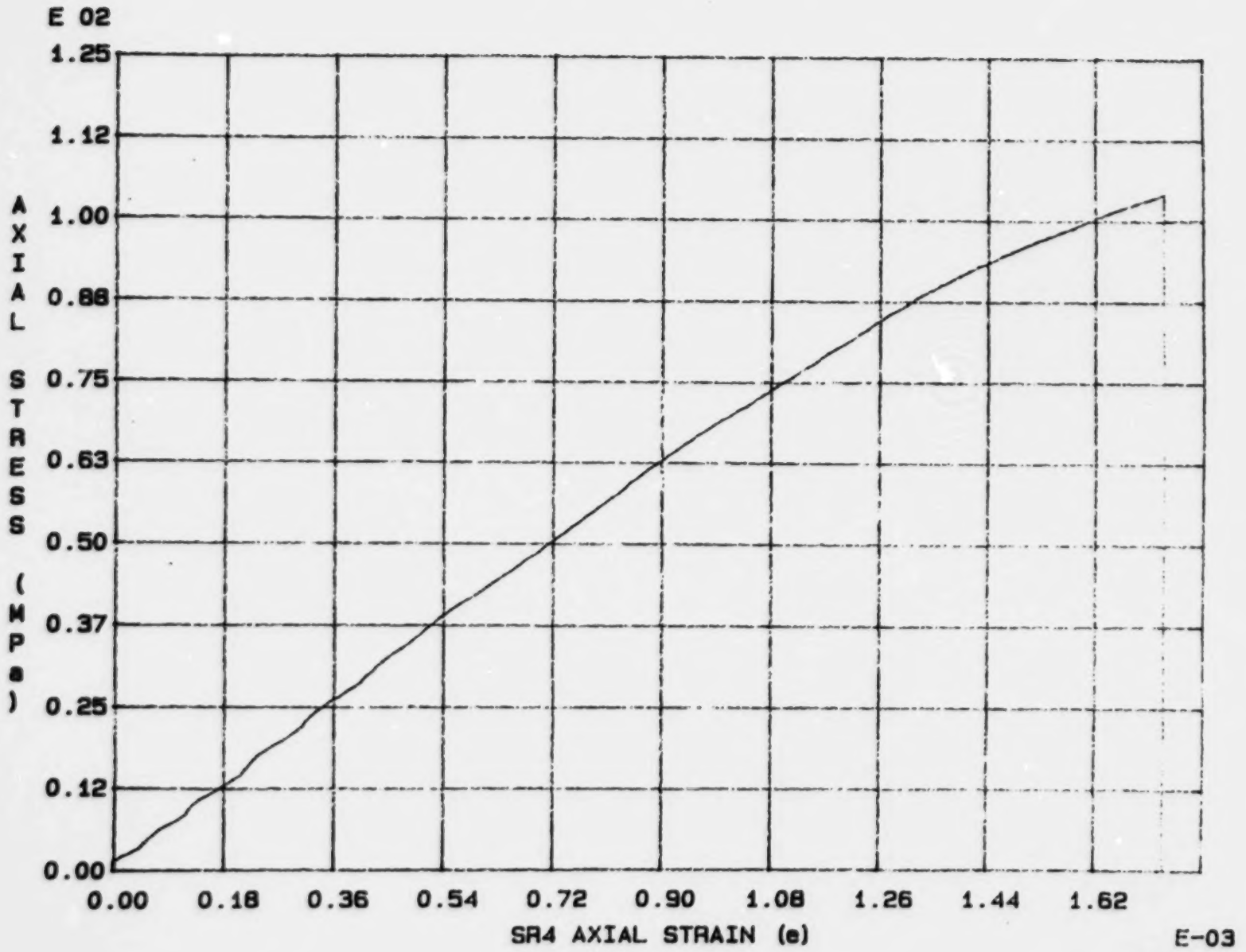

FIG. A-17 SPECIMEN 4013

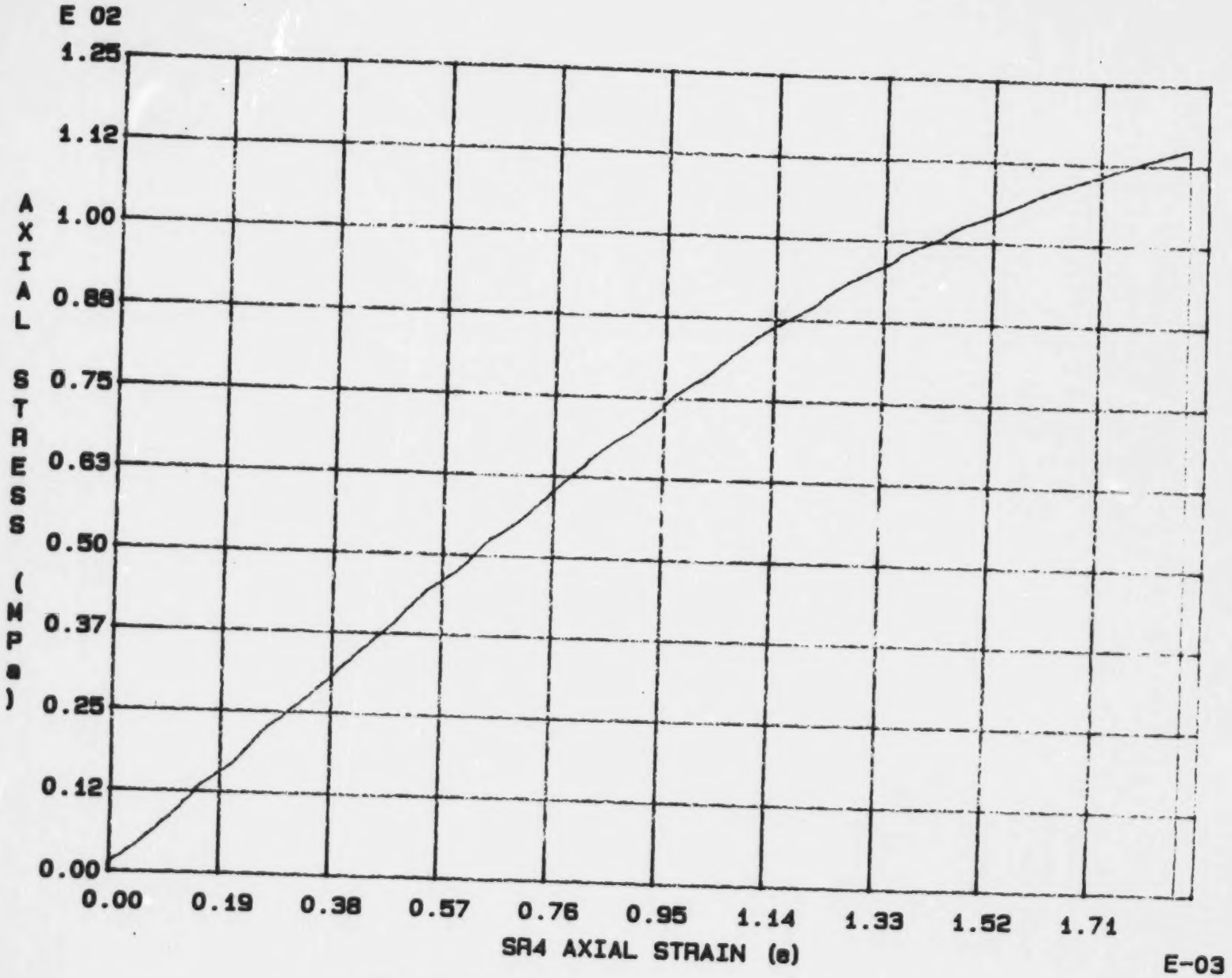

FIG. A-18 SPECIMEN 4015

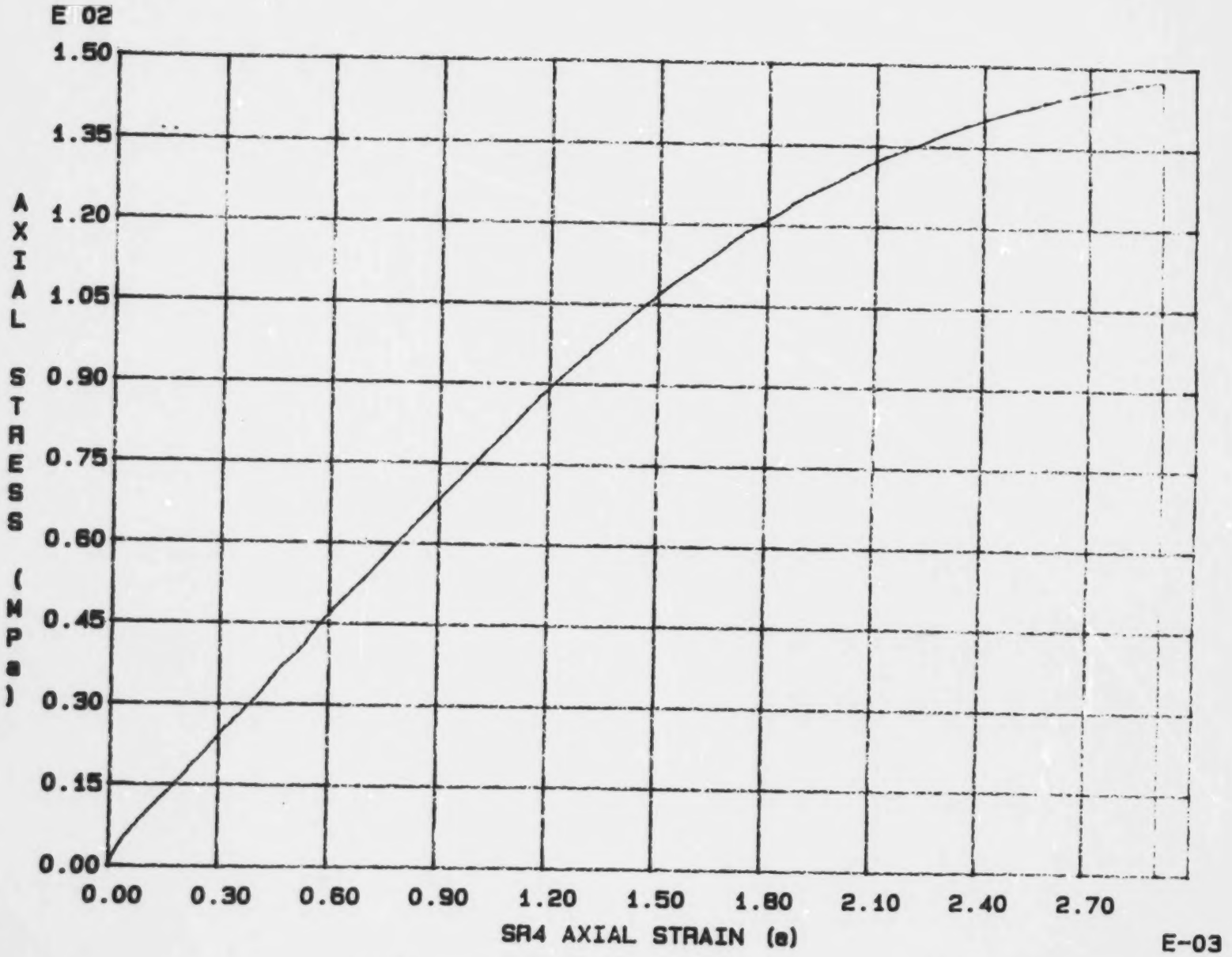

FIG. A-19 SPECIMEN 4017

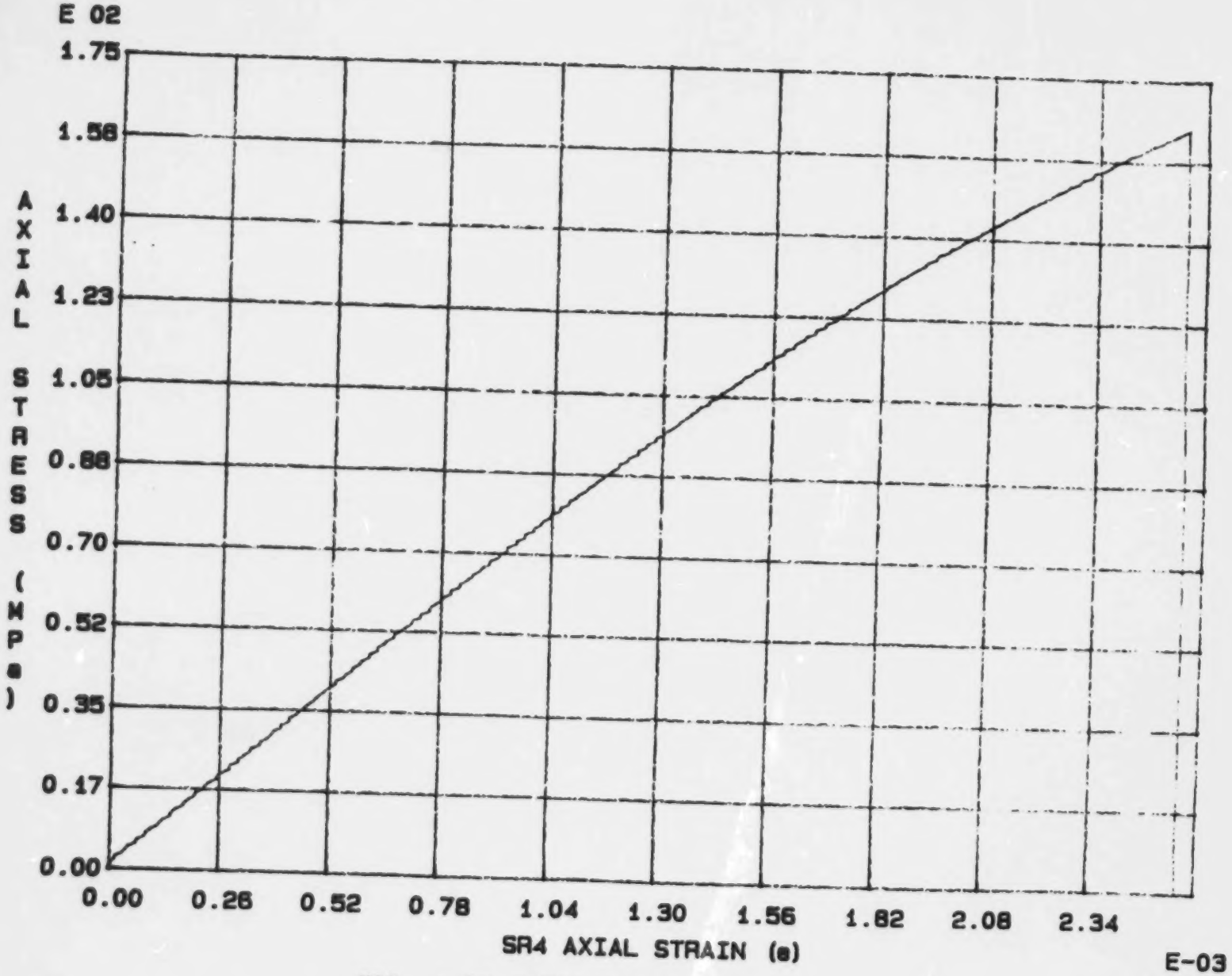

FIG. A-20 SPECIMEN 4021

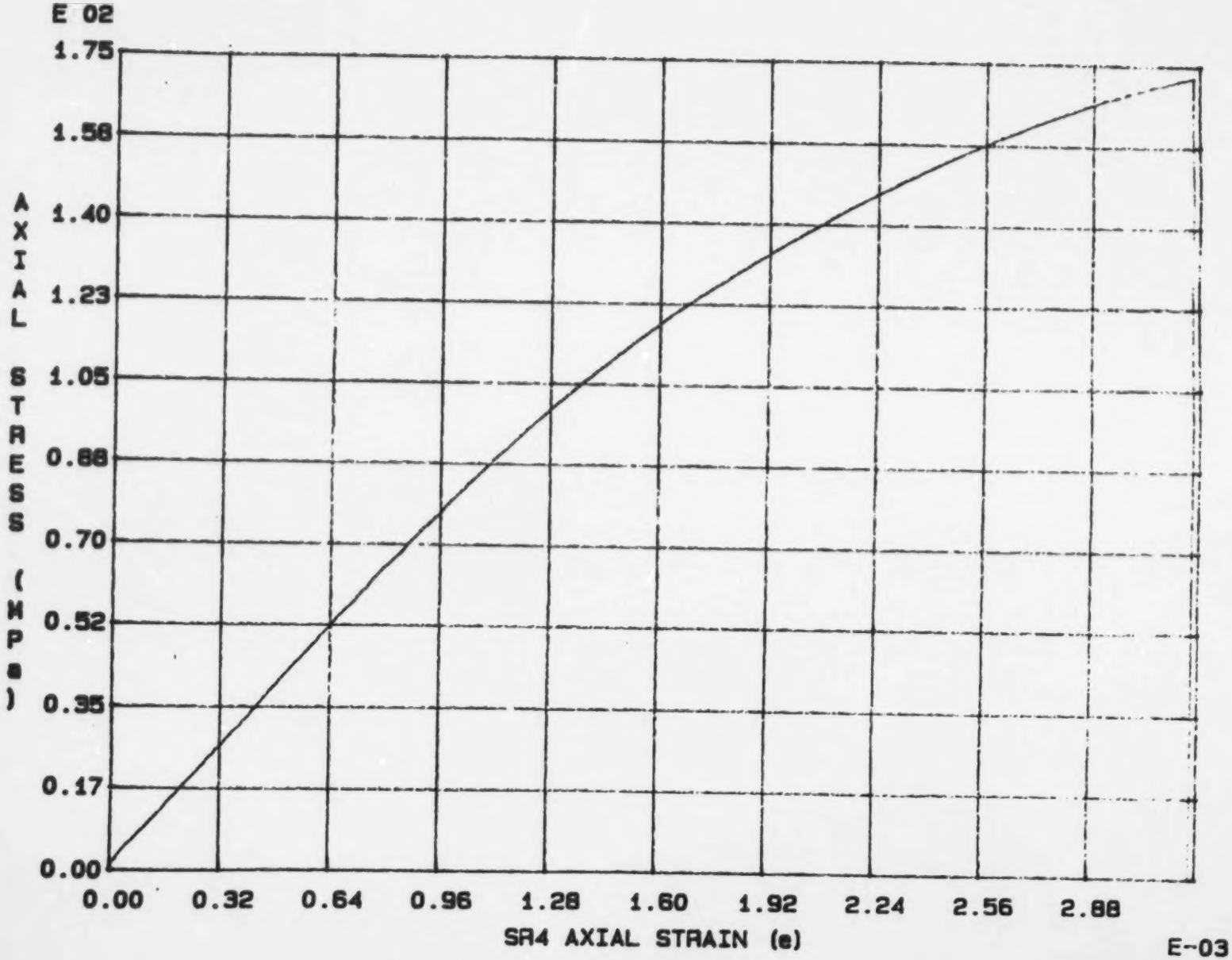

FIG. A-21 SPECIMEN 4023

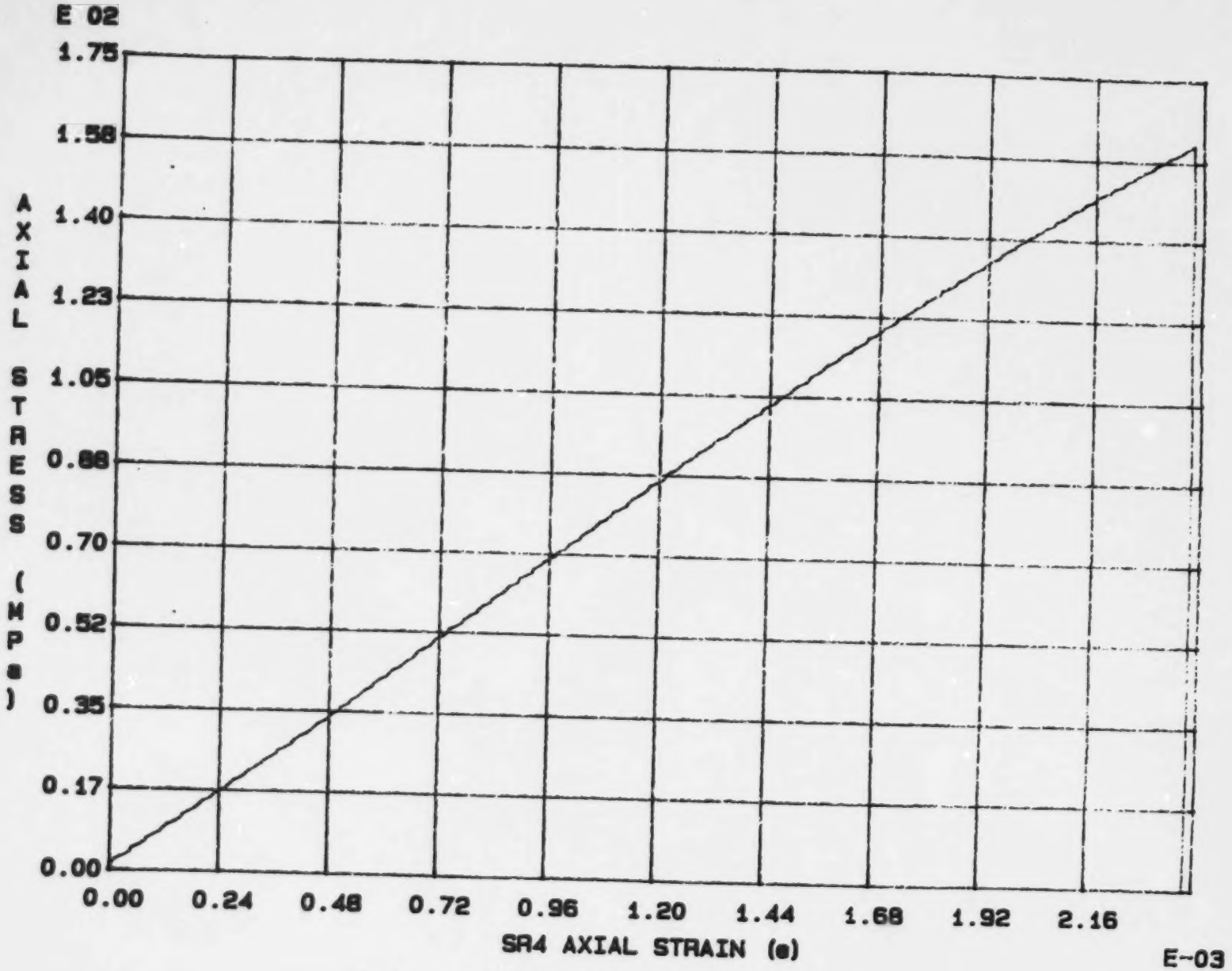

FIG. A-22 SPECIMEN 4031

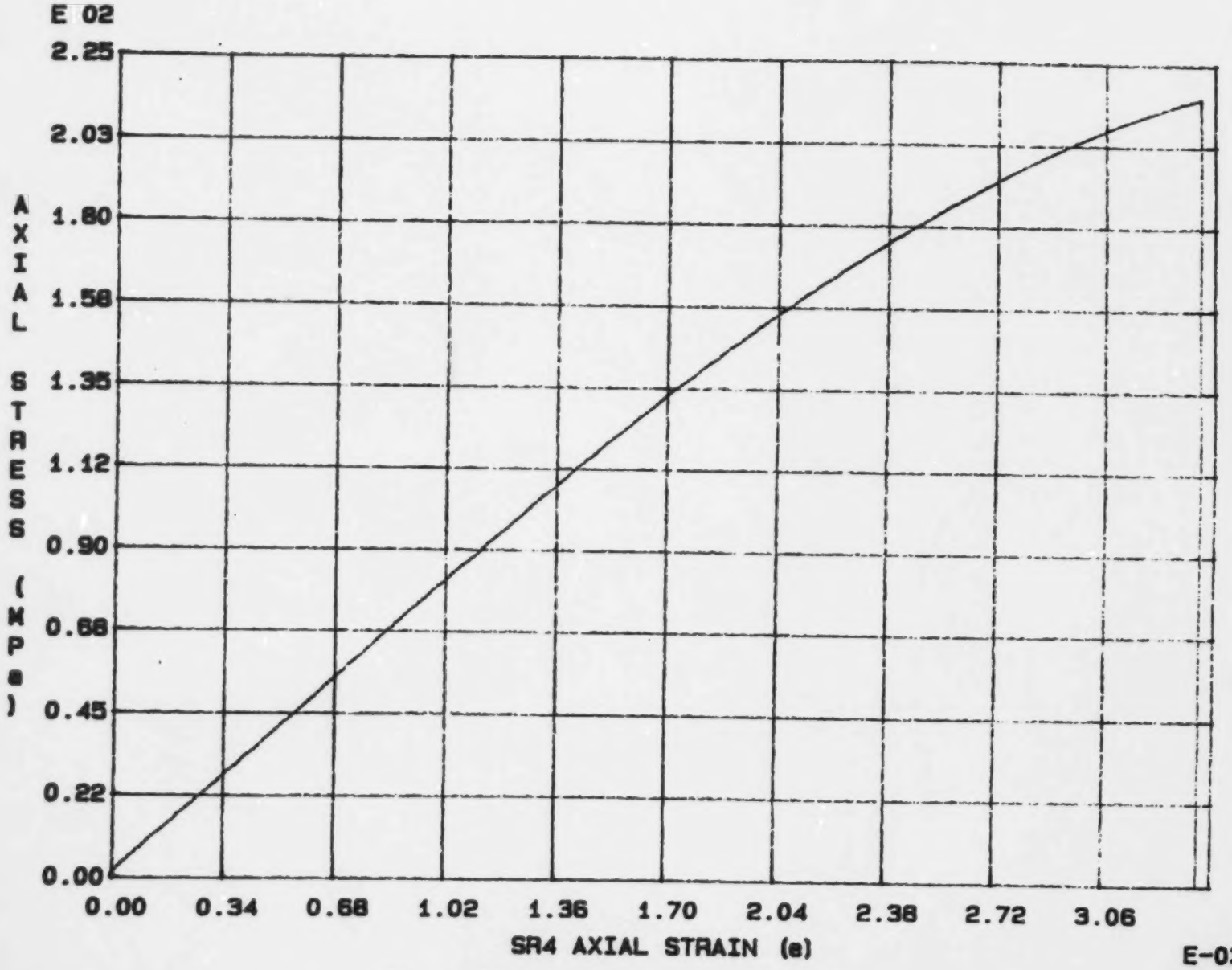

FIG. A-23 SPECIMEN 4033

APPENDIX B

CIRCUMFERENTIAL STRESS-STRAIN CURVES OF UNIAXIAL TESTS

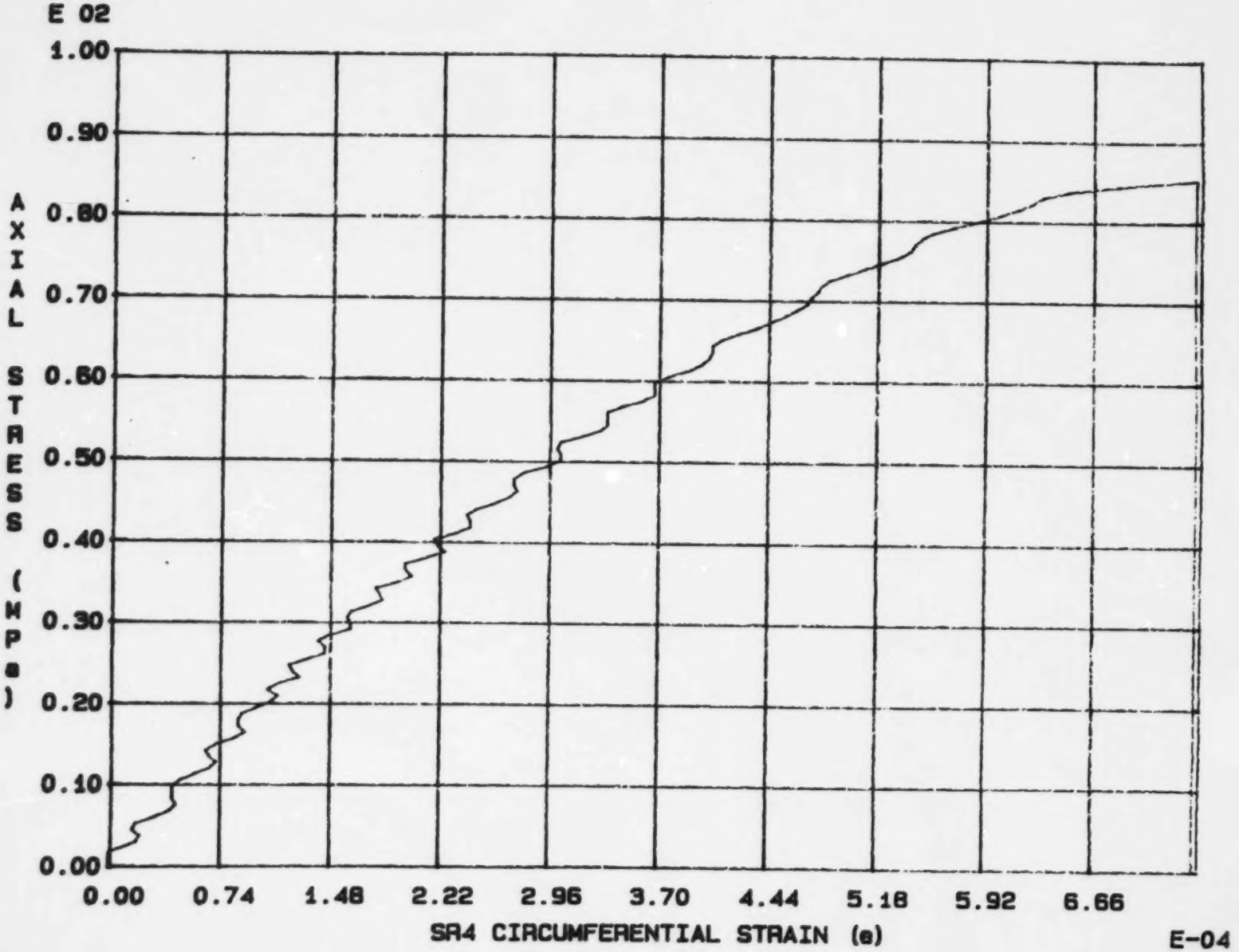

FIG. B-1 SPECIMEN 9011

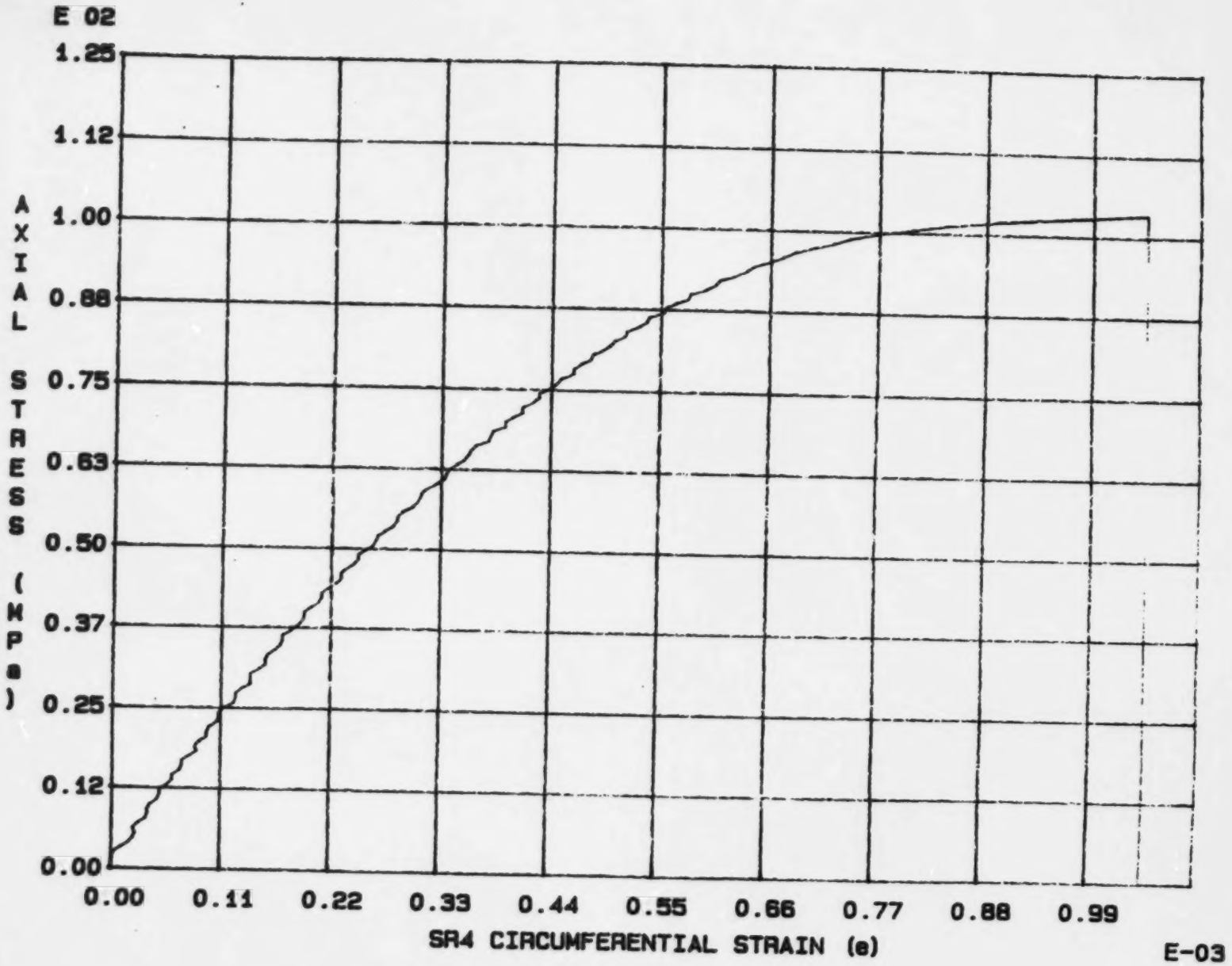

FIG. B-2 SPECIMEN 9013

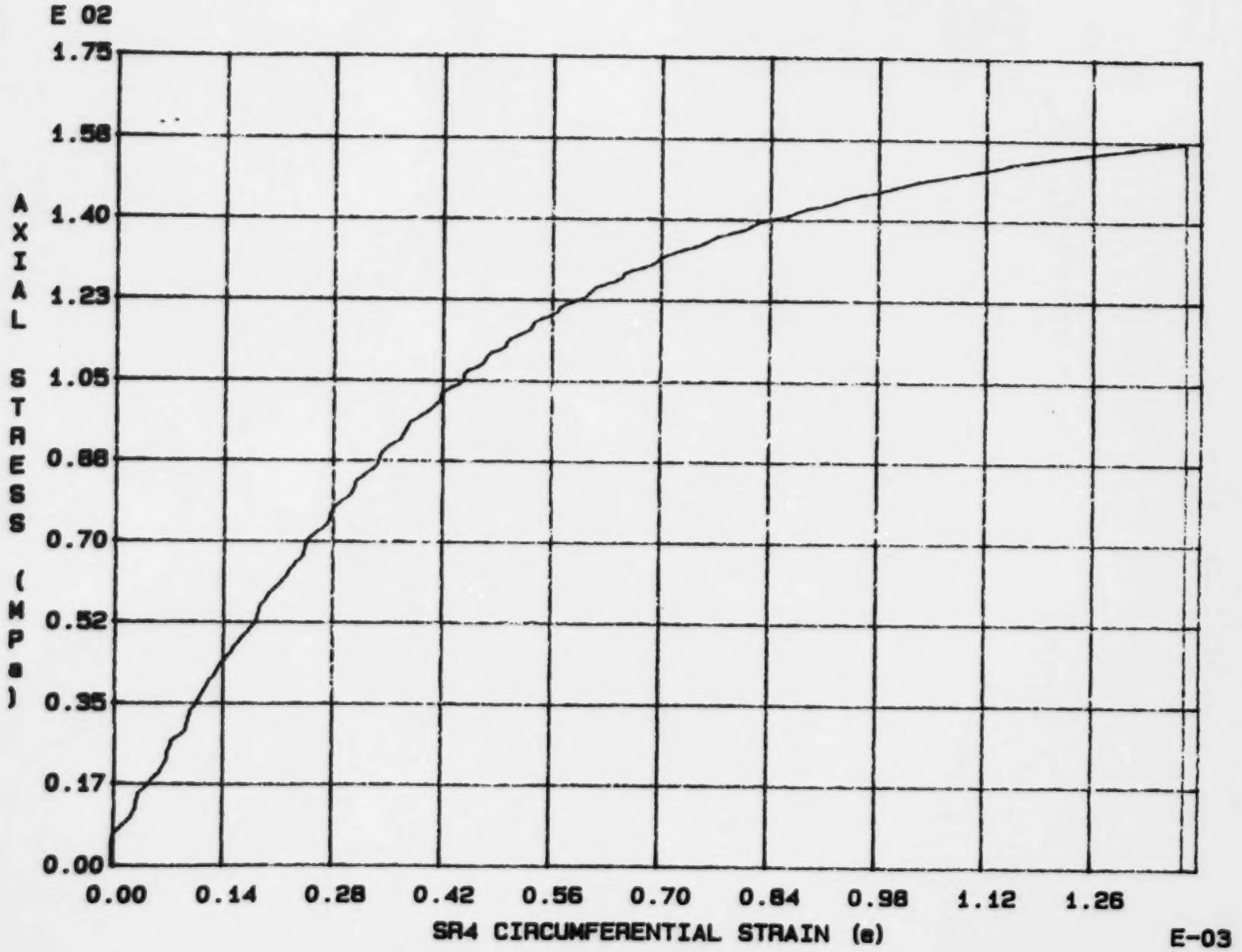

FIG. B-3 SPECIMEN 9015

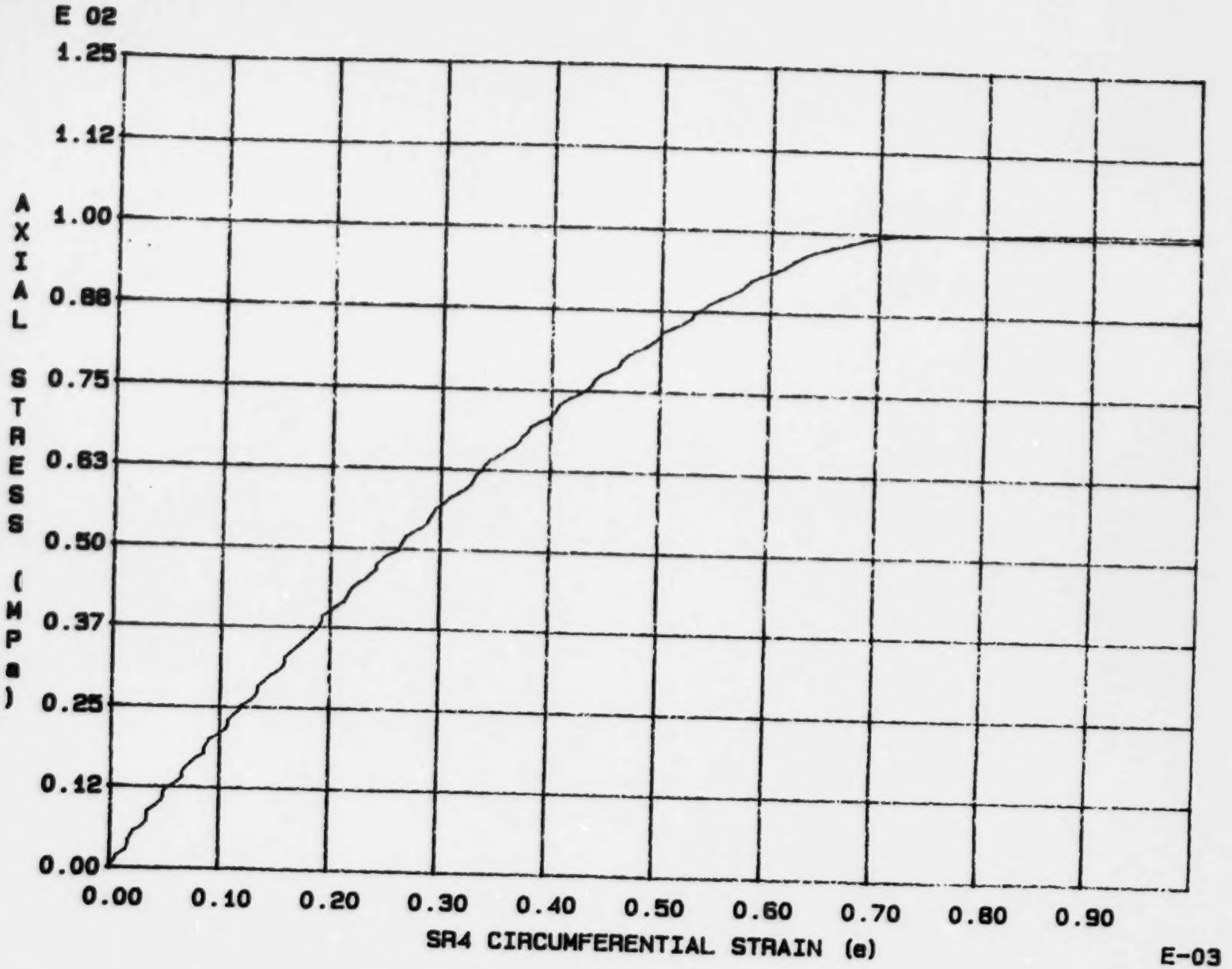

FIG. B-4 SPECIMEN 9021

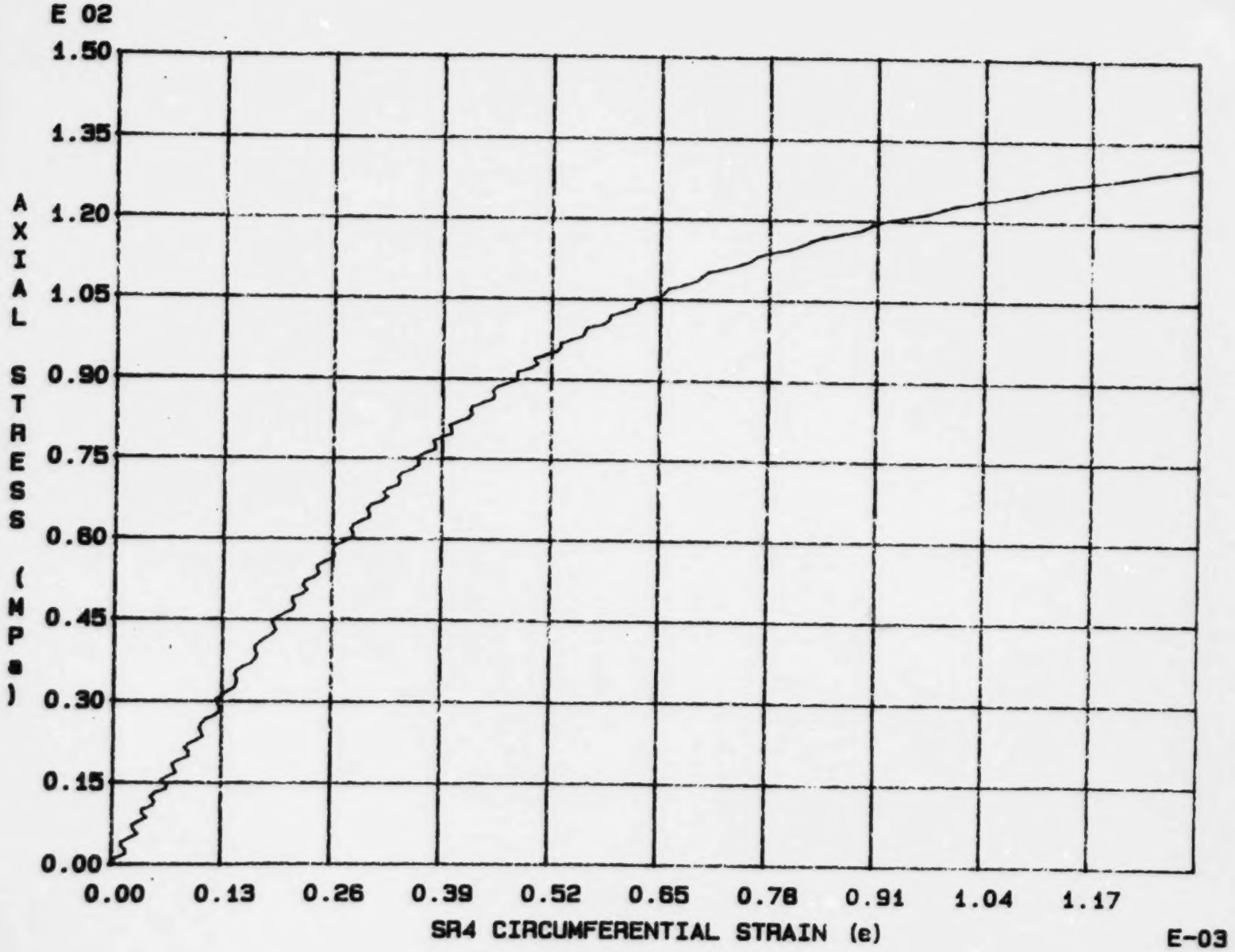

FIG. B-5 SPECIMEN 9023

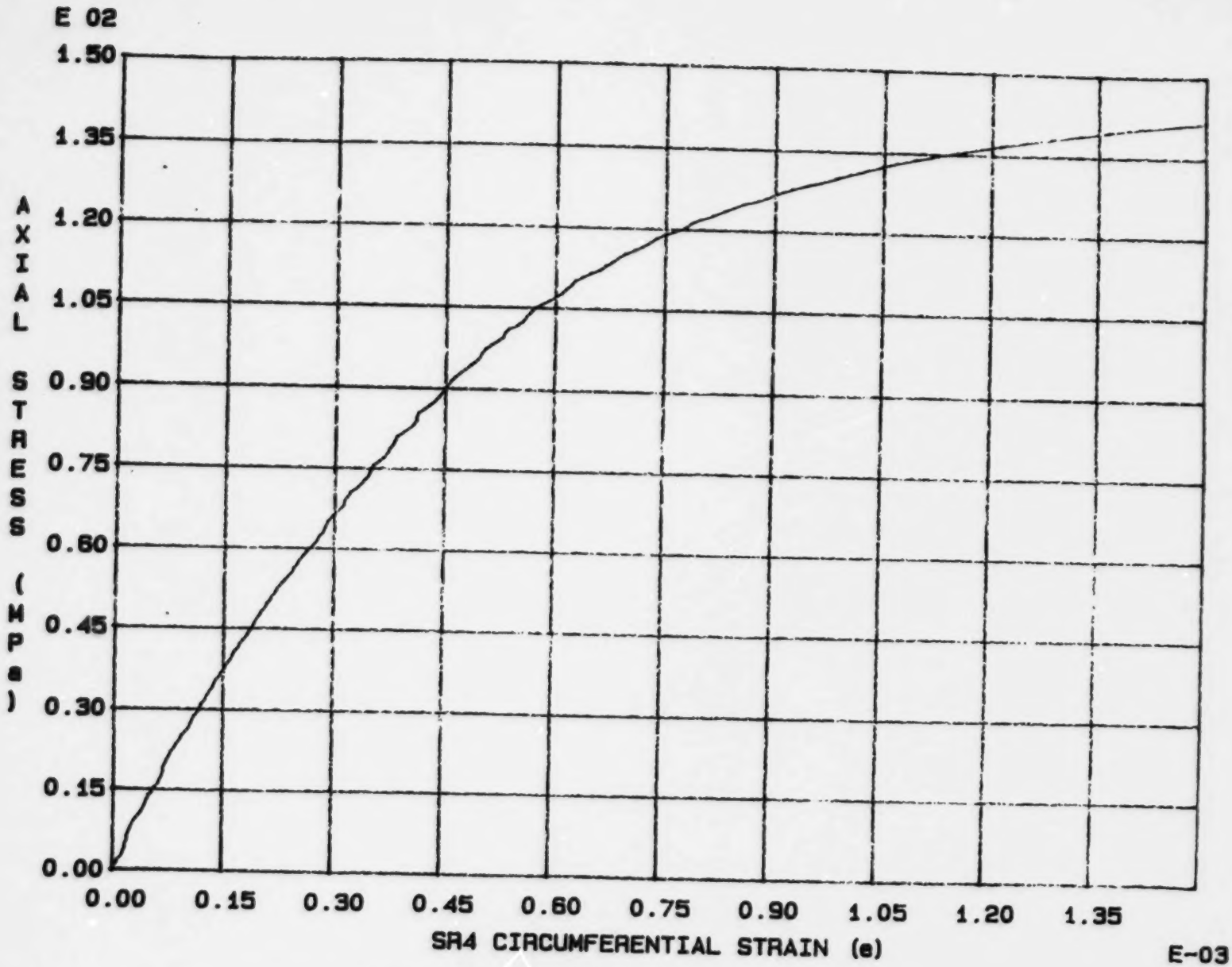

FIG. B-6 SPECIMEN 9031

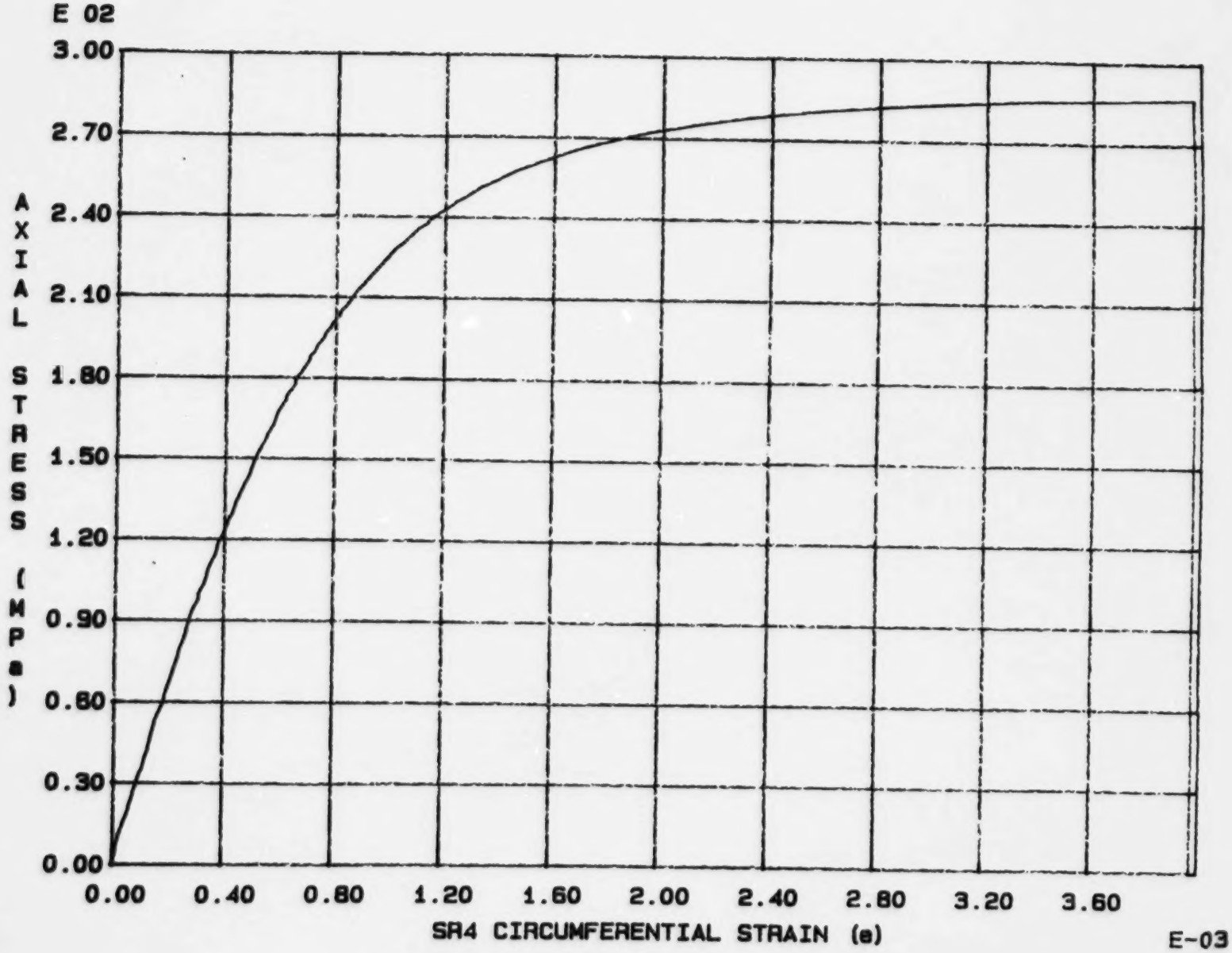

FIG. B-7 SPECIMEN 9033

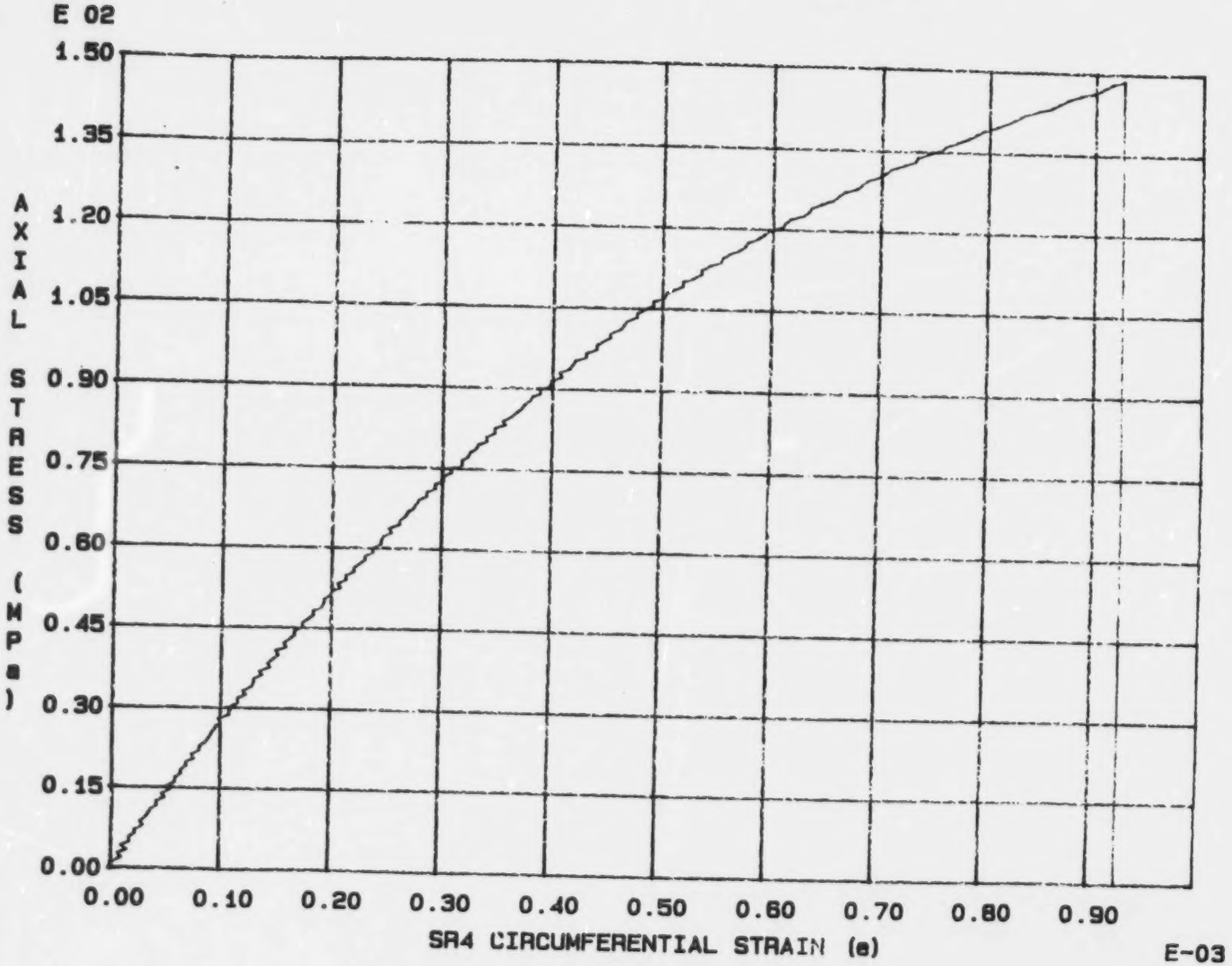

FIG. B-8 SPECIMEN 9035

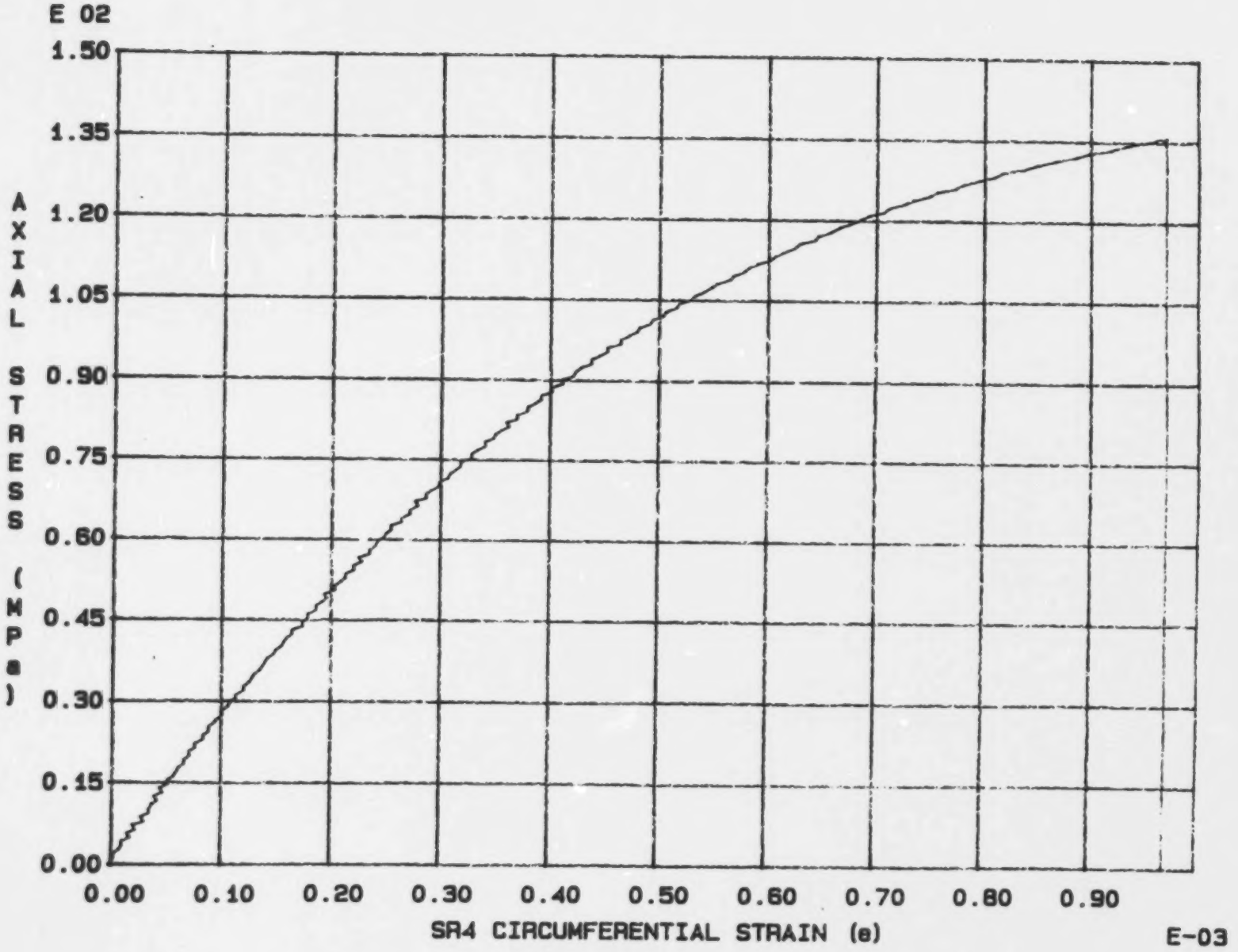

FIG. B-9 SPECIMEN 9511

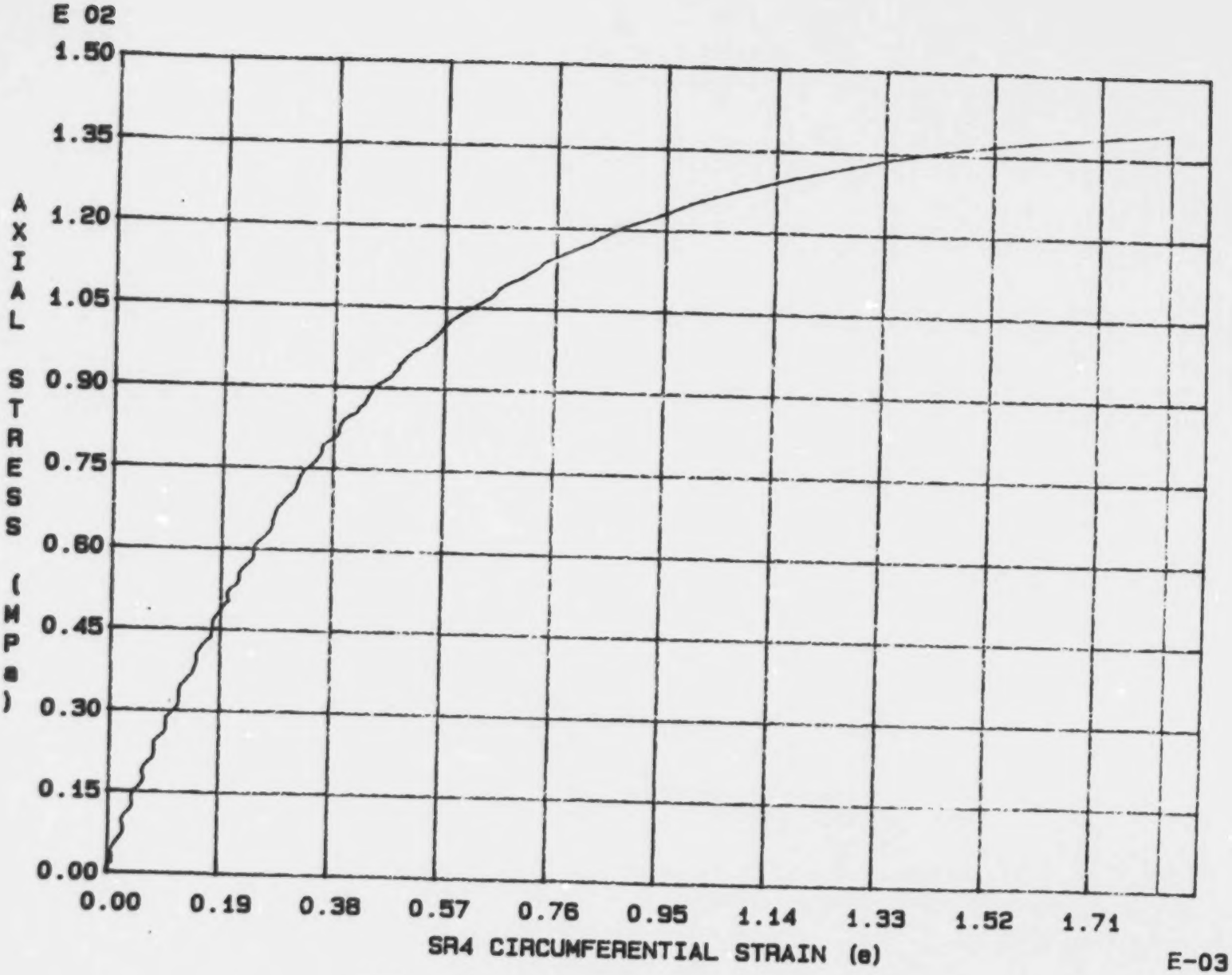

FIG. B-10 SPECIMEN 9513

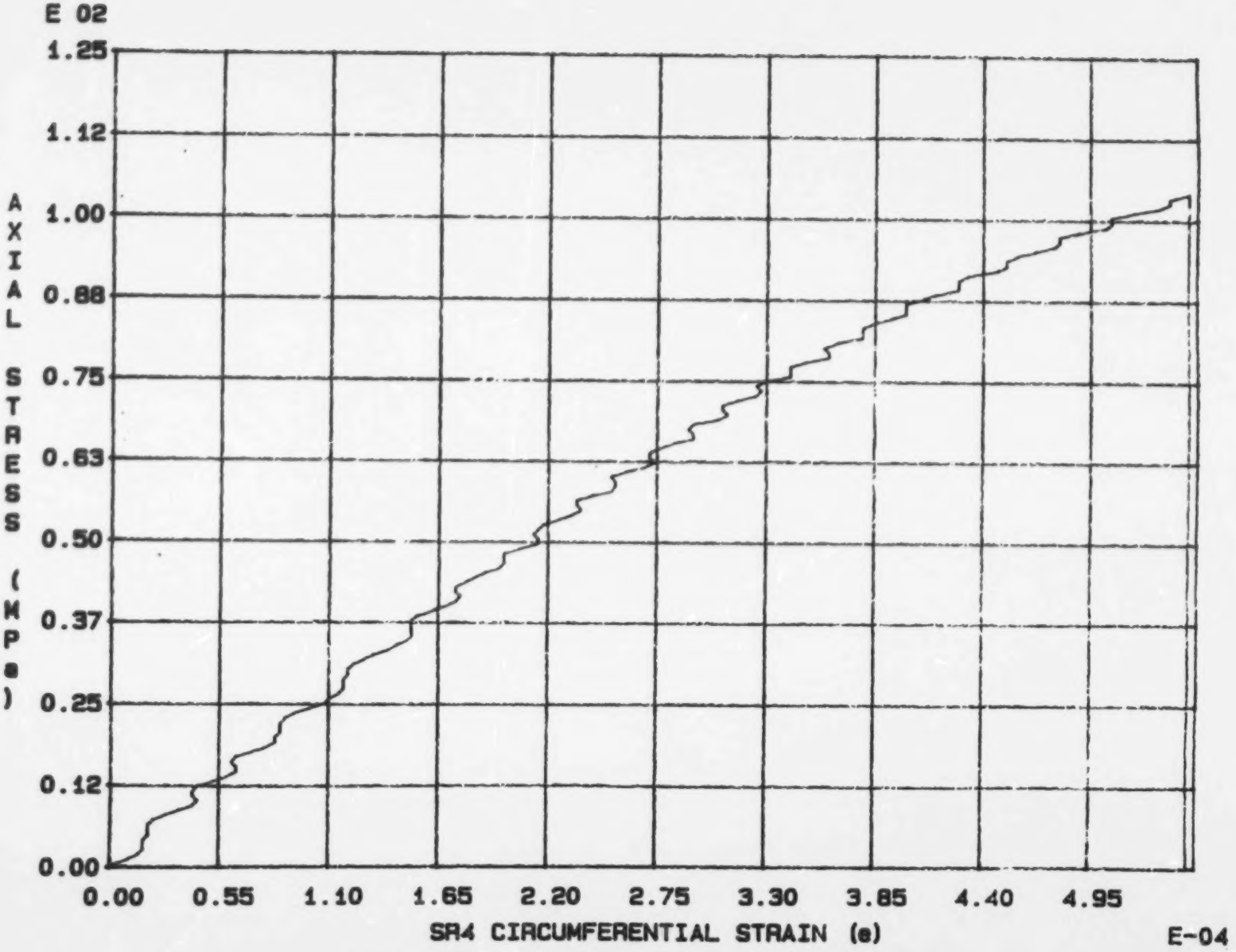

FIG. B-11 SPECIMEN 9521

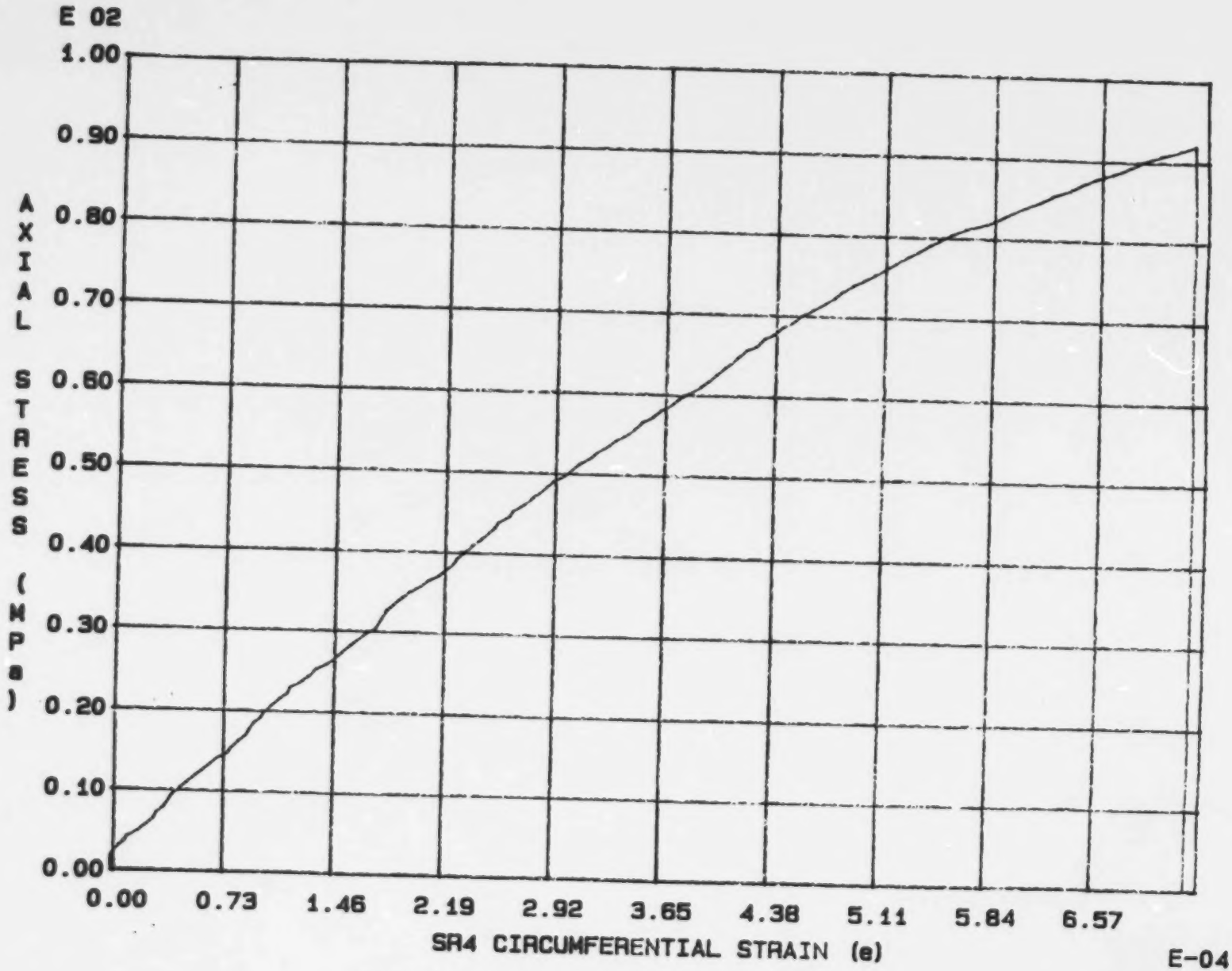

FIG. B-12 SPECIMEN 9523

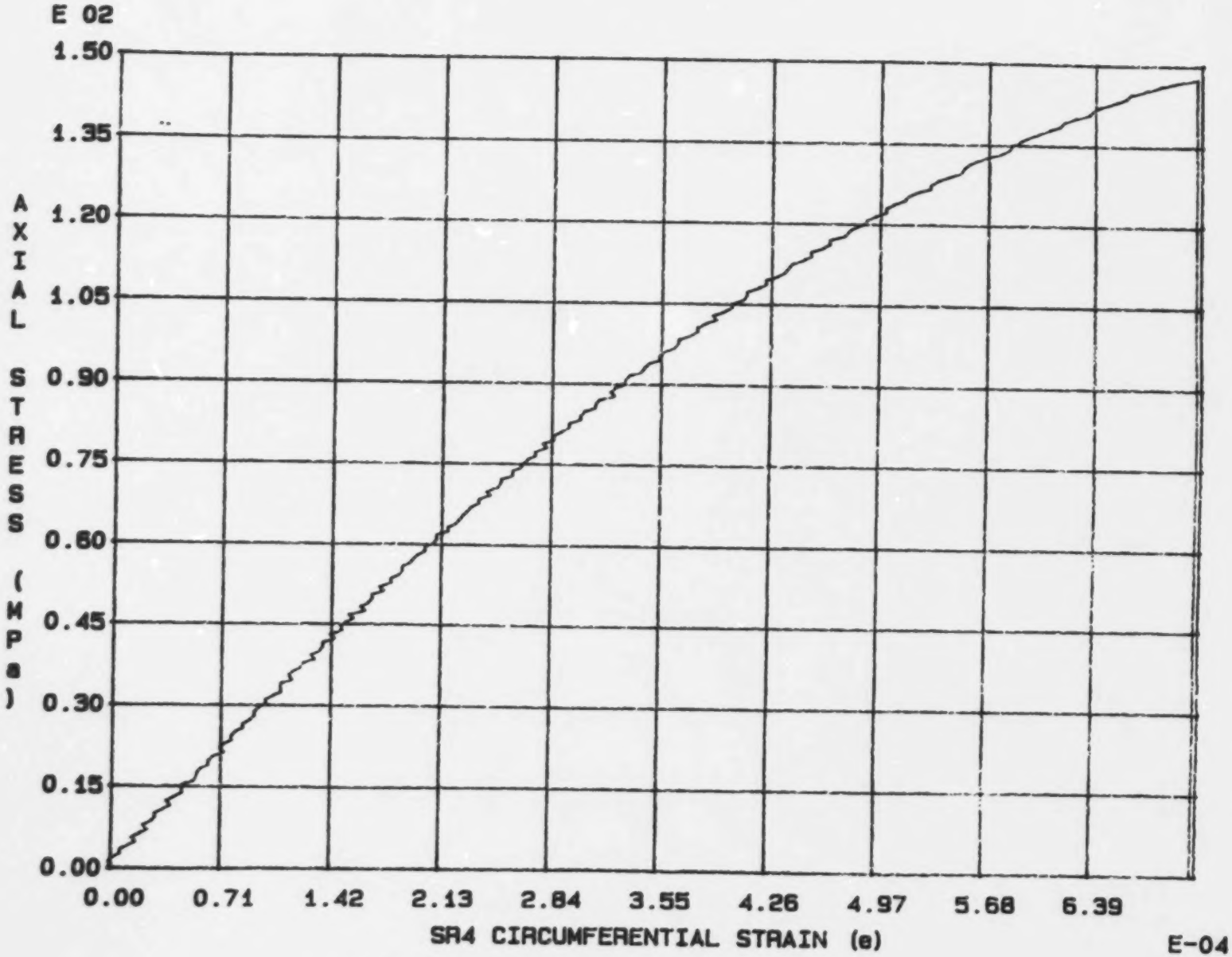

FIG. B-13 SPECIMEN 9531

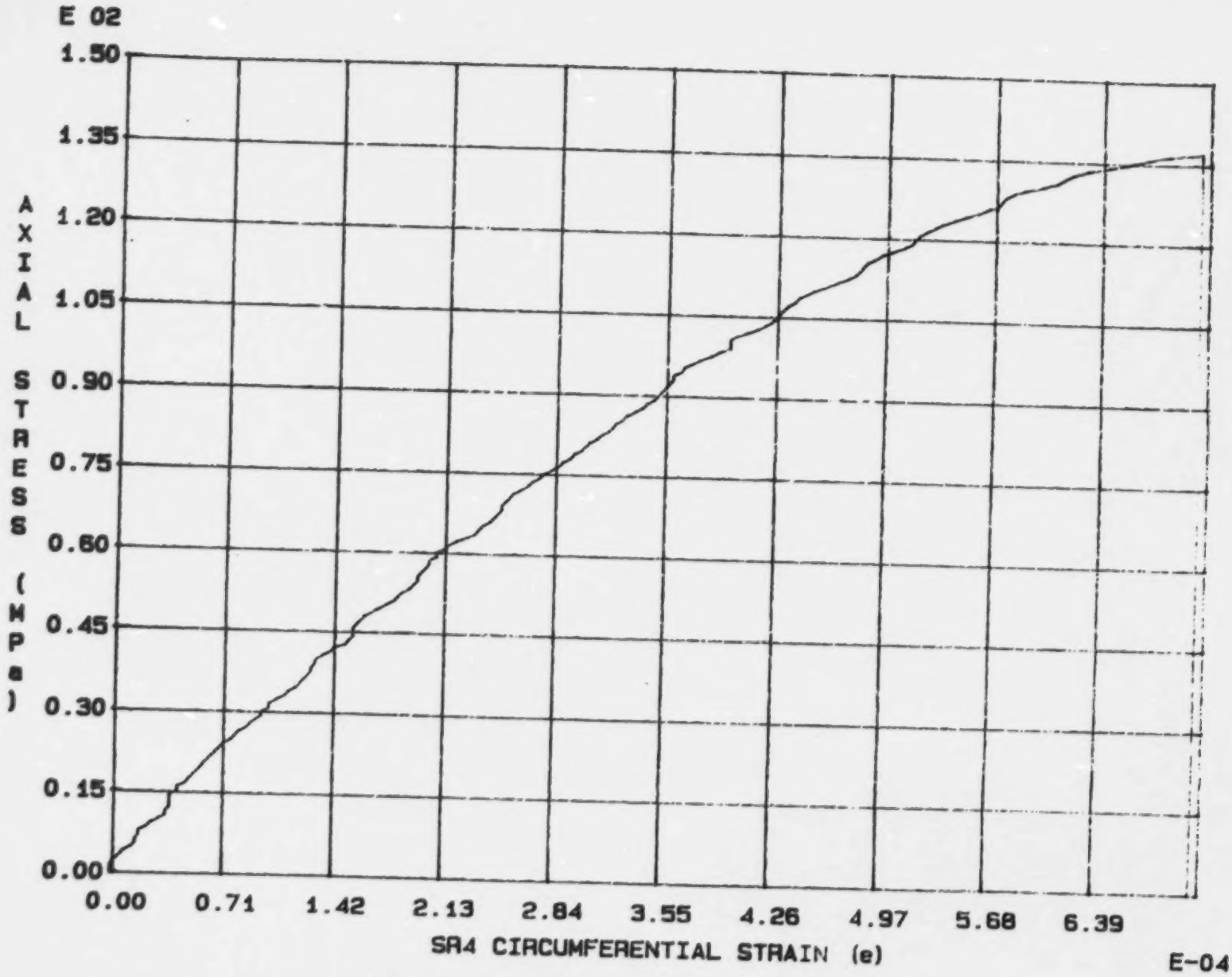

FIG. B-14 SPECIMEN 9533

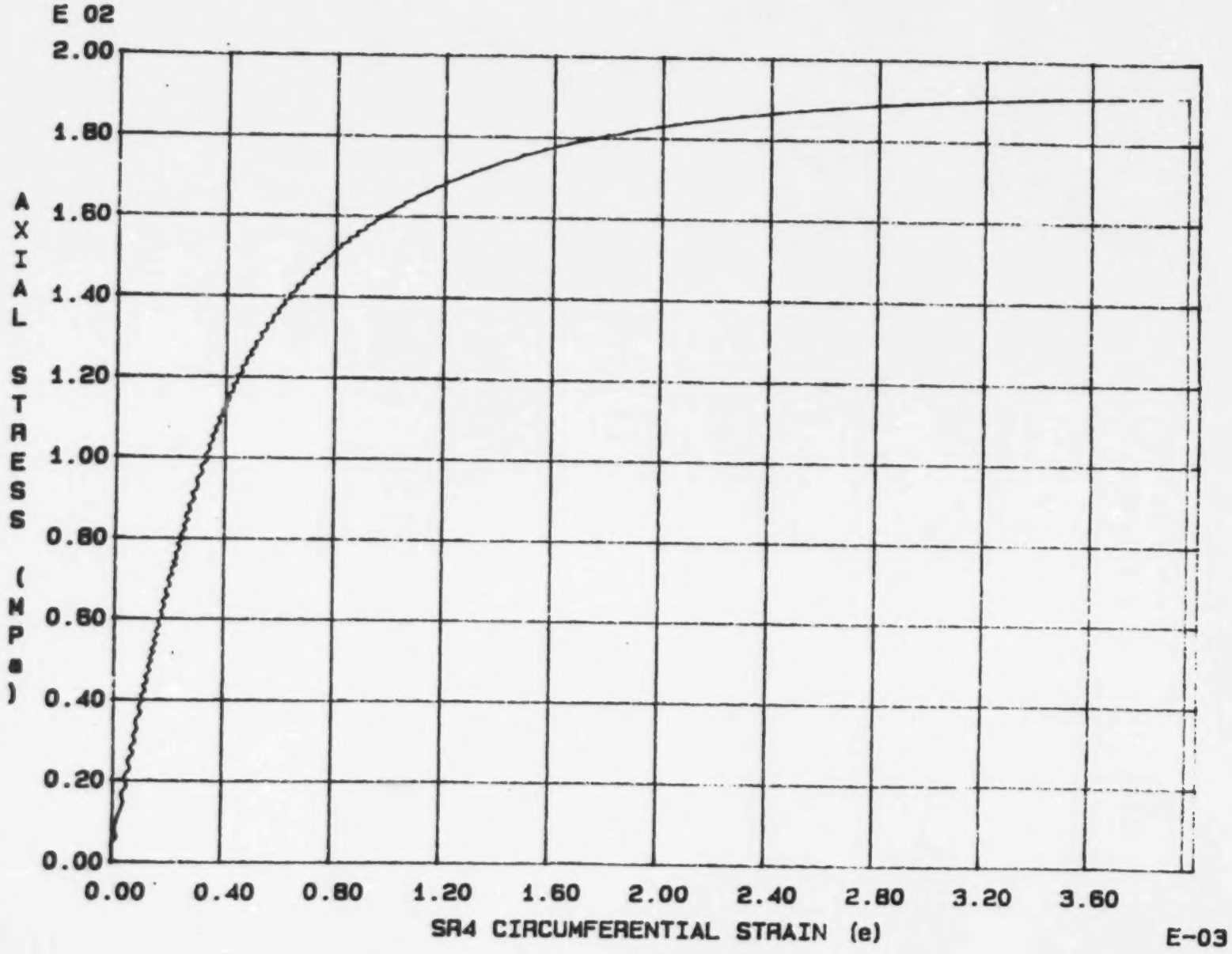

FIG. B-15 SPECIMEN 9535

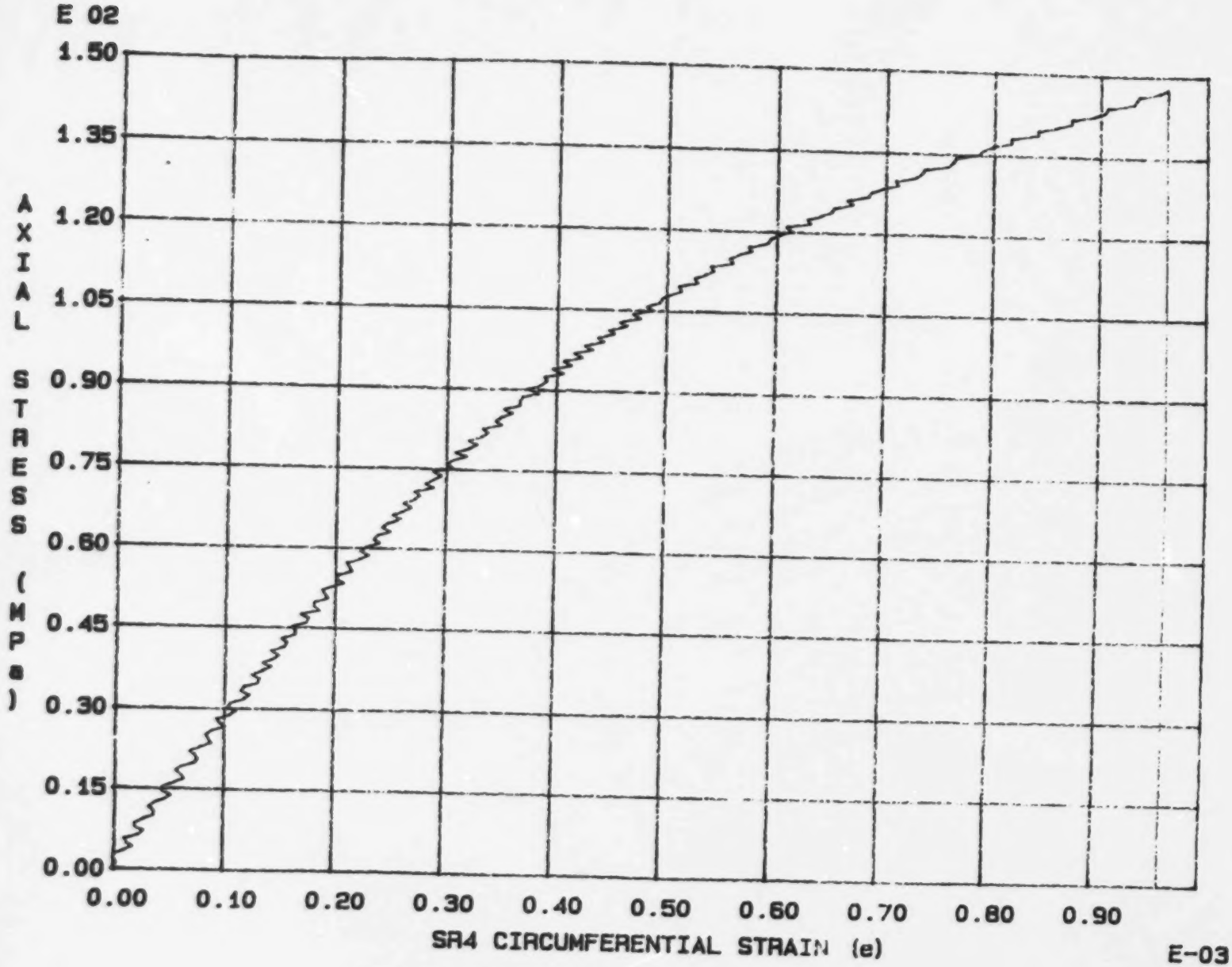

FIG. B-16 SPECIMEN 4011

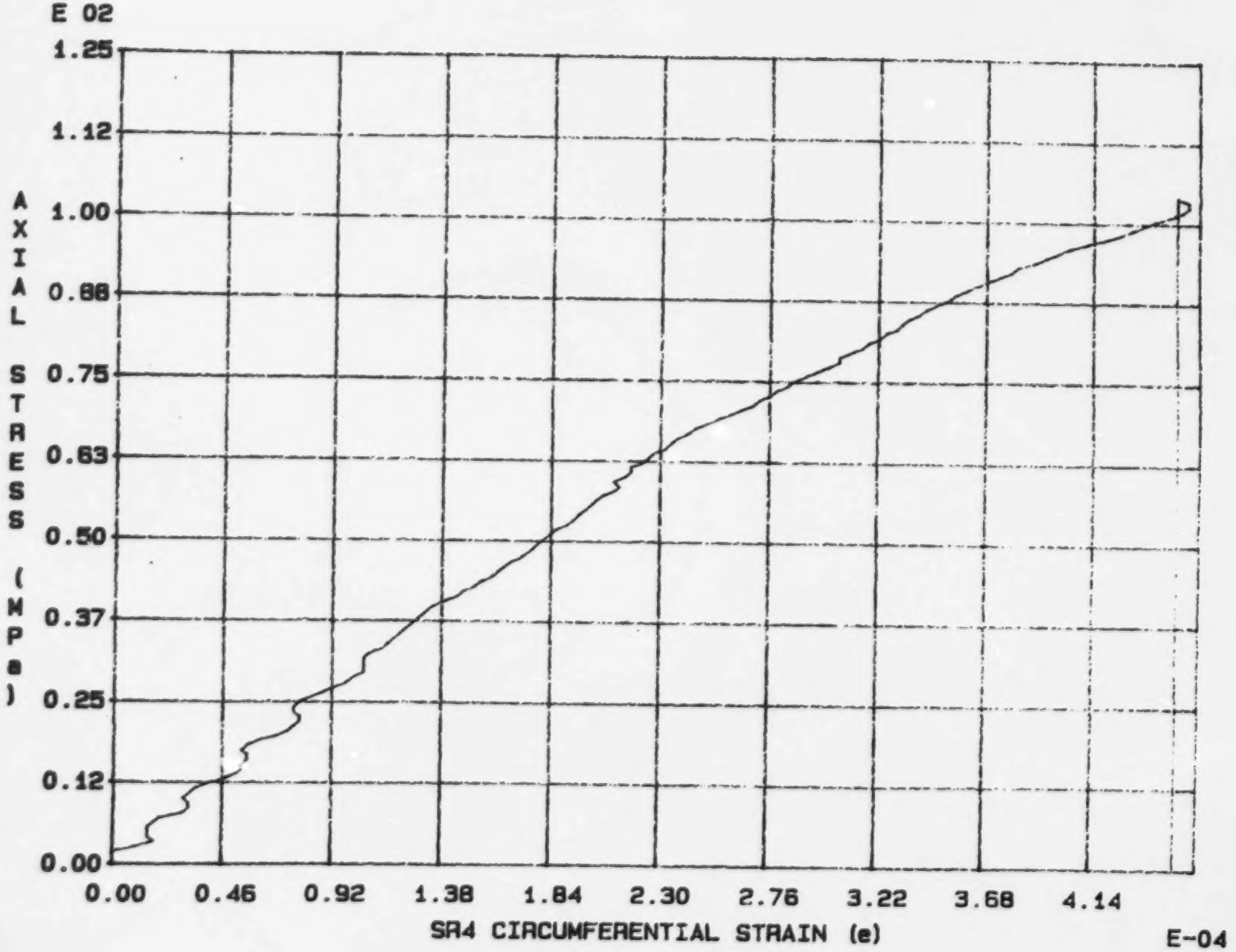

FIG. B-17 SPECIMEN 4013

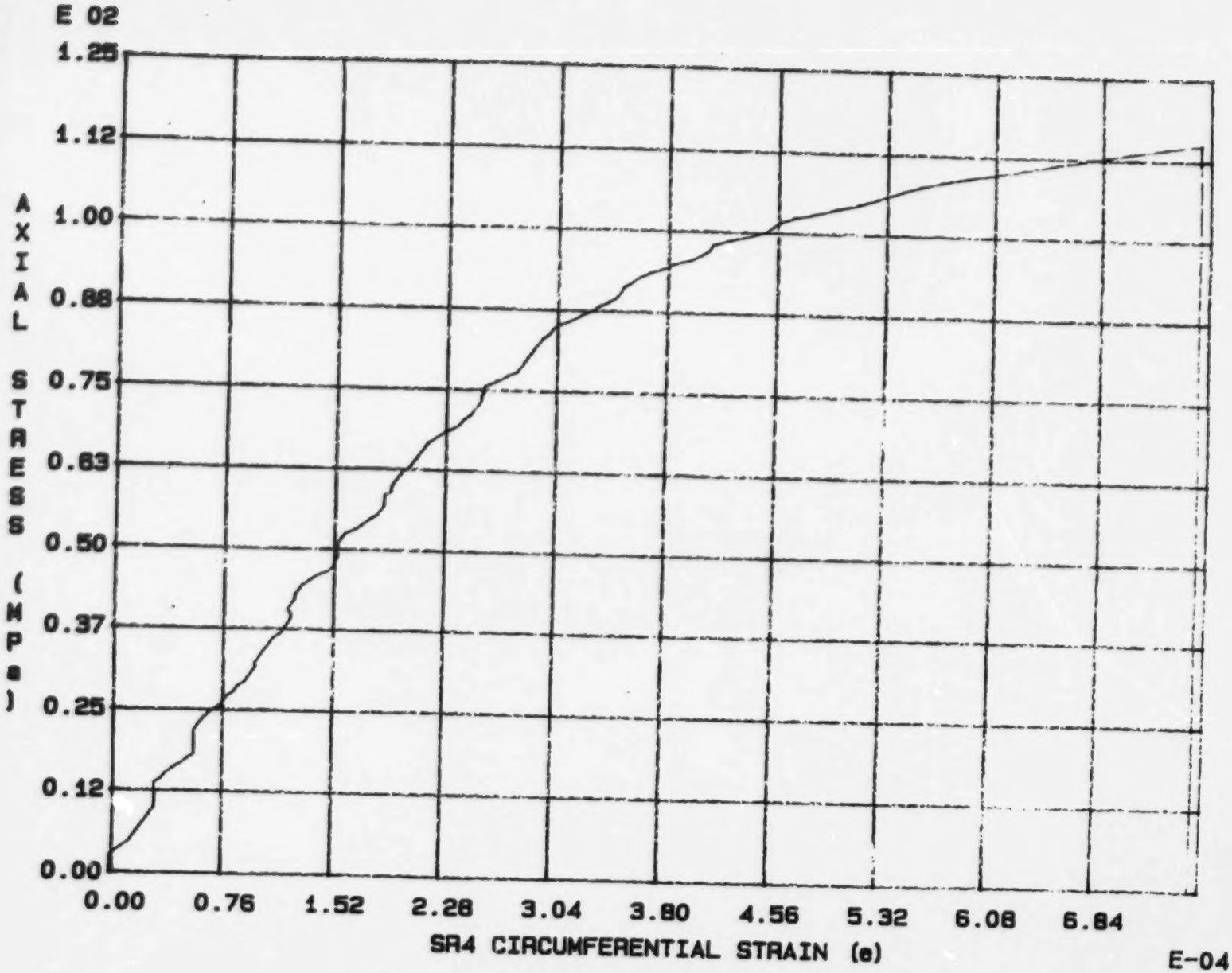

FIG. B-18 SPECIMEN 4015

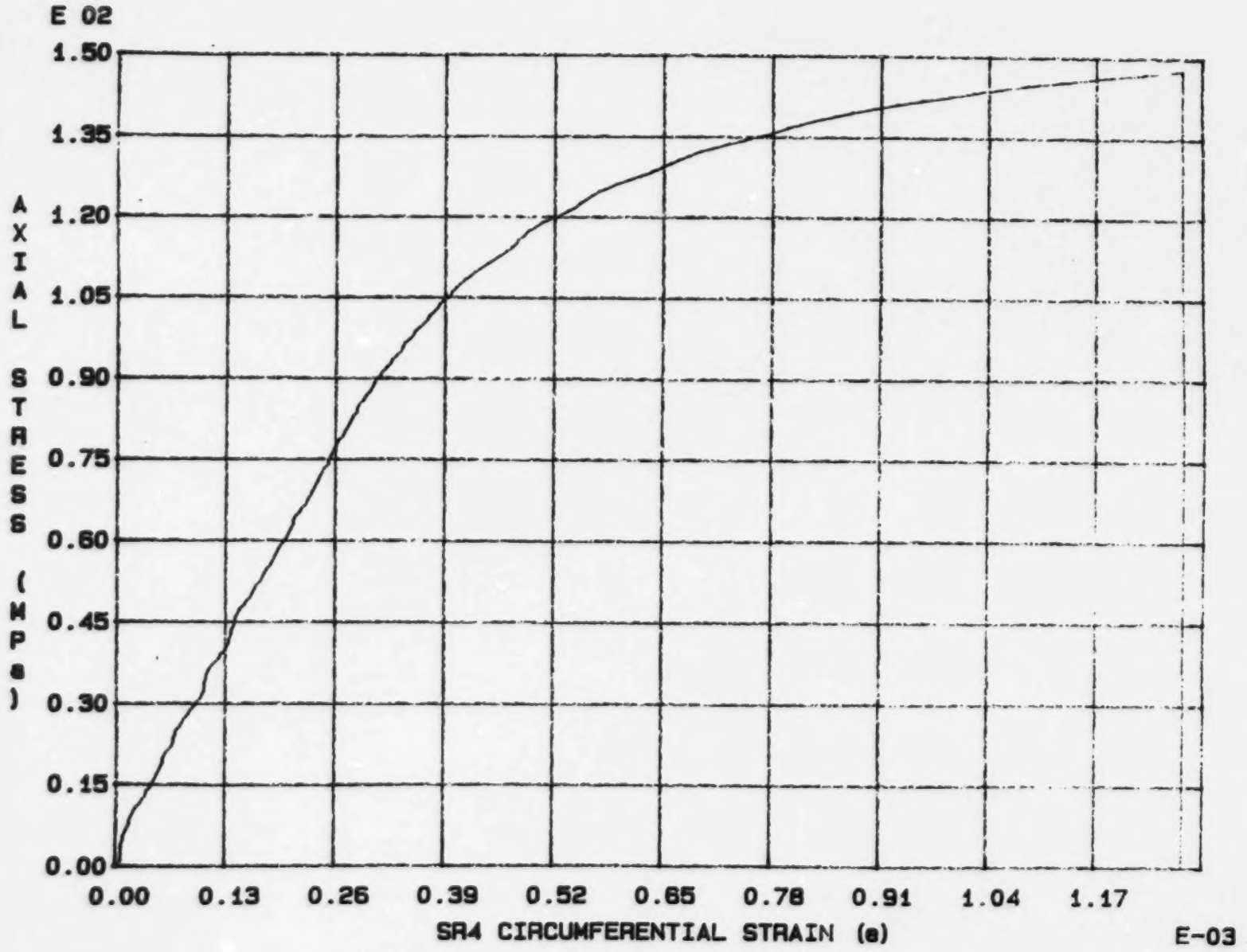

FIG. B-19 SPECIMEN 4017

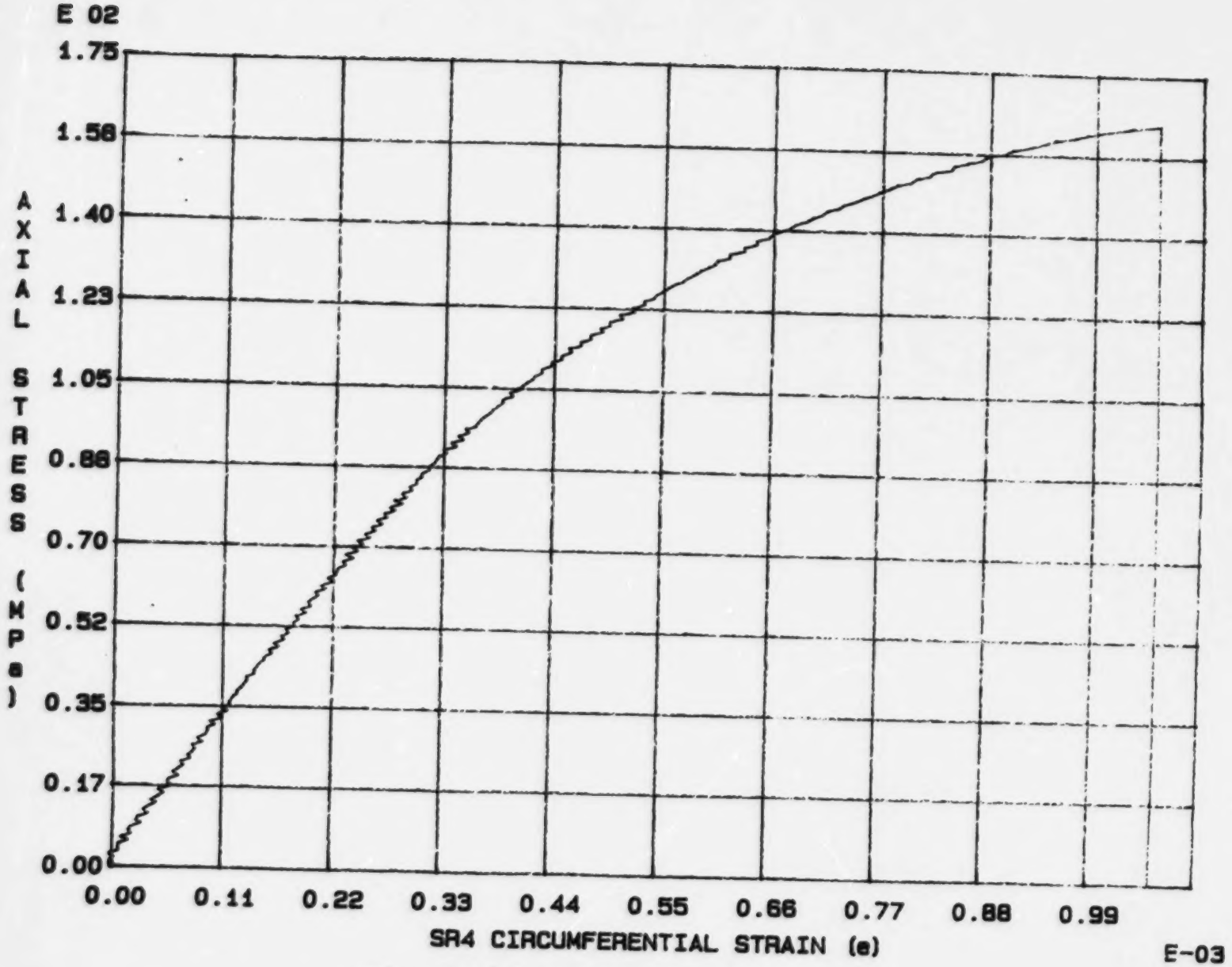

FIG. B-20 SPECIMEN 4021

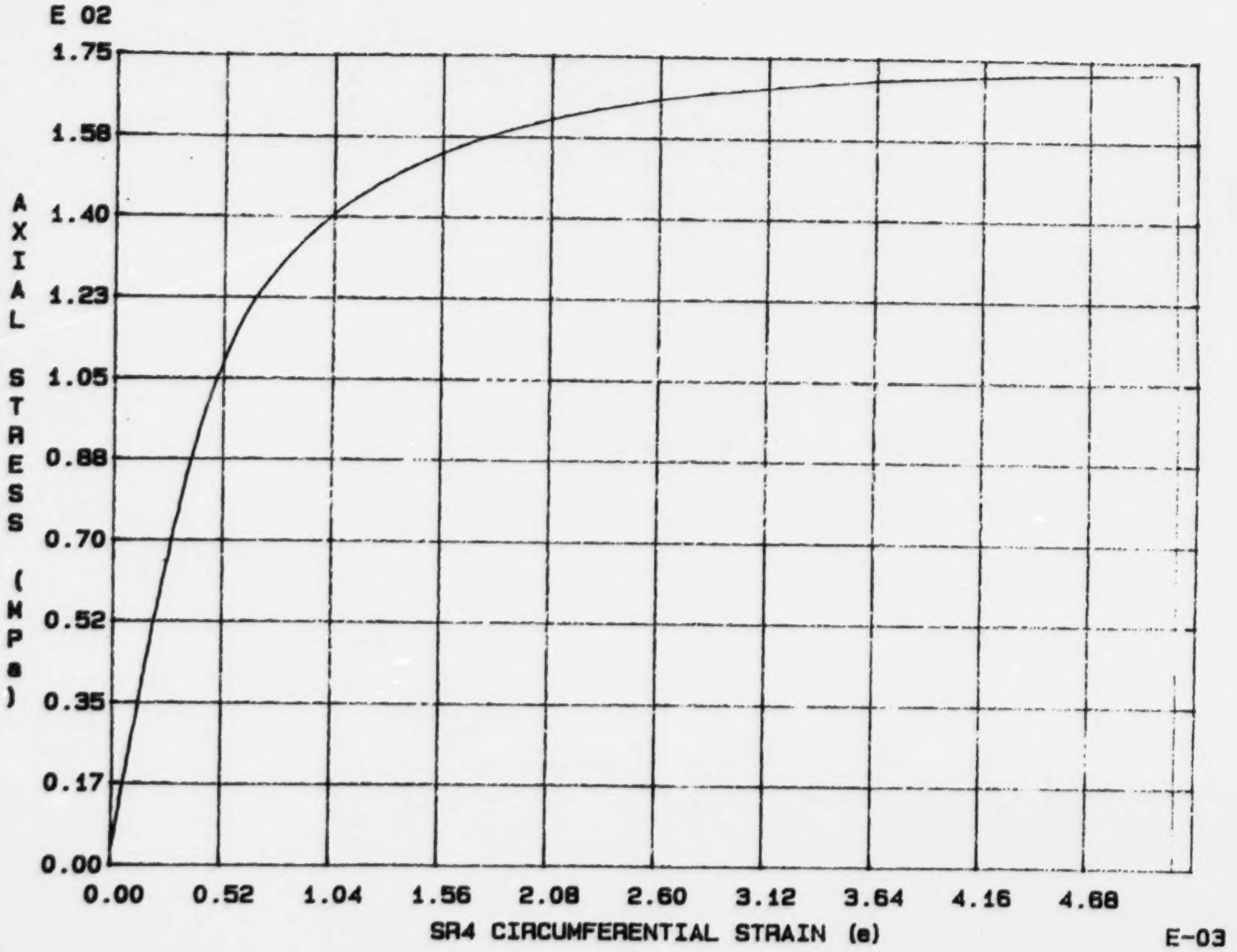

FIG. B-21 SPECIMEN 4023

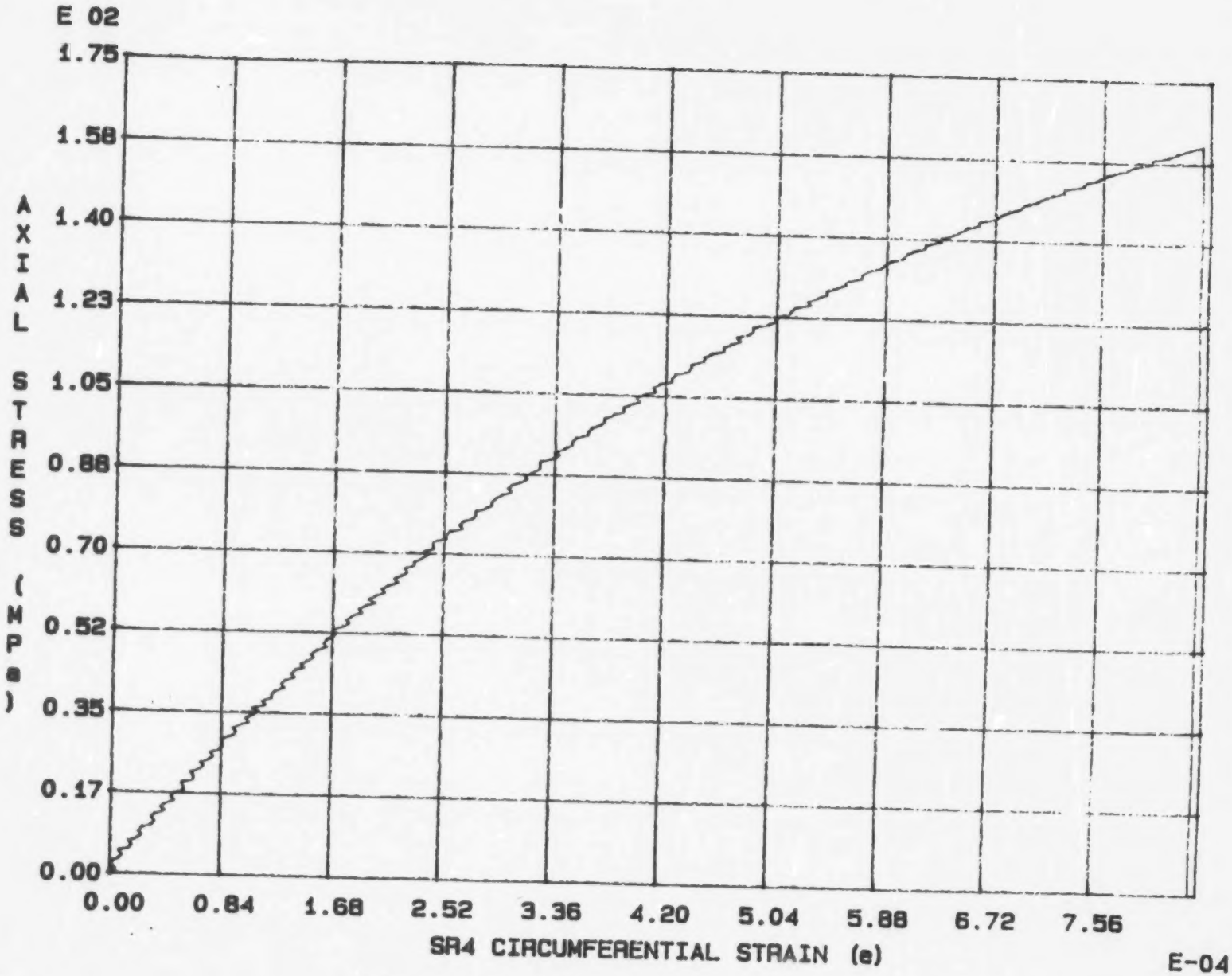

FIG. B-22 SPECIMEN 4031

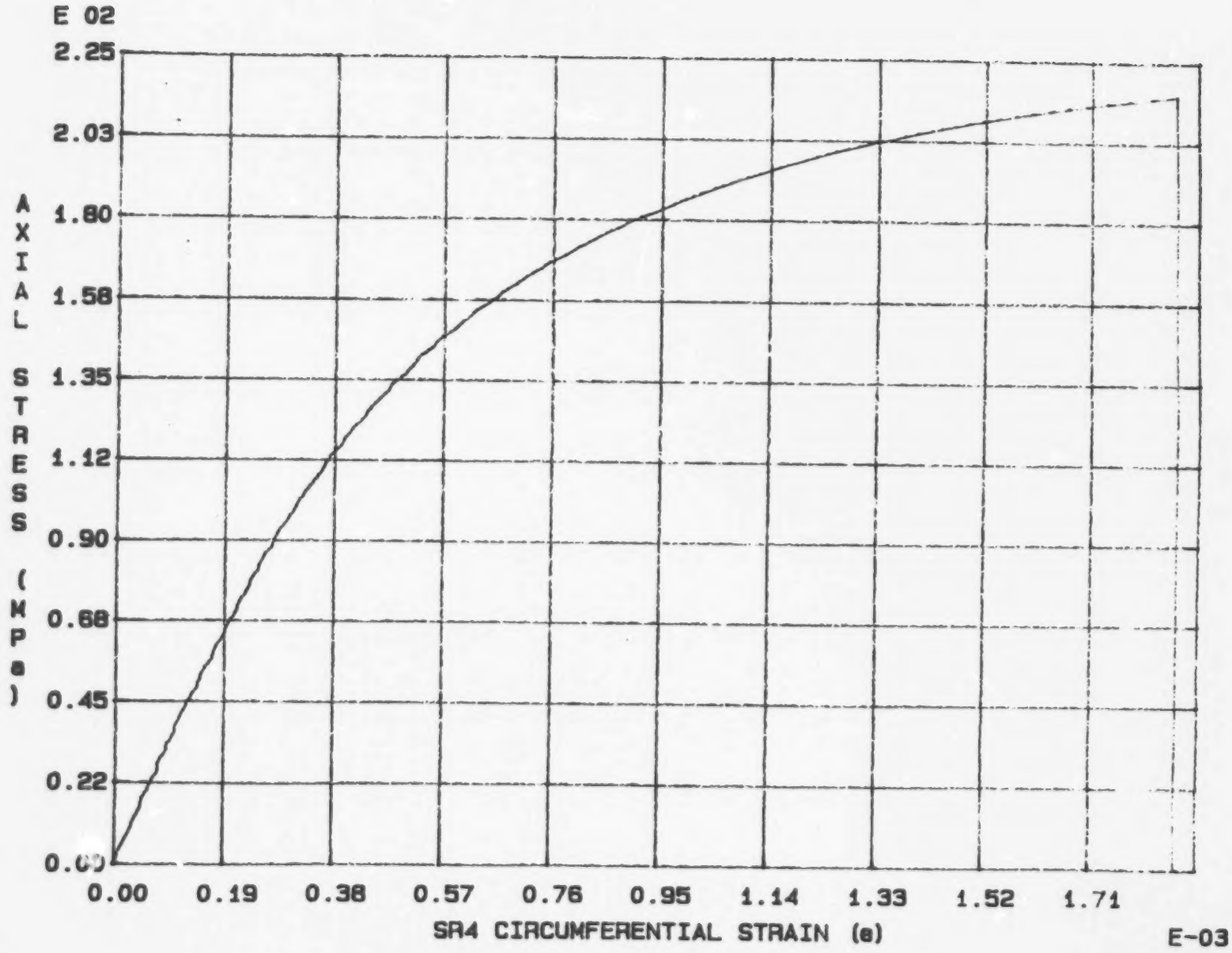

FIG. B-23 SPECIMEN 4033

APPENDIX C

AXIAL STRESS-STRAIN CURVES OF MULTI-STAGE TESTS

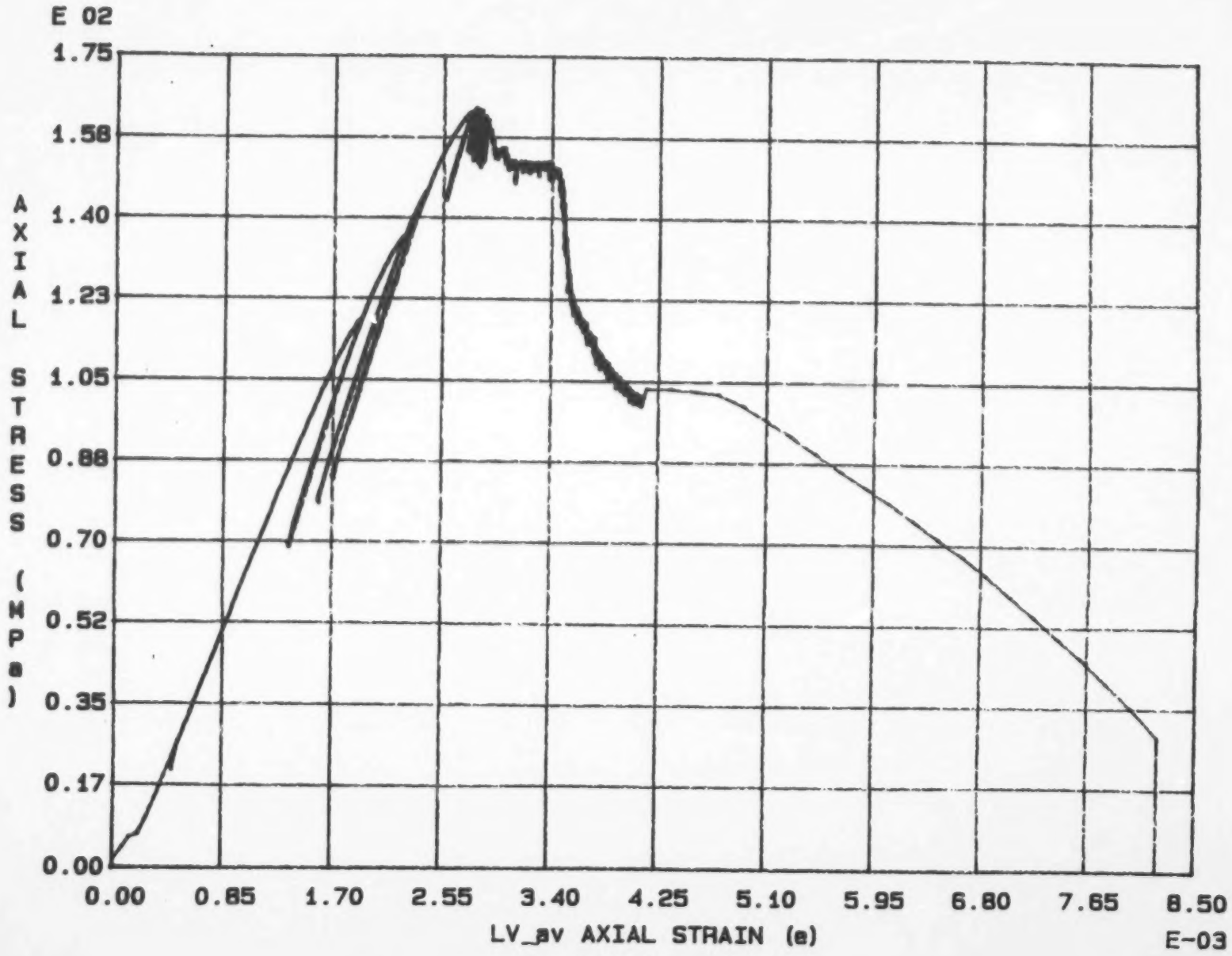

FIG. C-1 SPECIMEN 9012

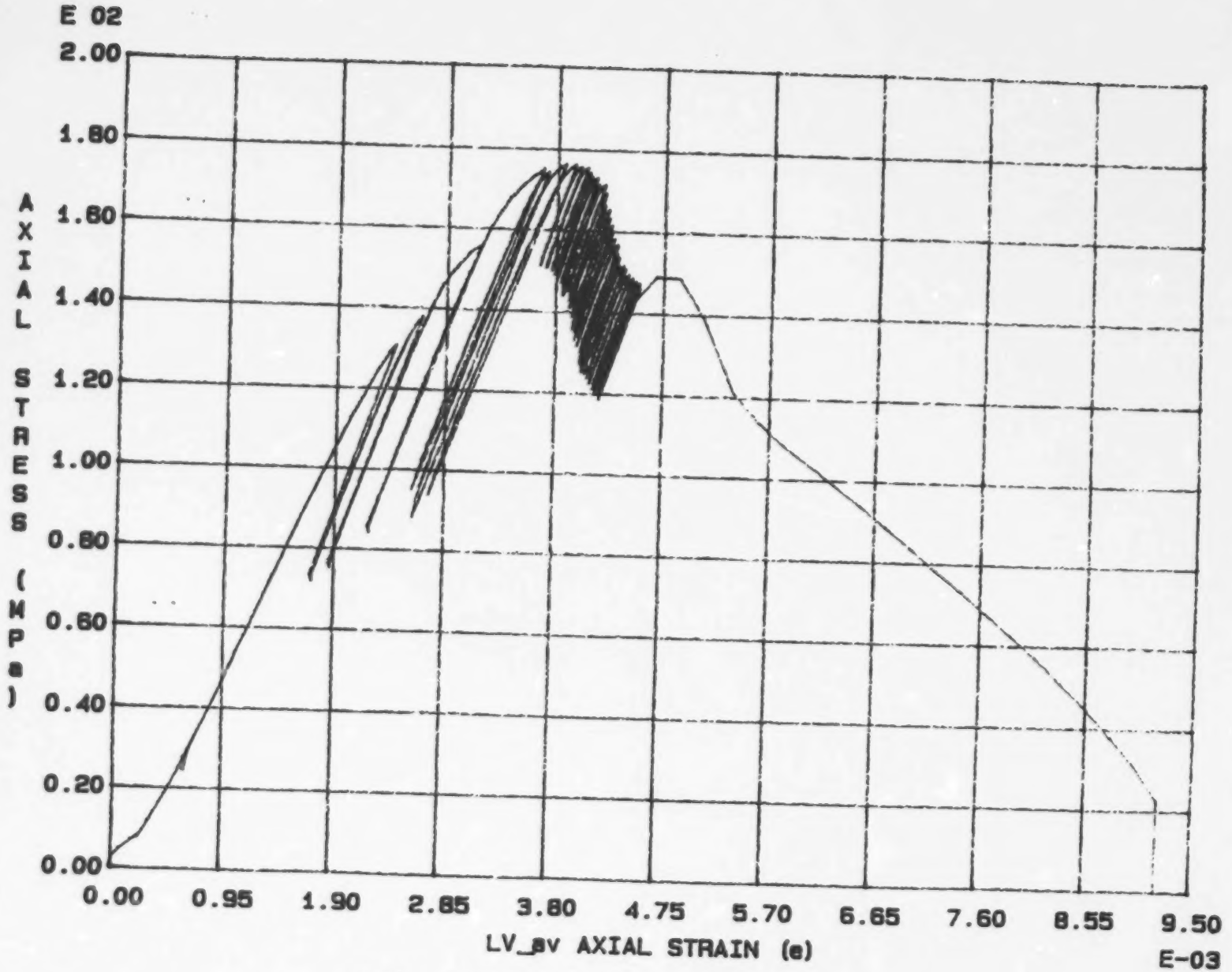

FIG. C-2 SPECIMEN 9014

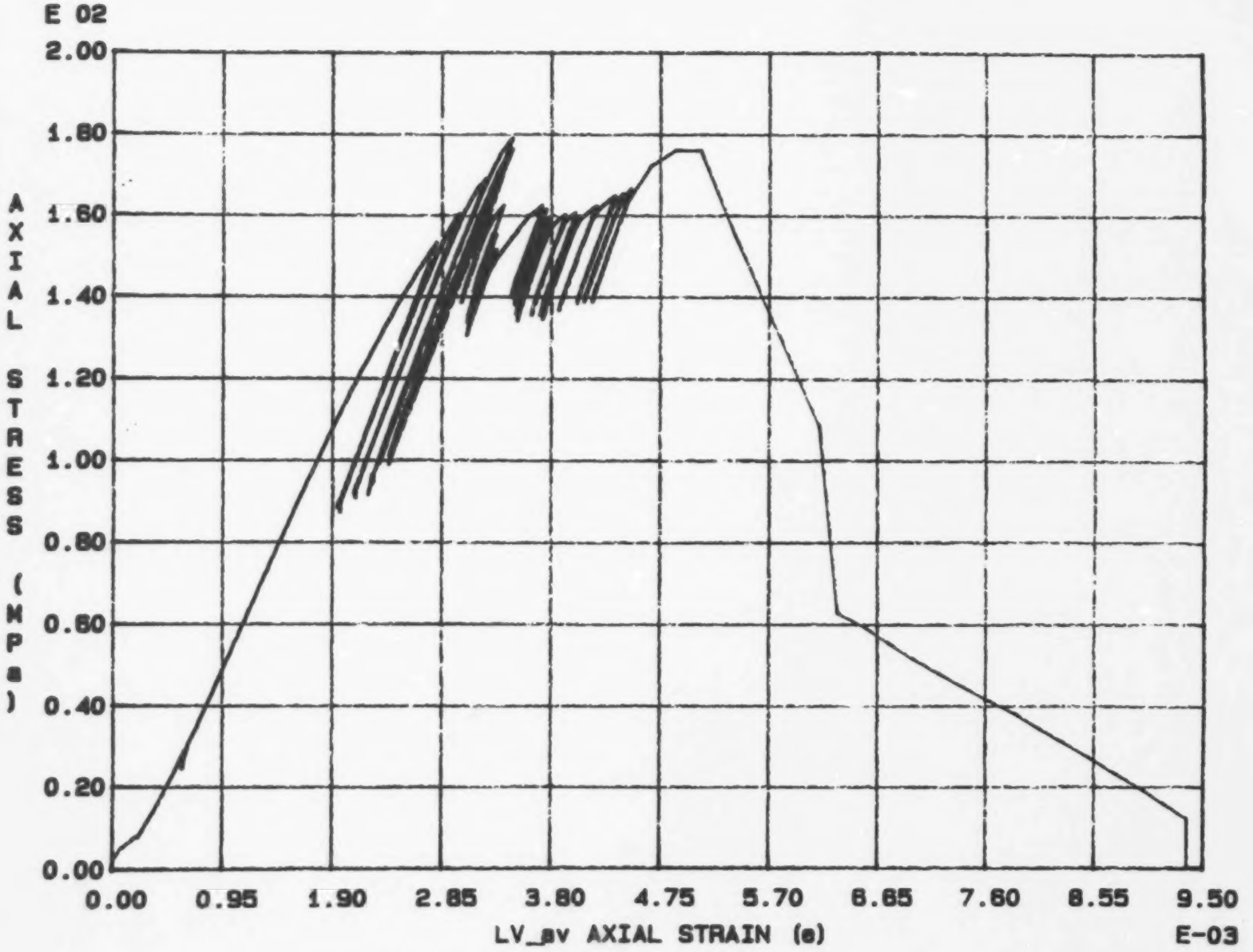

FIG. C-3 SPECIMEN 9016

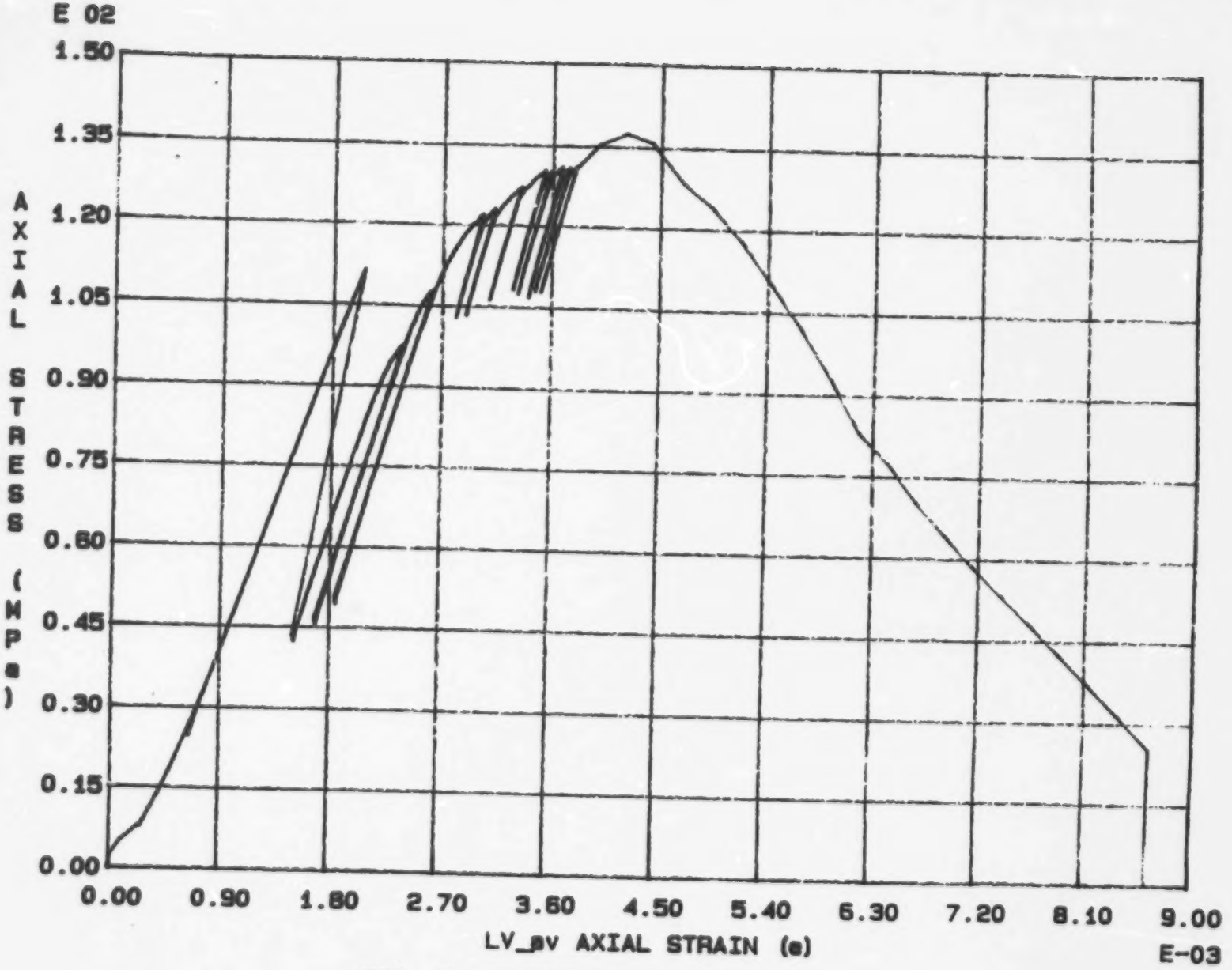

FIG. C-4 SPECIMEN 9022

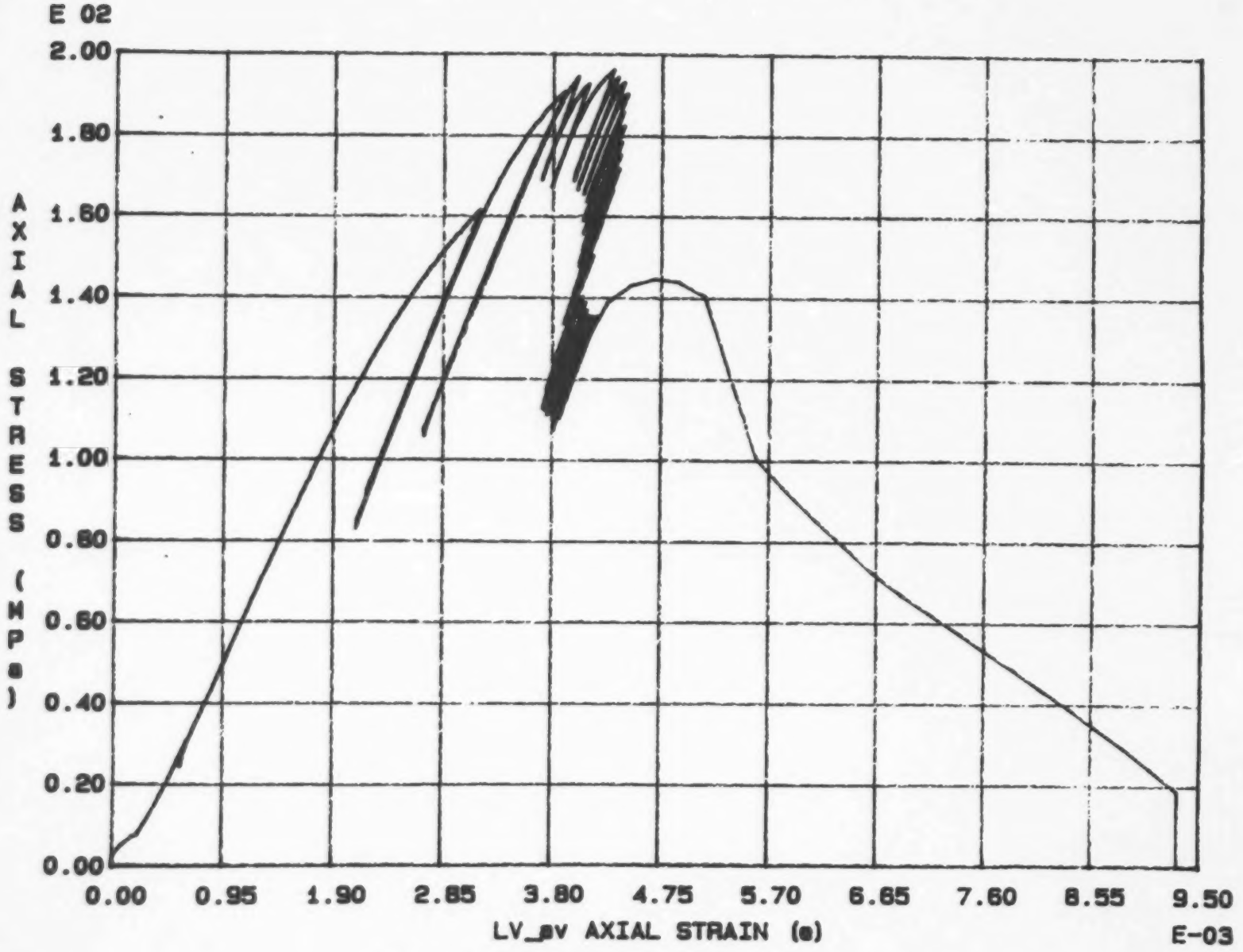

FIG. C-5 SPECIMEN 9024

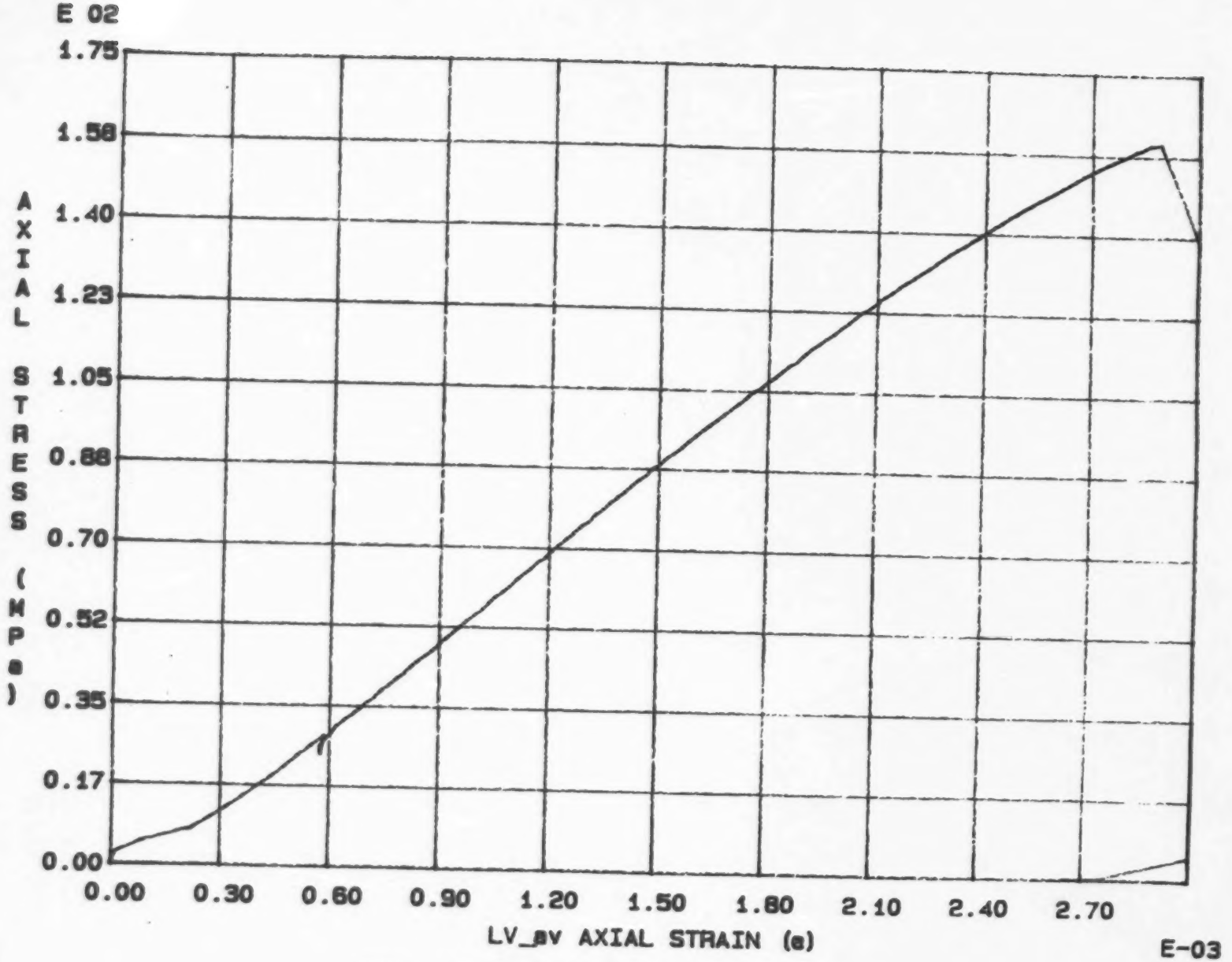

FIG. C-6 SPECIMEN 9032

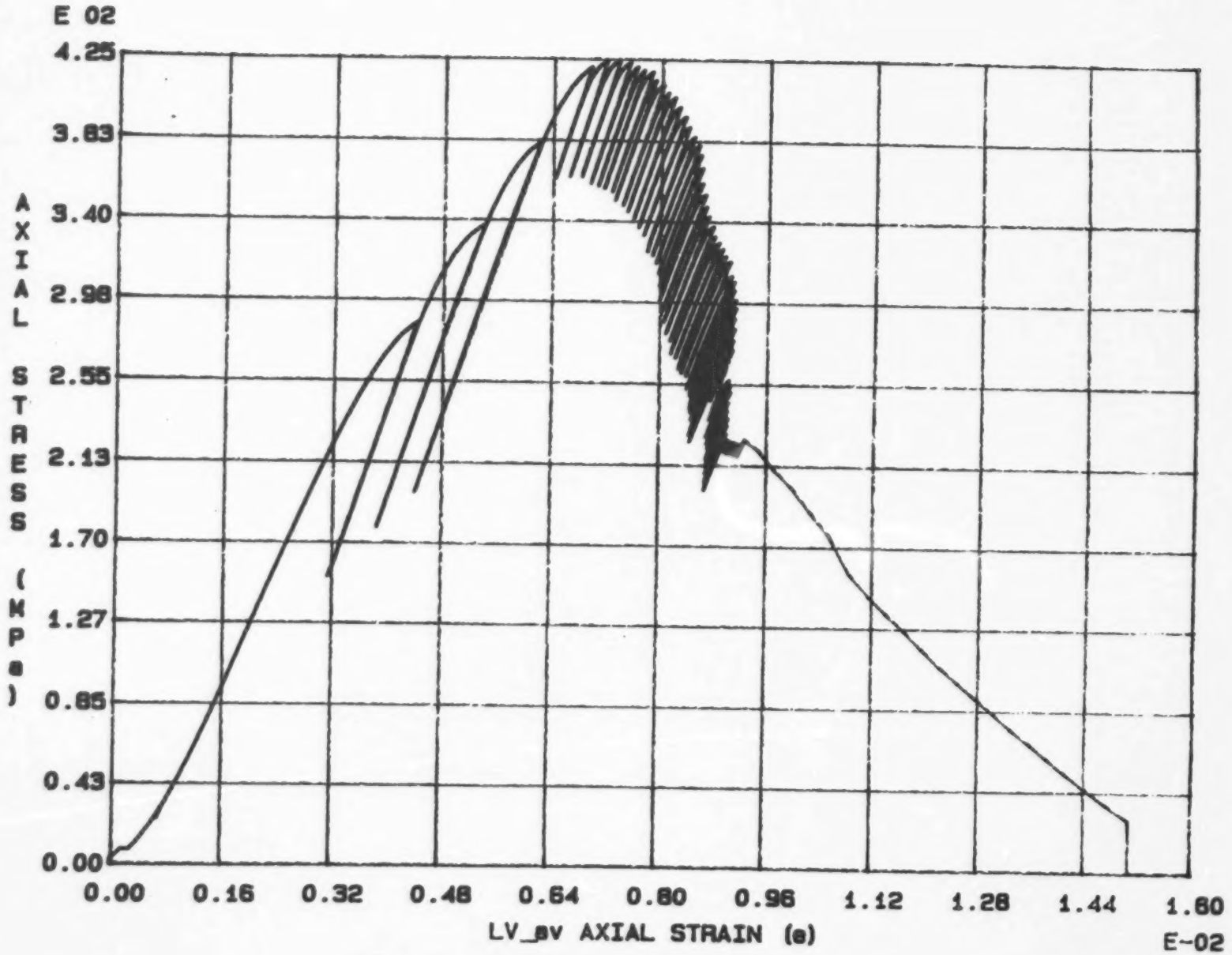

FIG. C-7 SPECIMEN 9034

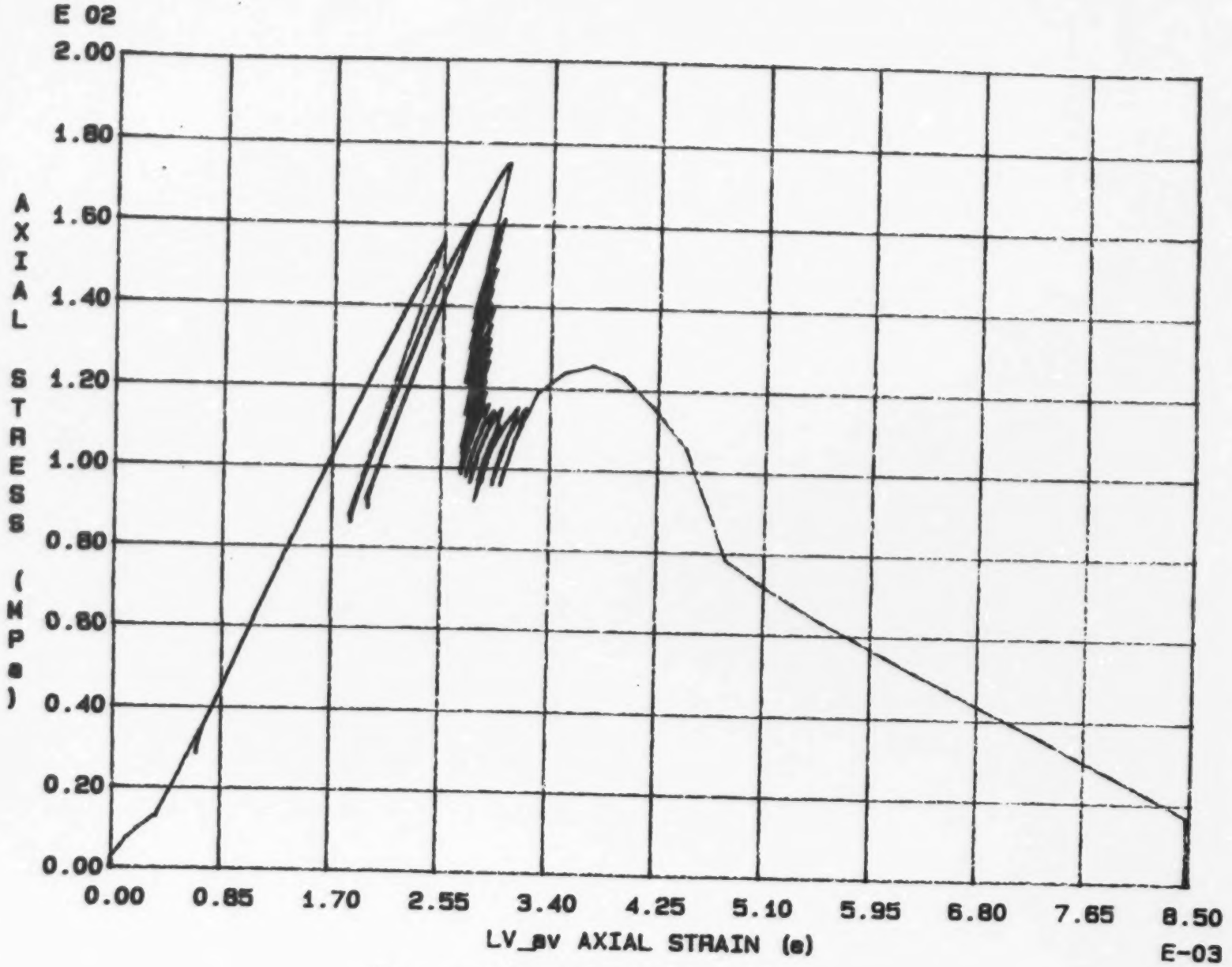

FIG. C-8 SPECIMEN 9036

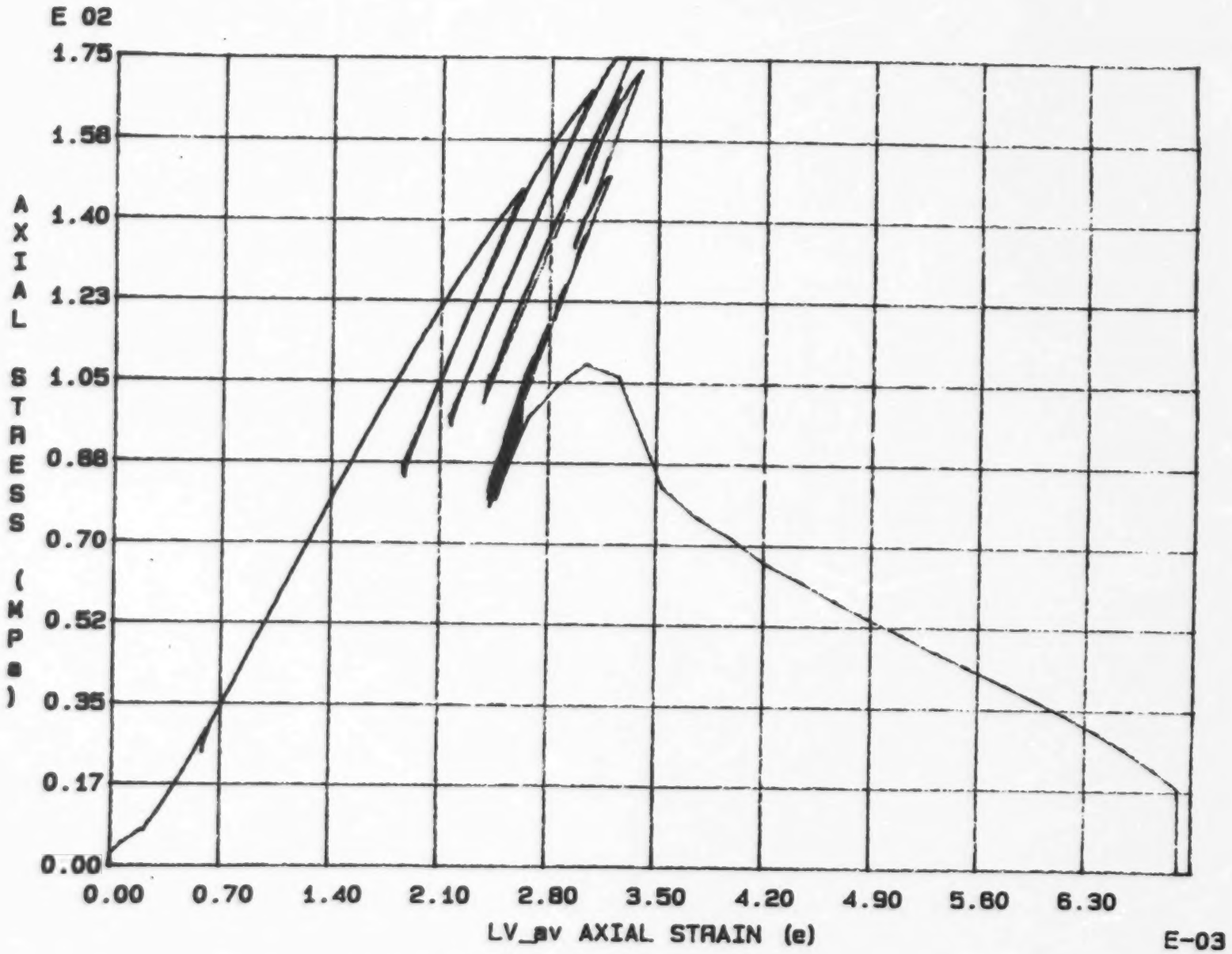

FIG. C-9 SPECIMEN 9512

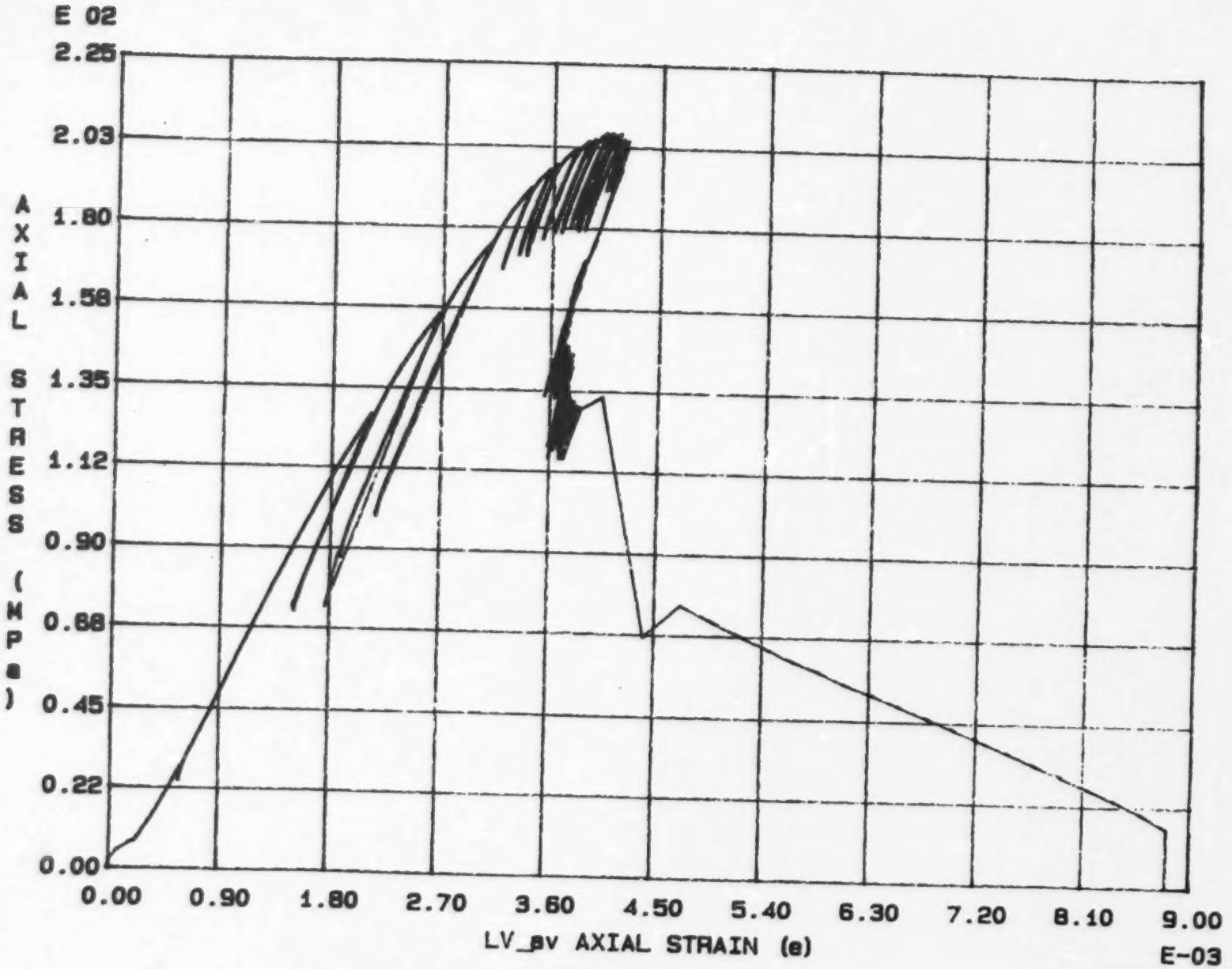

FIG. C-10 SPECIMEN 9514

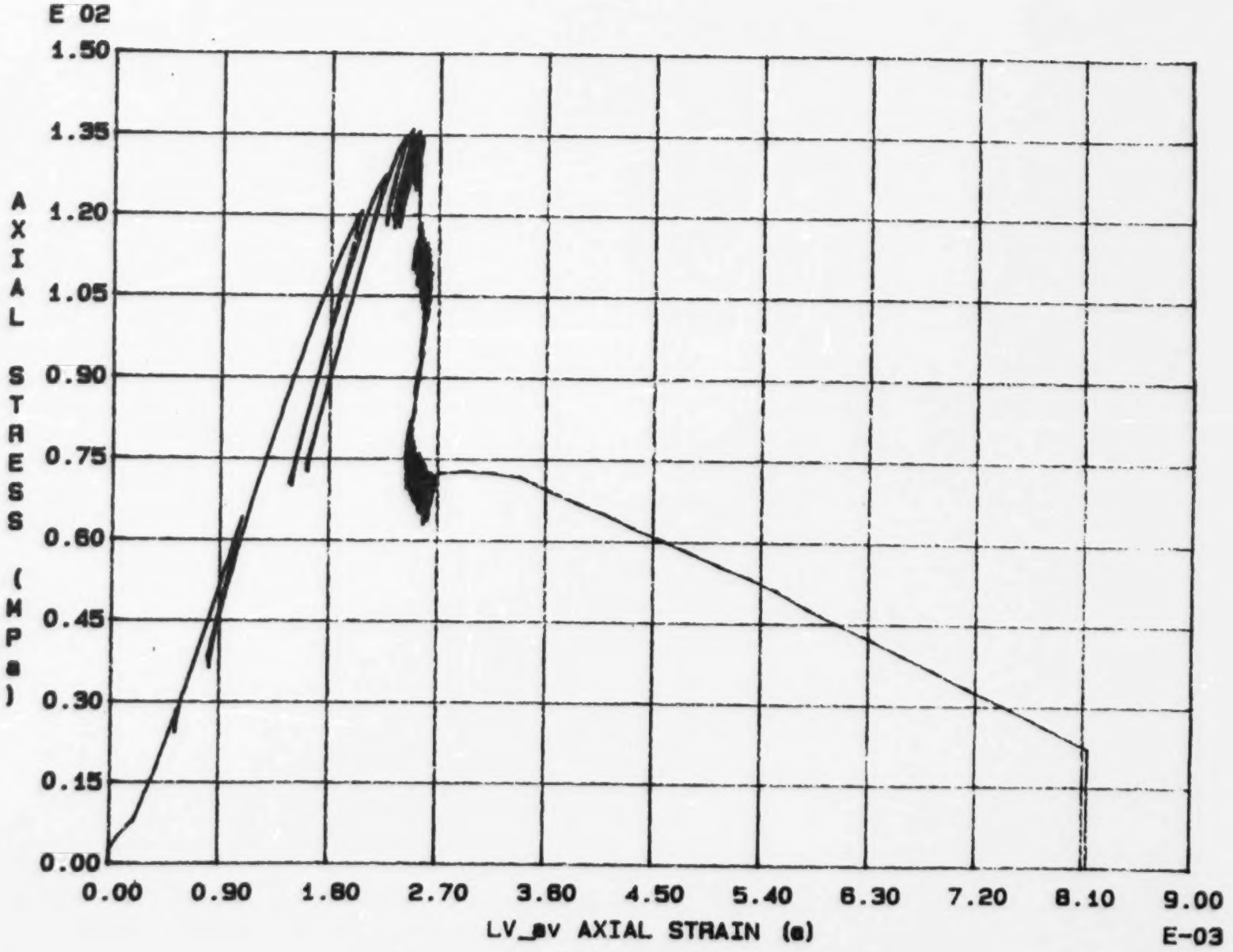

FIG. C-11 SPECIMEN 9522

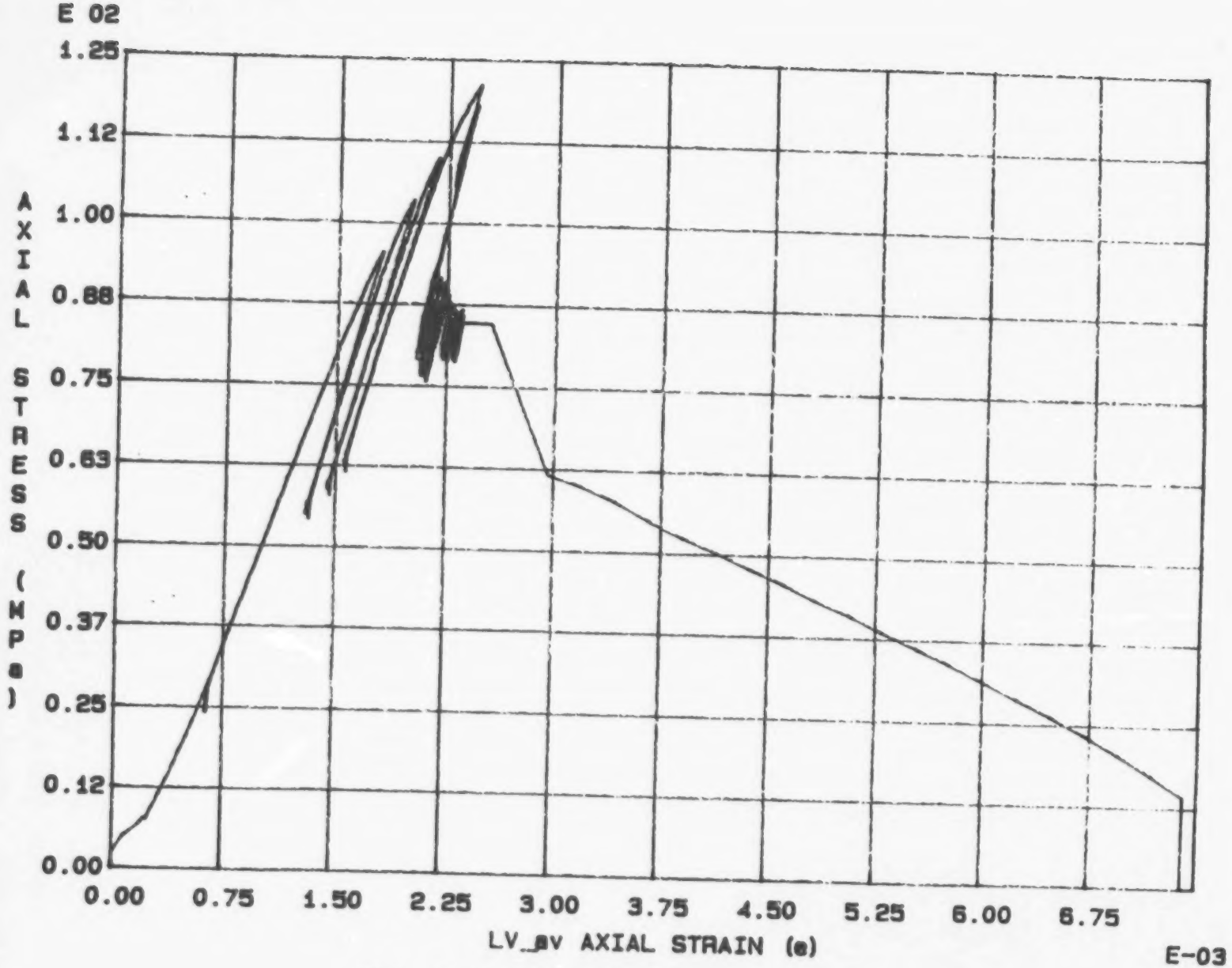

FIG. C-12 SPECIMEN 9524

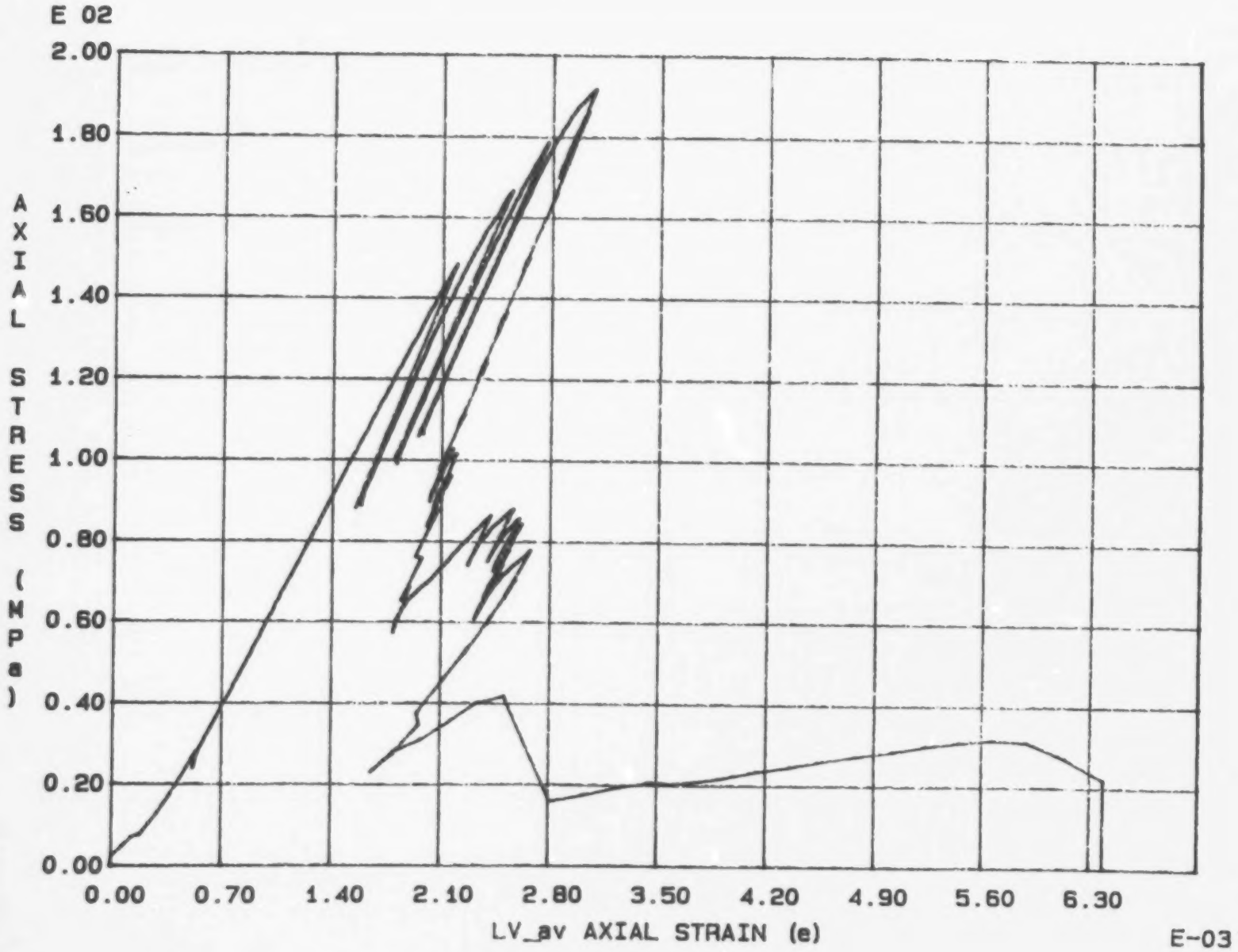

FIG. C-13 SPECIMEN 9532

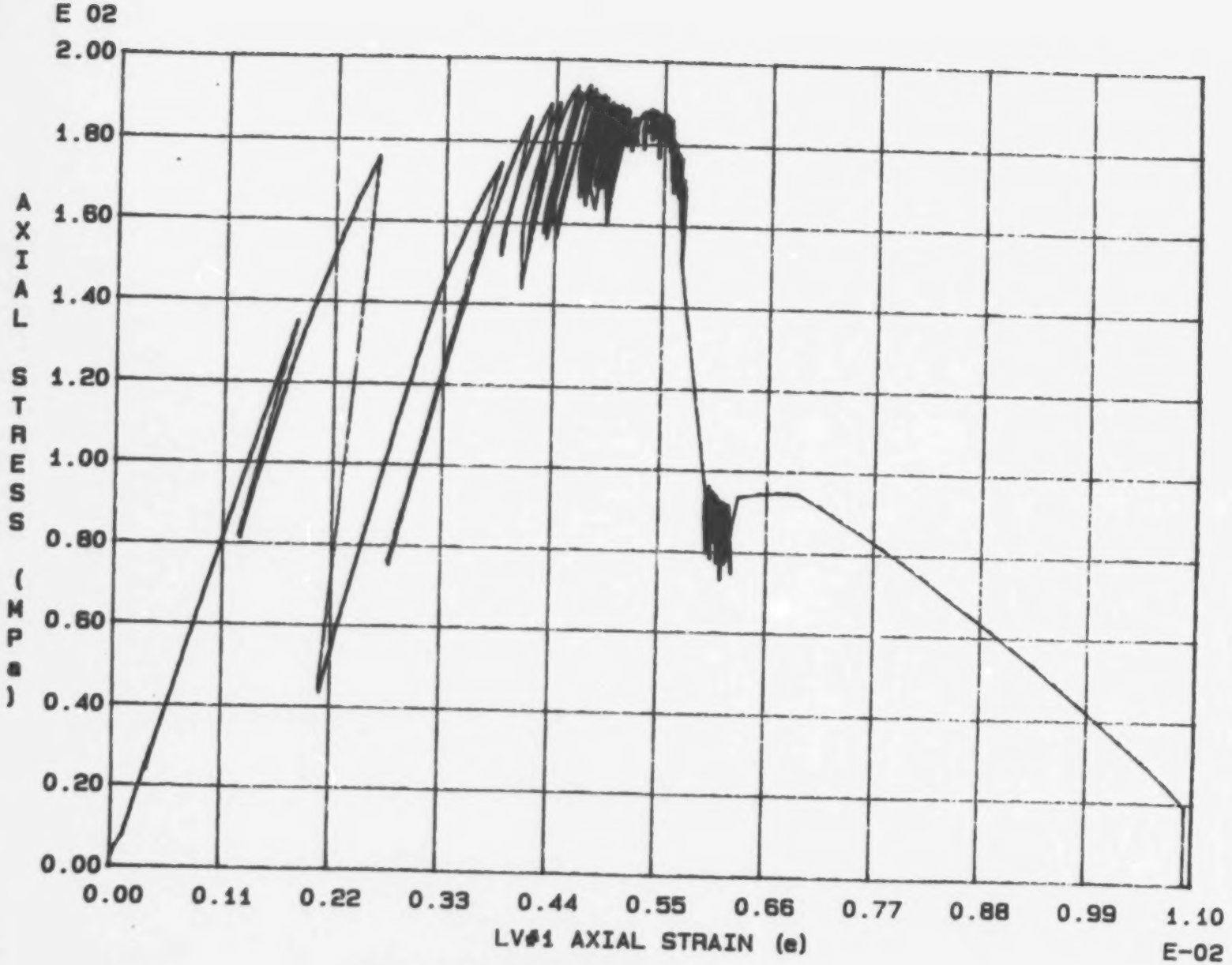

FIG. C-14 SPECIMEN 9534

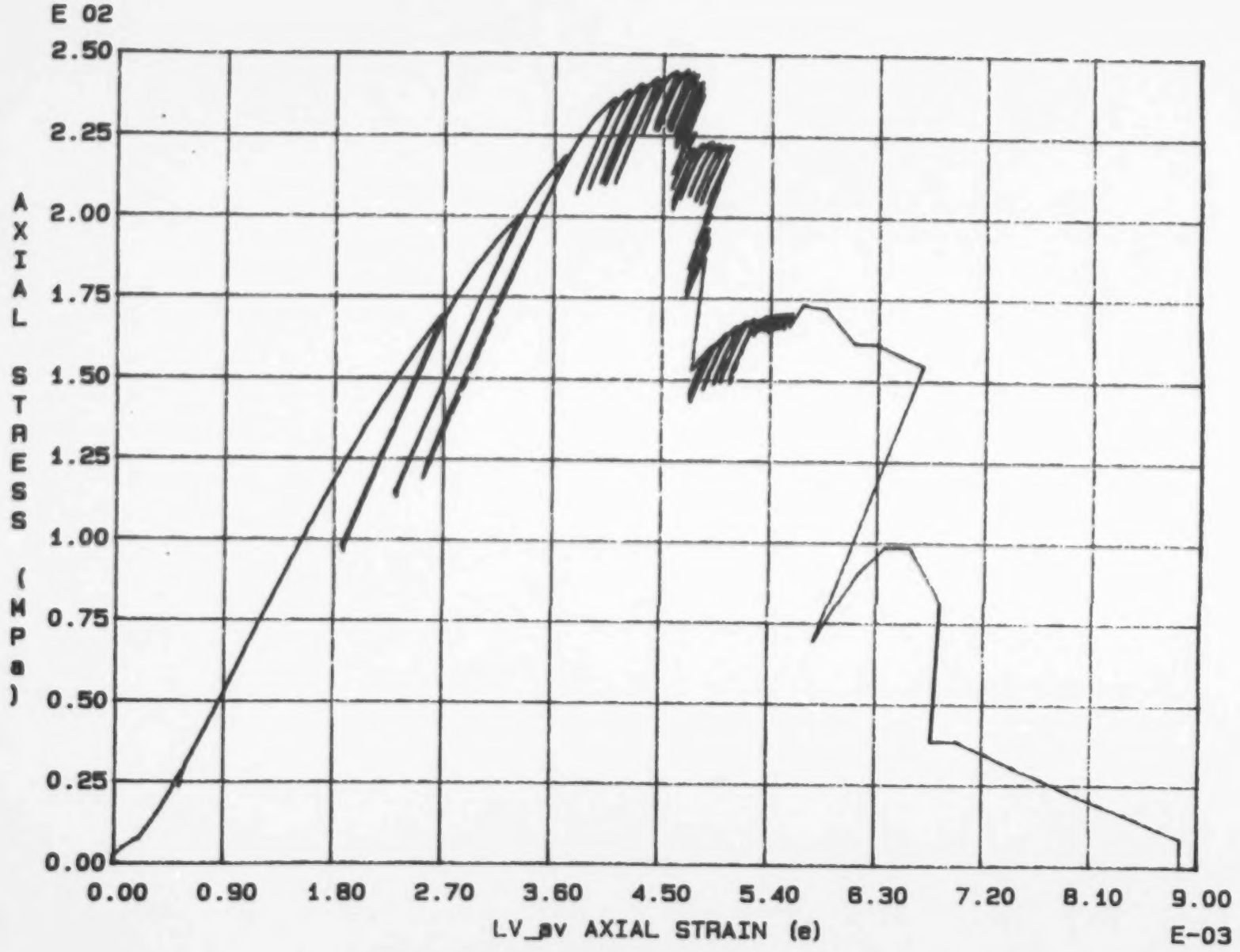

FIG. C-15 SPECIMEN 9536

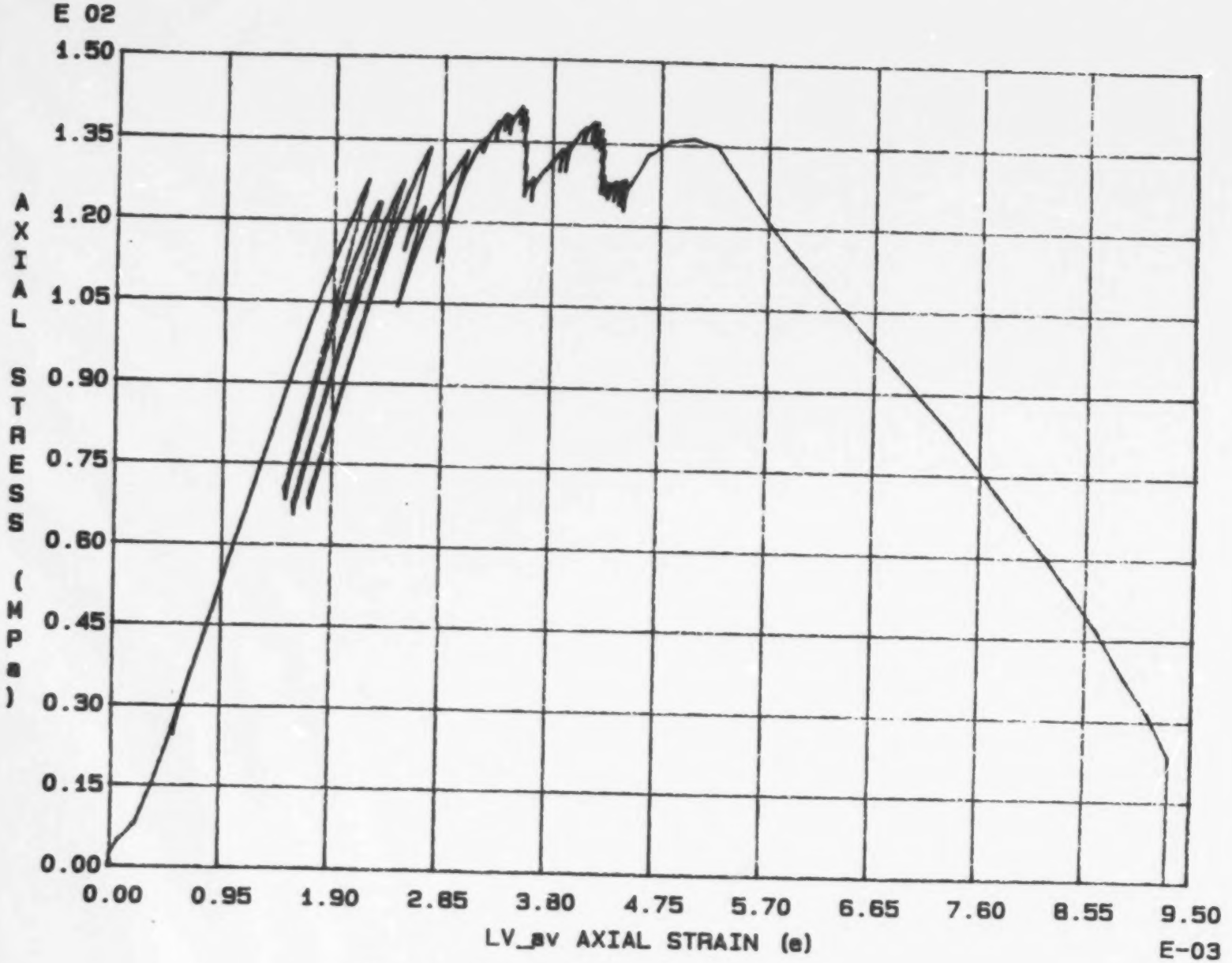

FIG. C-16 SPECIMEN 4012

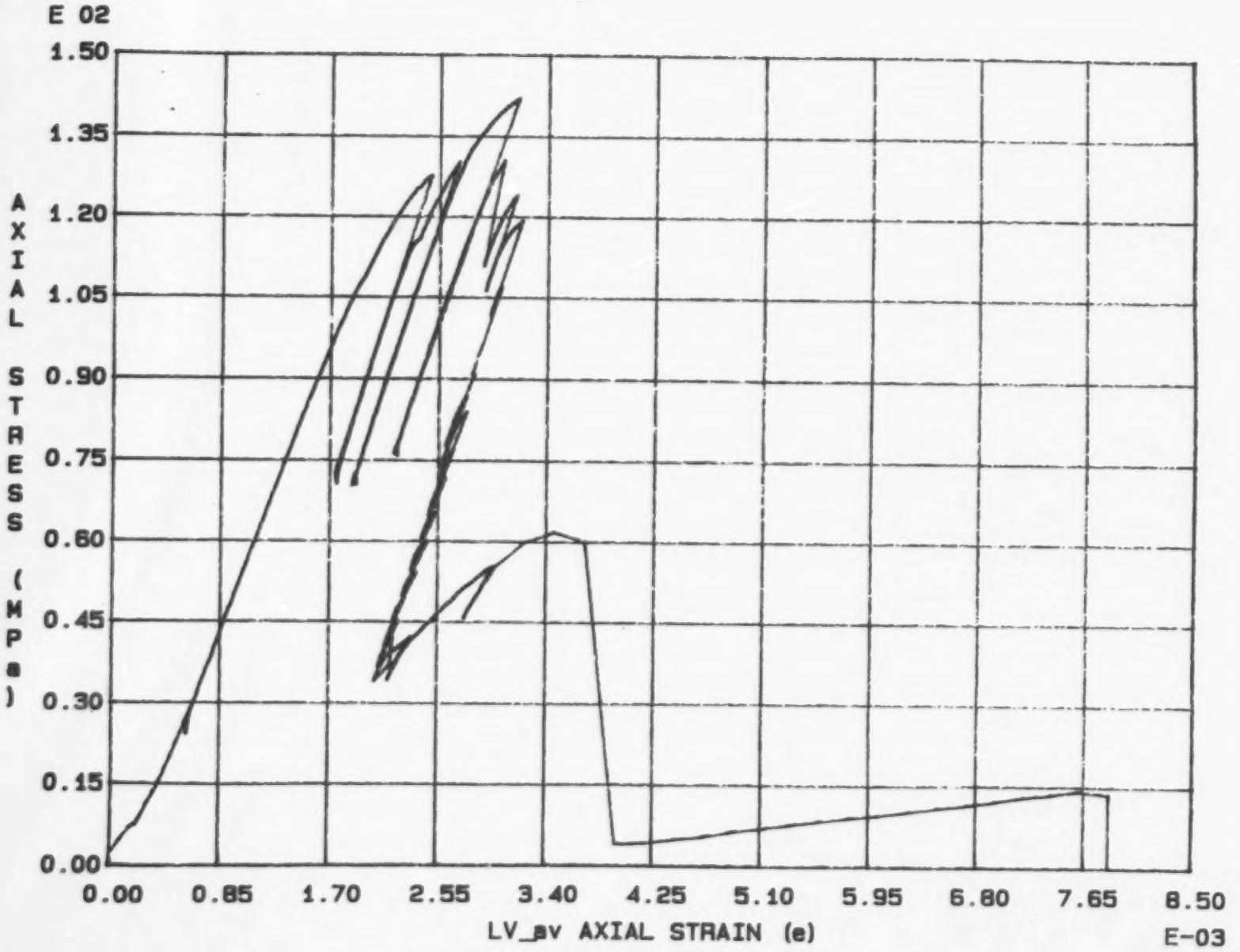

FIG. C-17 SPECIMEN 4014

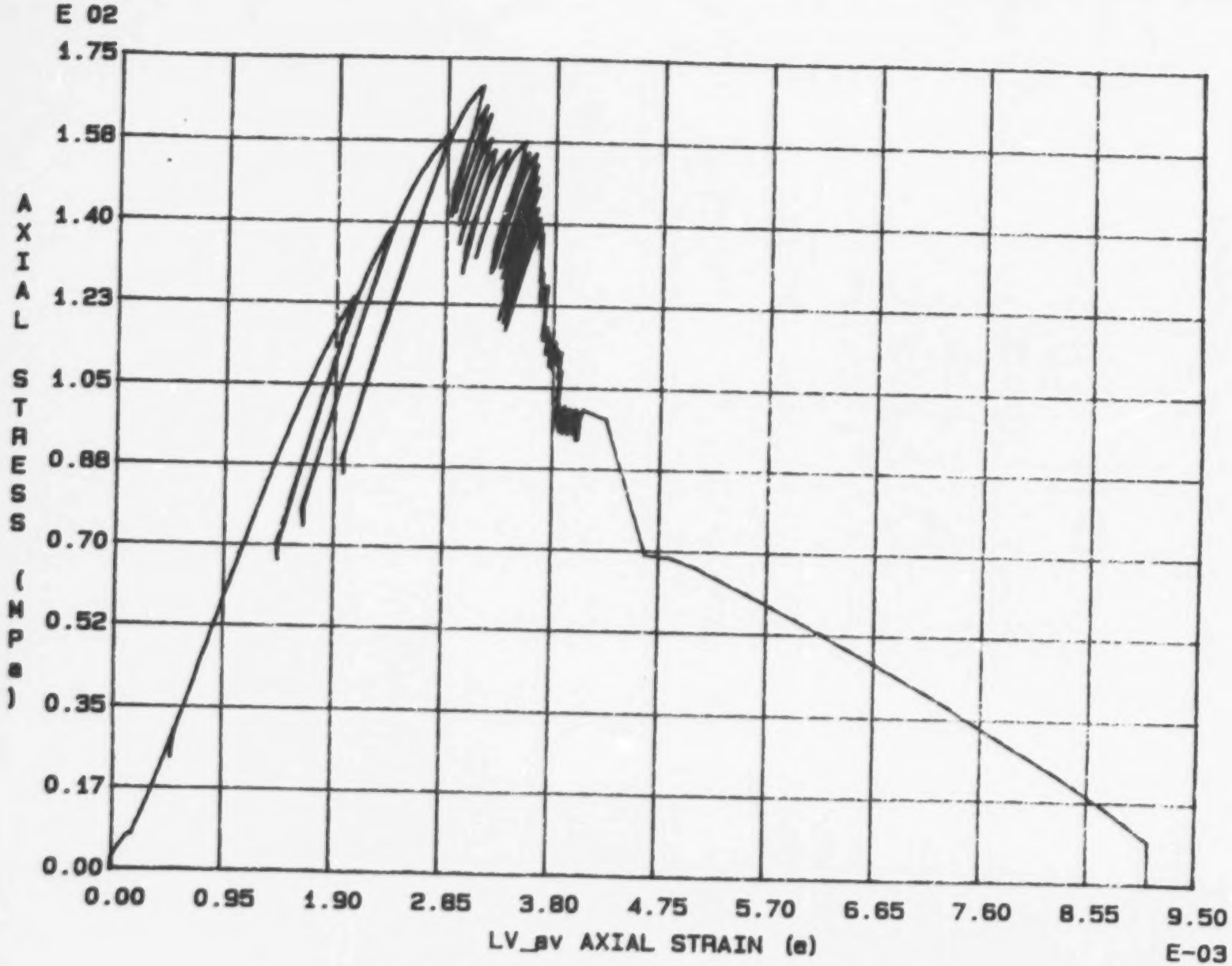

FIG. C-18 SPECIMEN 4016

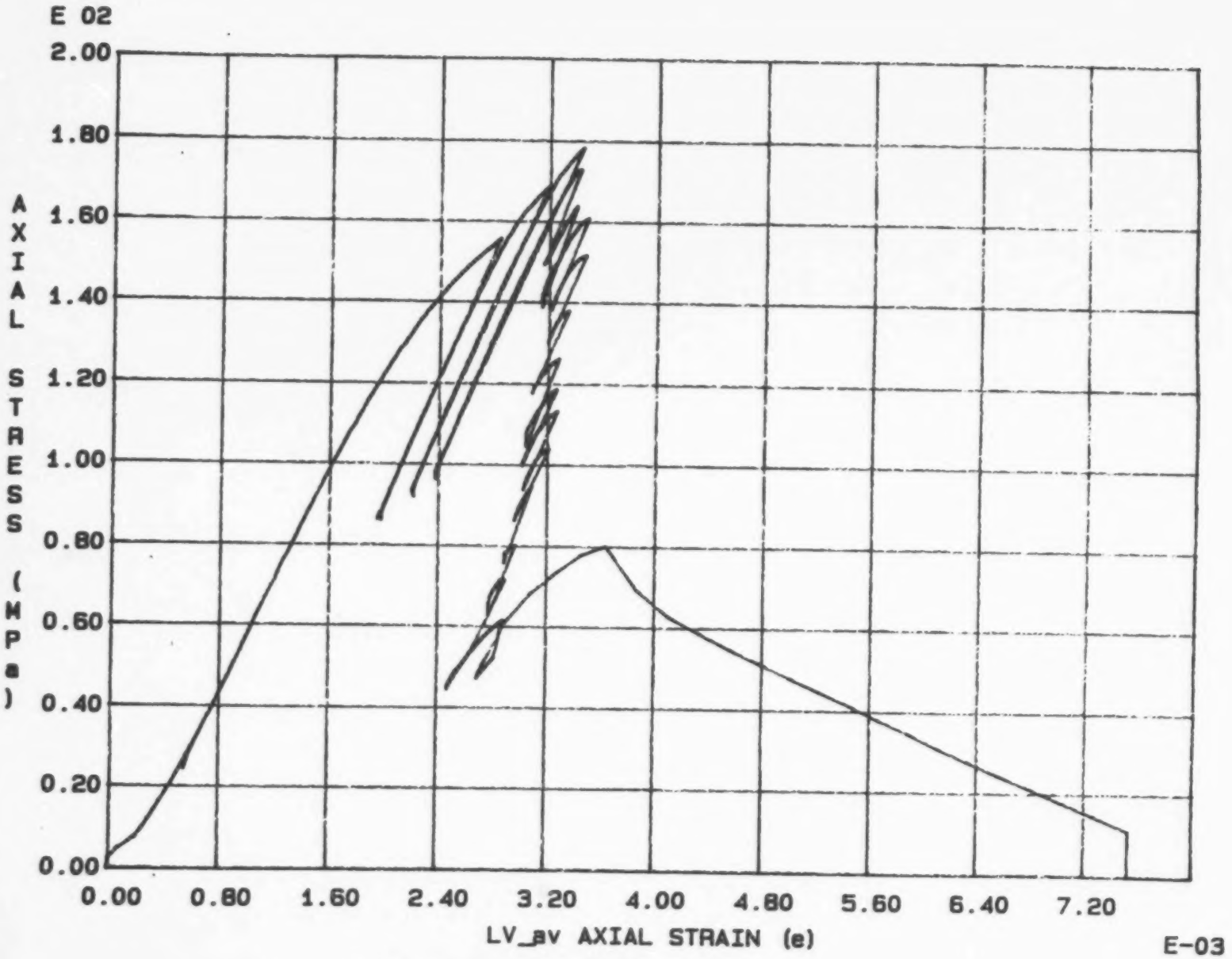

FIG. C-19 SPECIMEN 4018

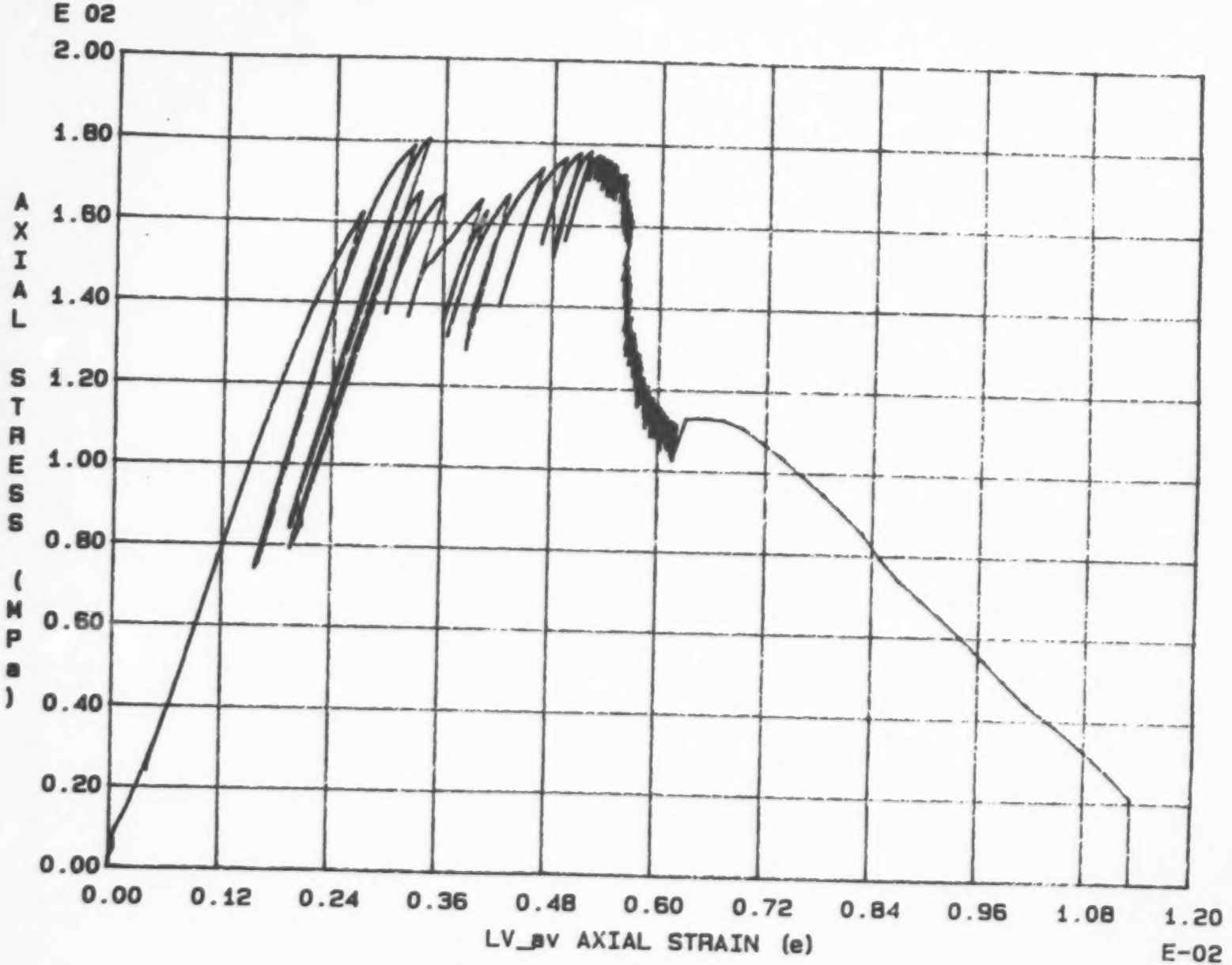

FIG. C-20 SPECIMEN 4022

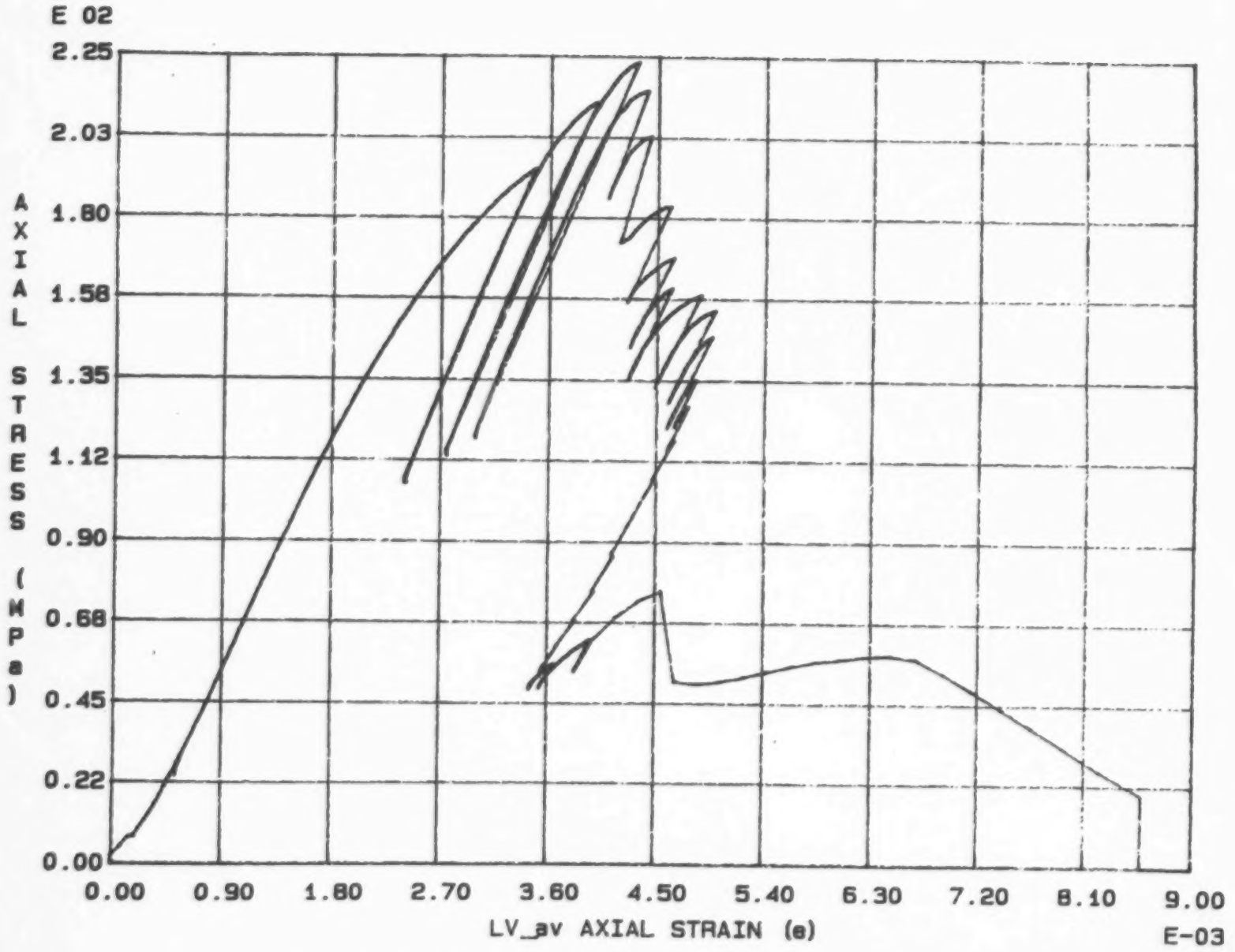

FIG. C-21 SPECIMEN 4024

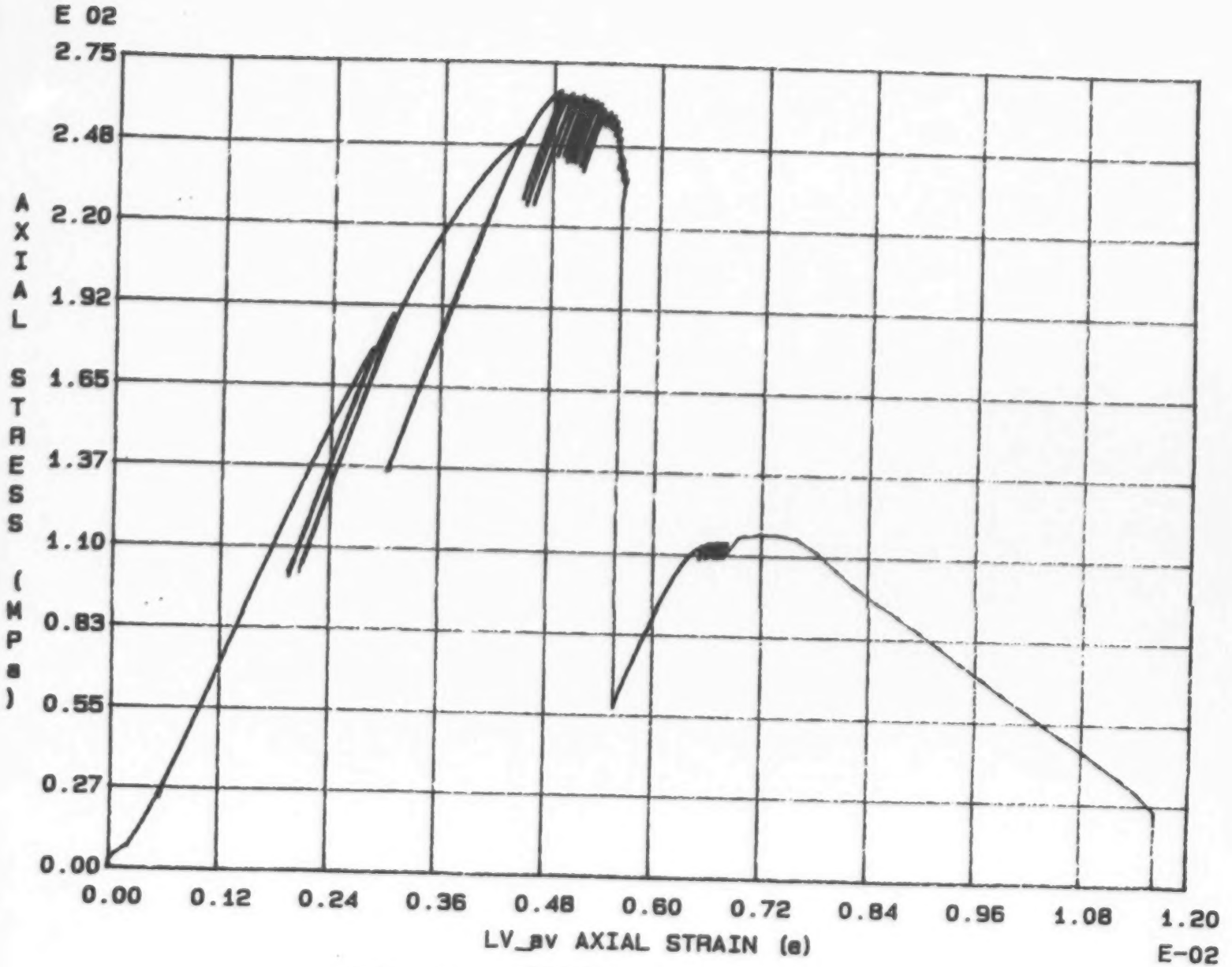

FIG. C-22 SPECIMEN 4032

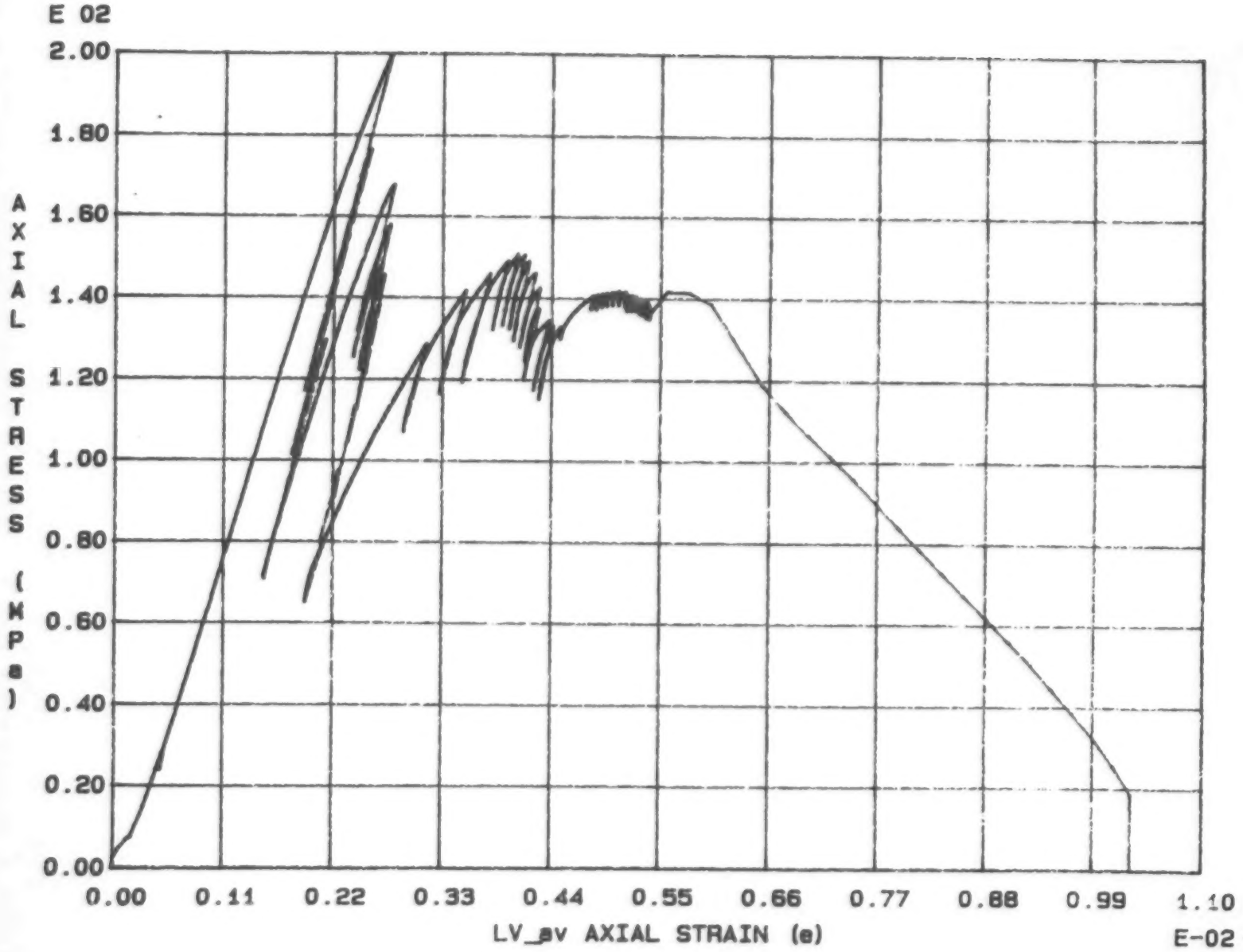

FIG. C-23 SPECIMEN 4034

APPENDIX D

CIRCUMFERENTIAL STRESS-STRAIN CURVES OF MULTI-STAGE TESTS

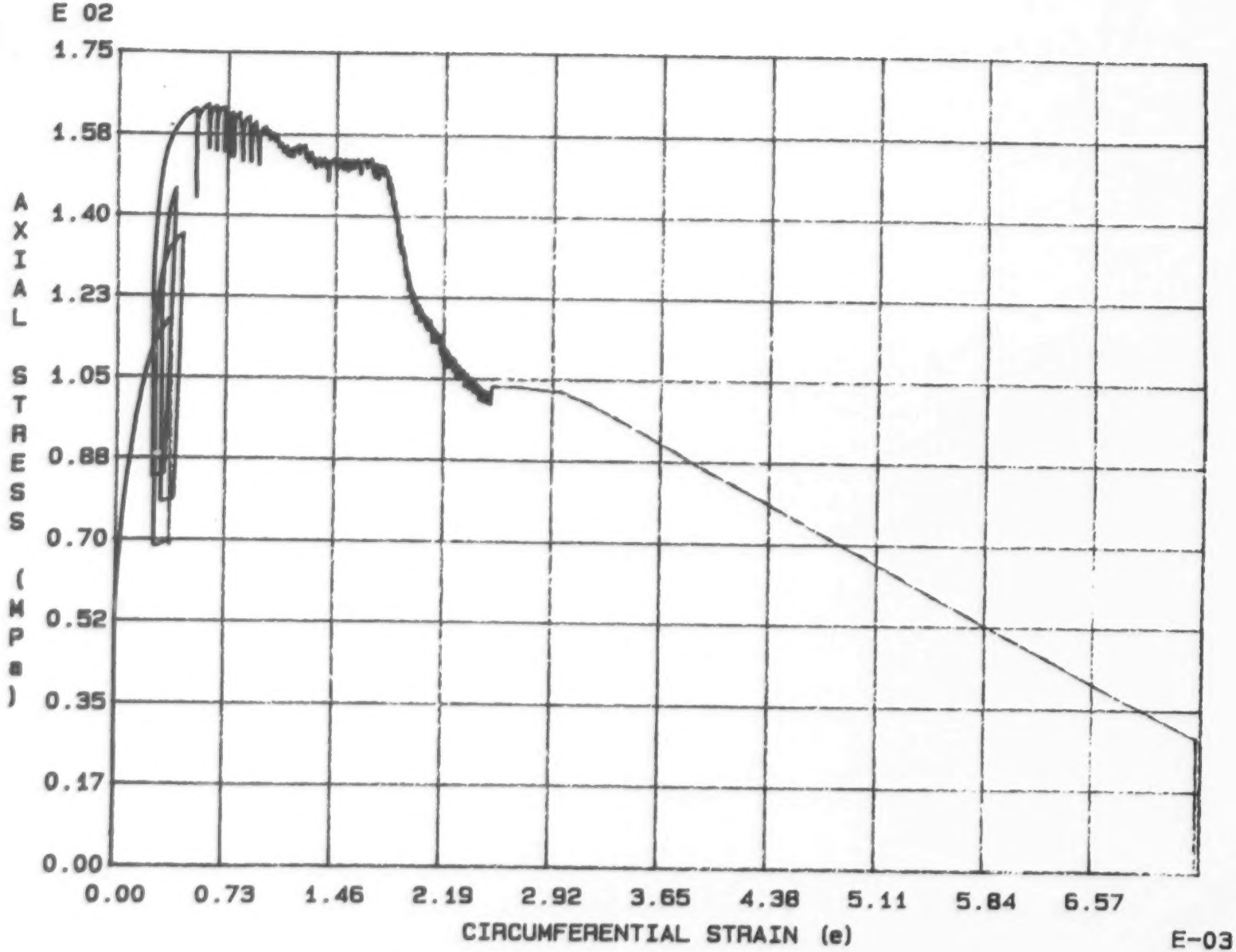

FIG. D-1 SPECIMEN 9012

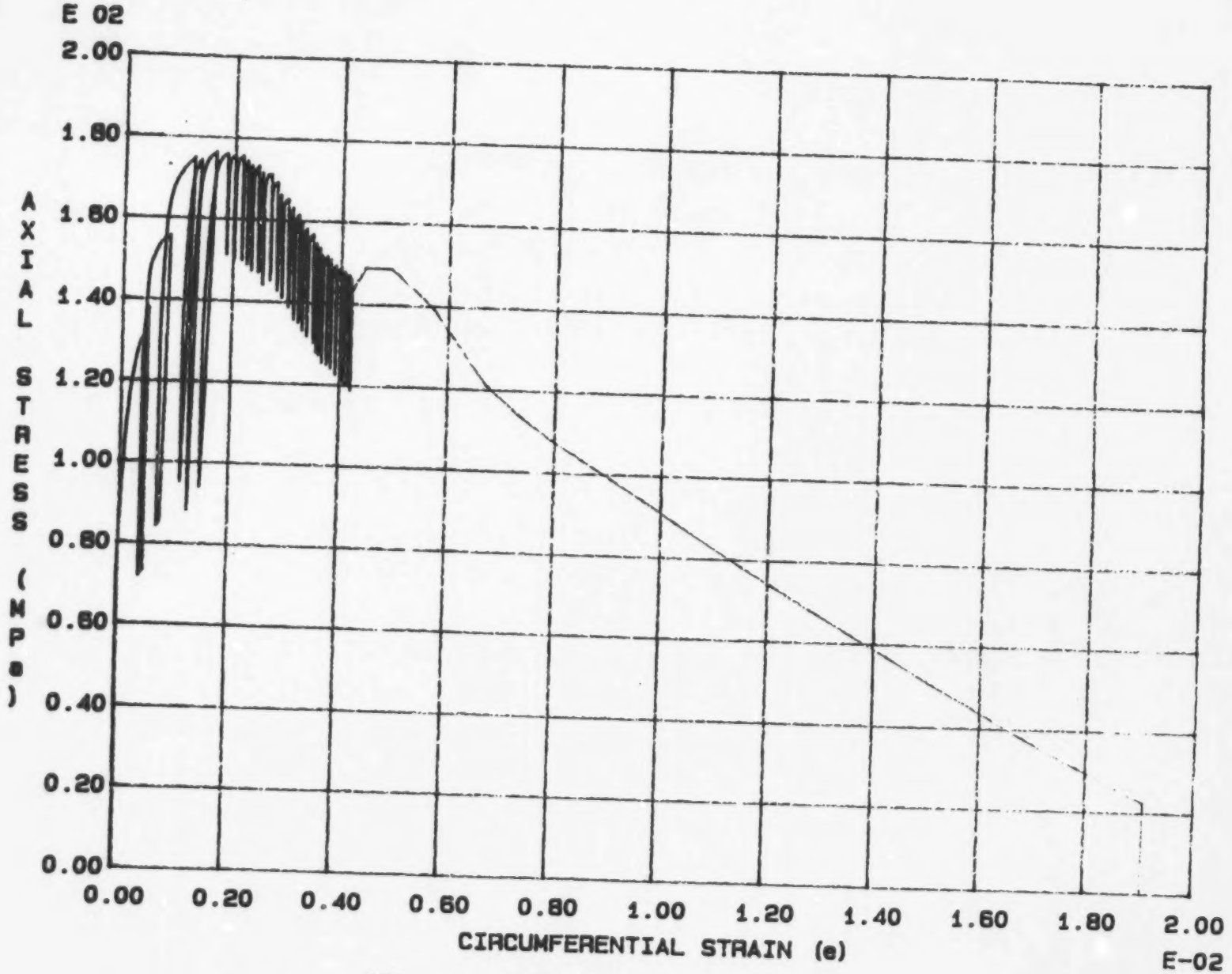

FIG. D-2 SPECIMEN 9014

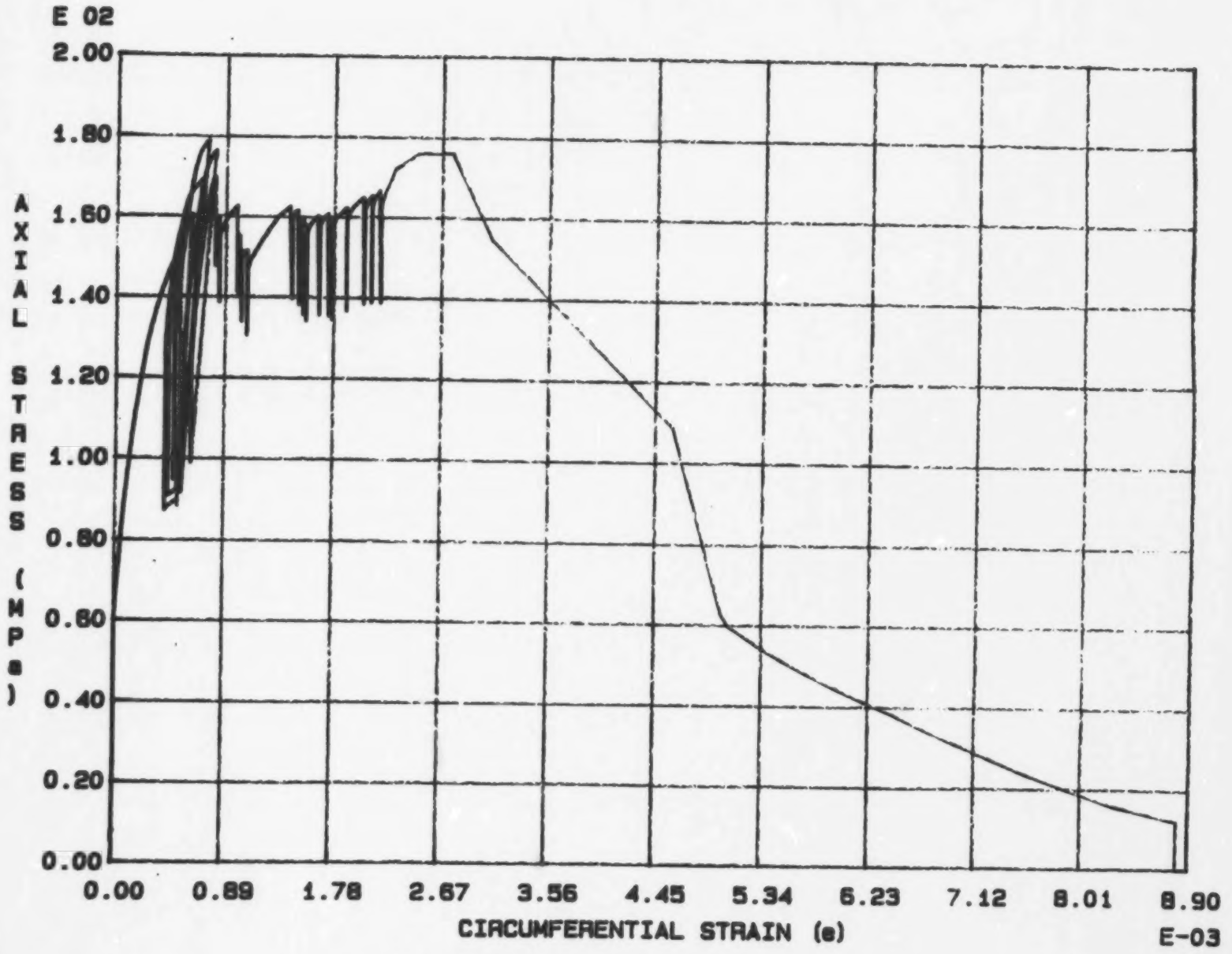

FIG. D-3 SPECIMEN 9016

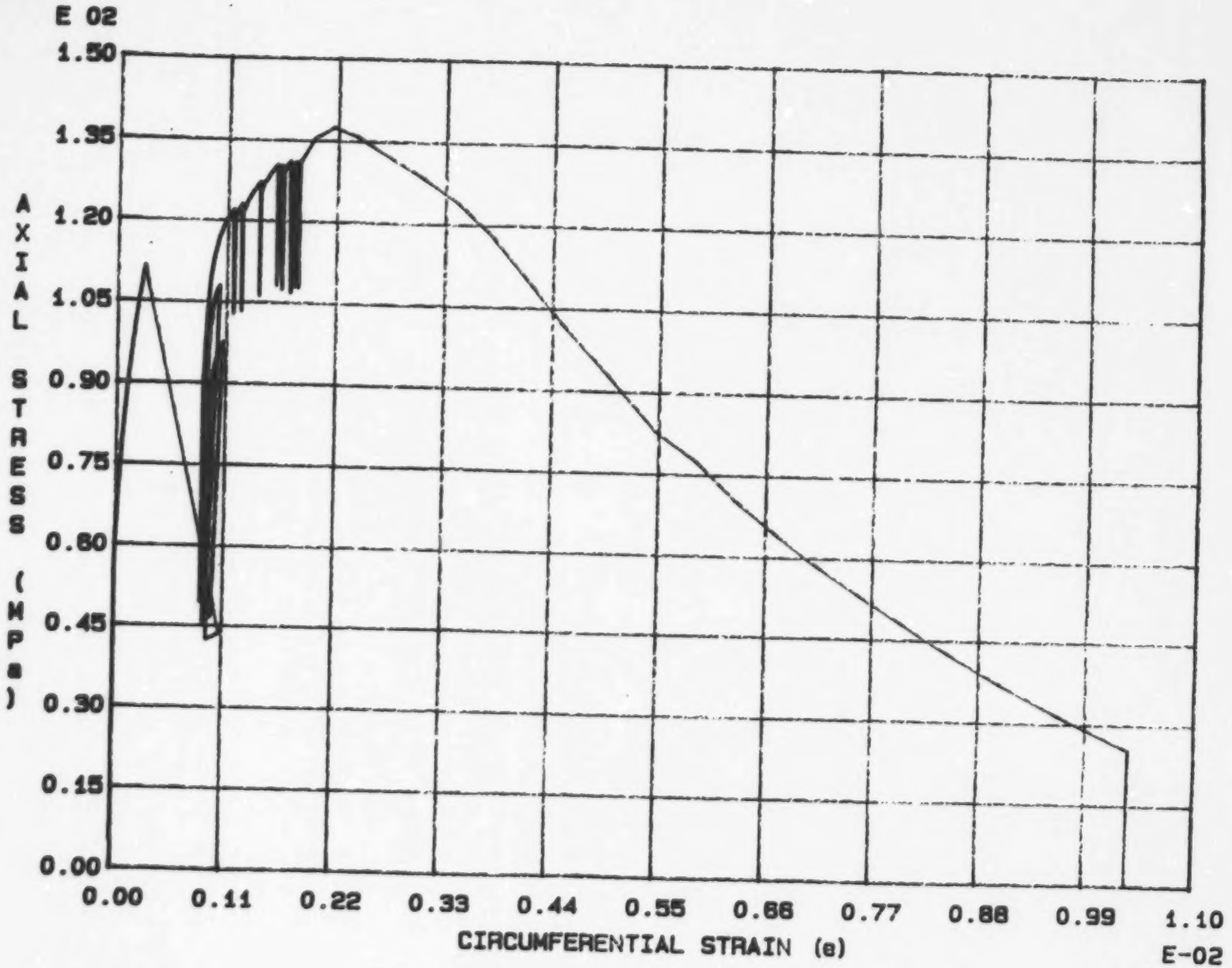

FIG. D-4 SPECIMEN 9022

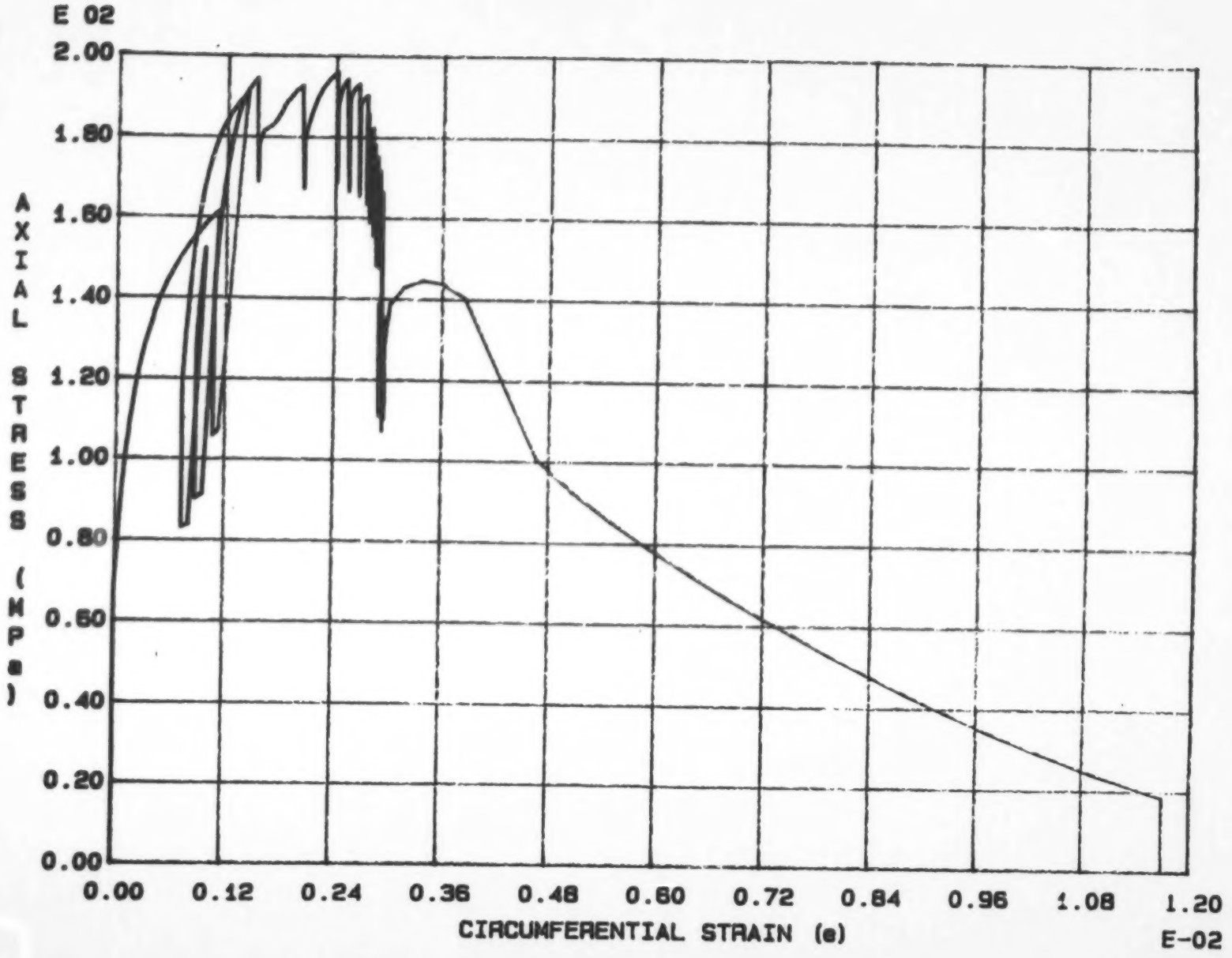

FIG. D-5 SPECIMEN 9024

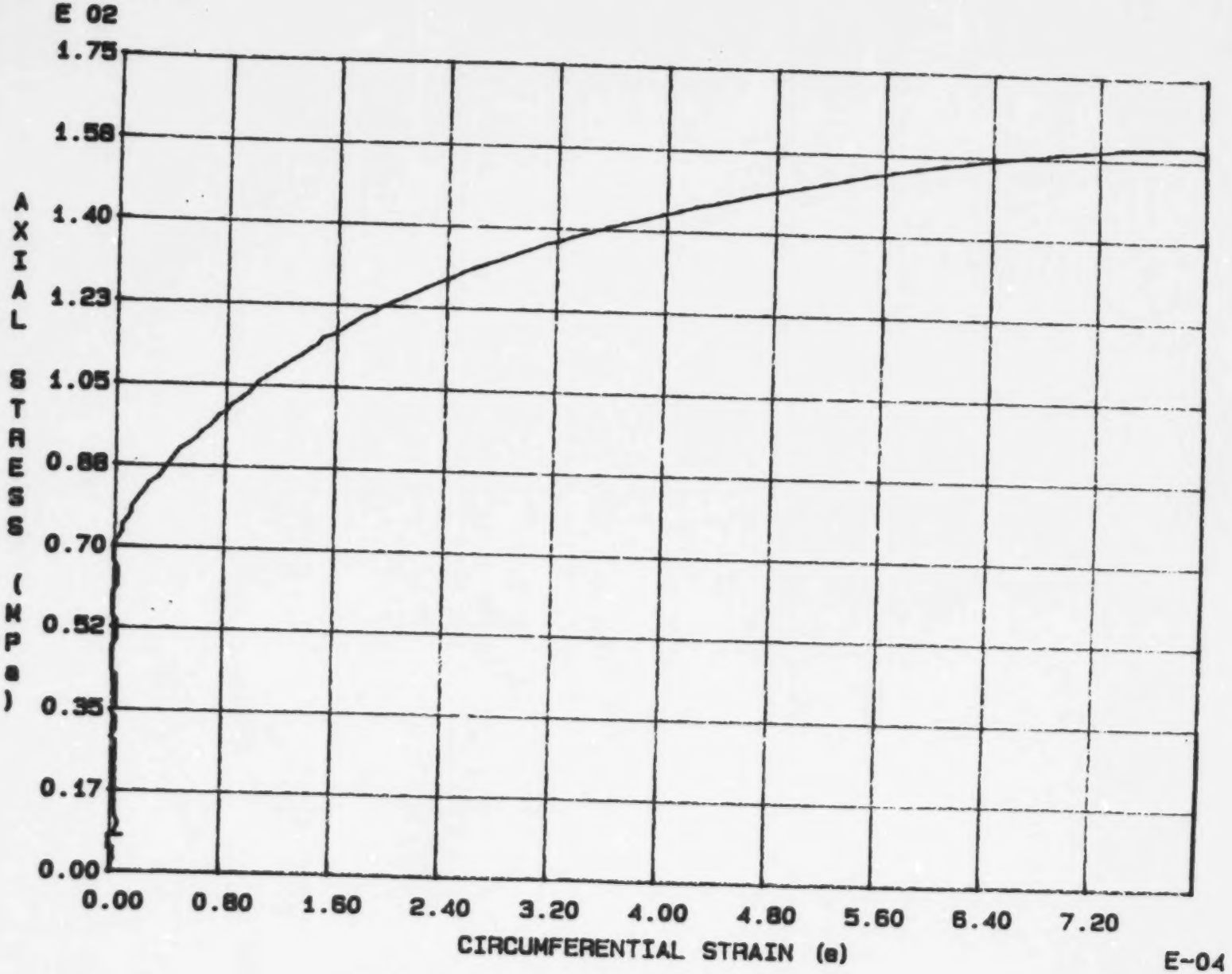

FIG. D-6 SPECIMEN 9032

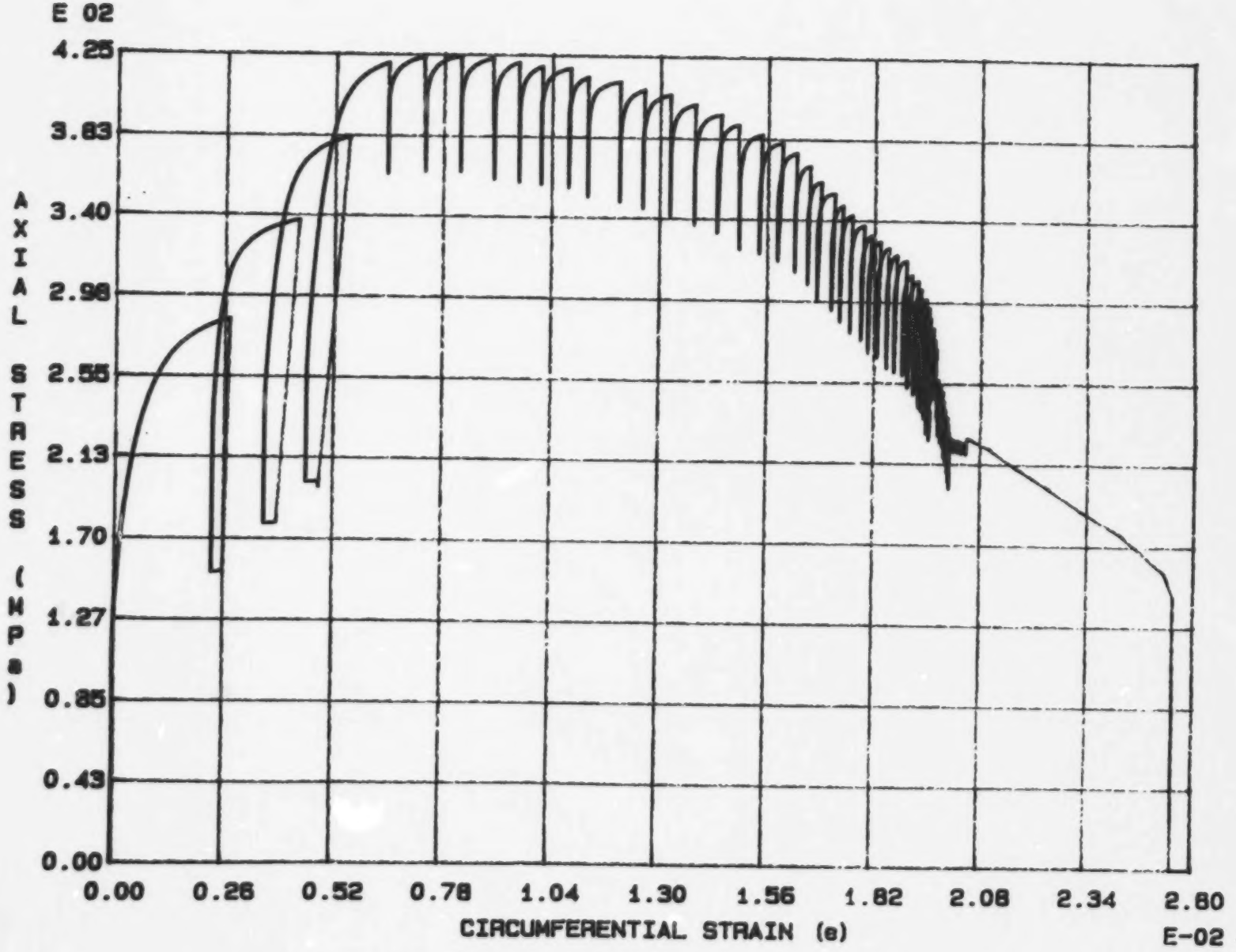

FIG. D-7 SPECIMEN 9034

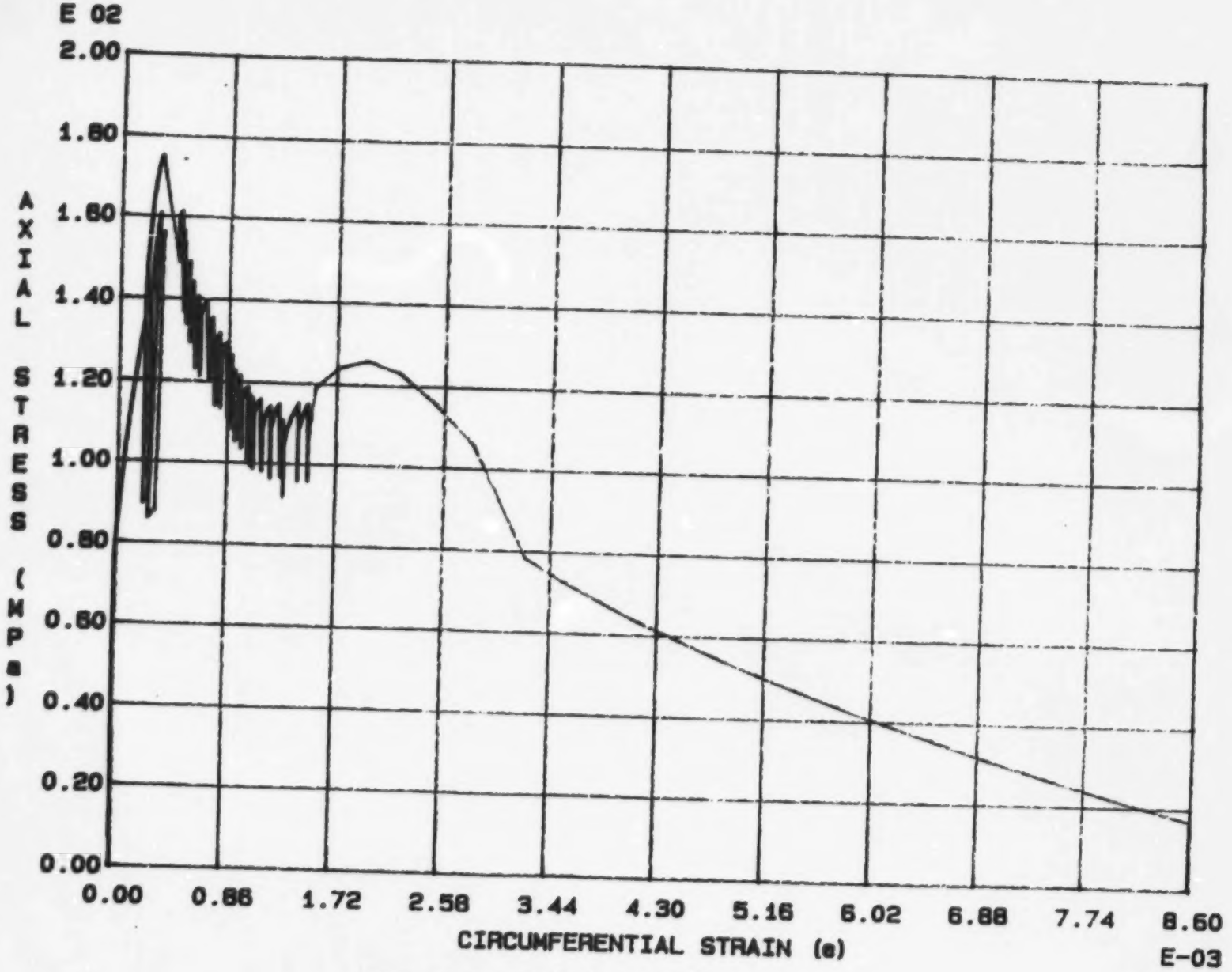

FIG. D-8 SPECIMEN 9036

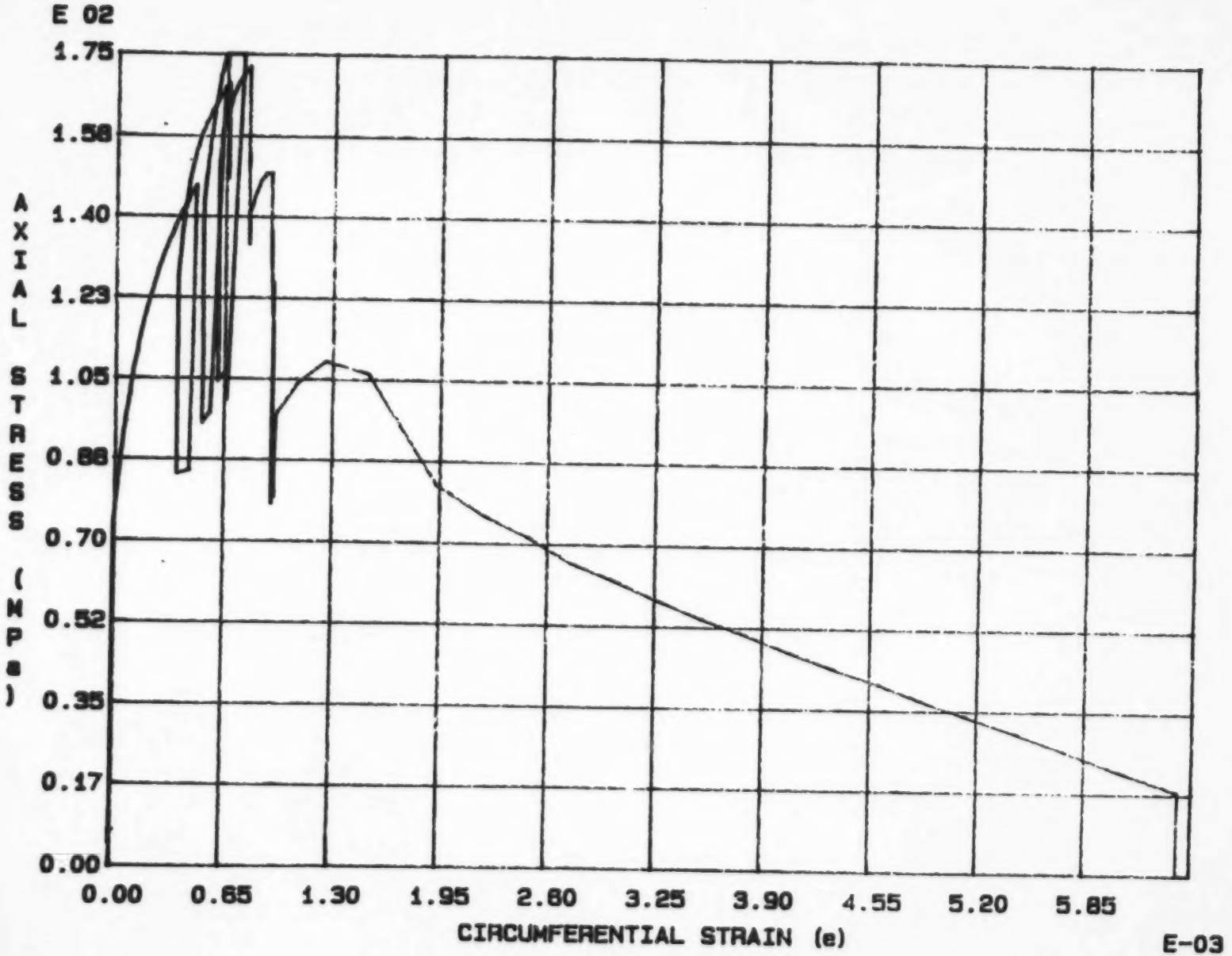

FIG. D-9 SPECIMEN 9512

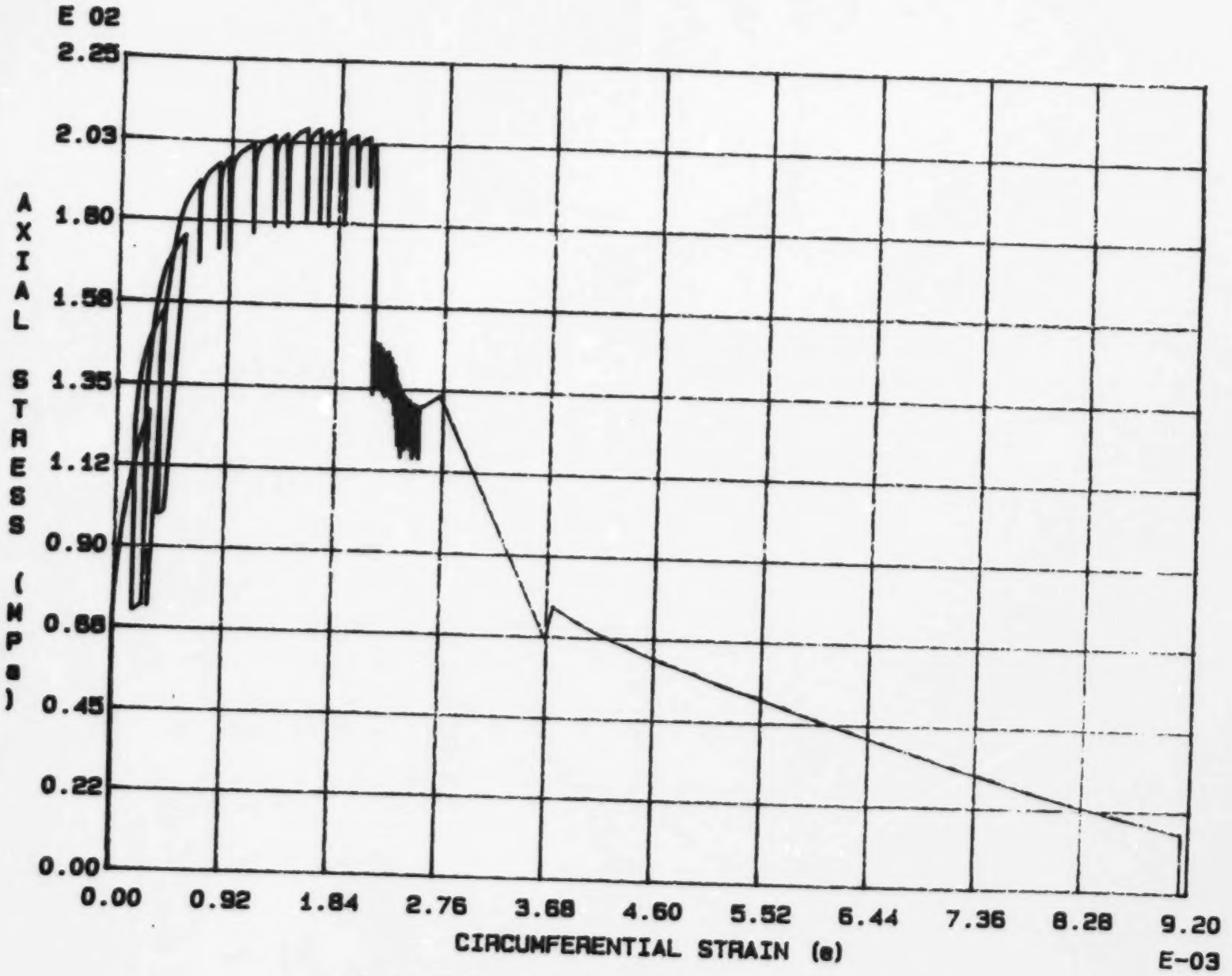

FIG. D-10 SPECIMEN 9514

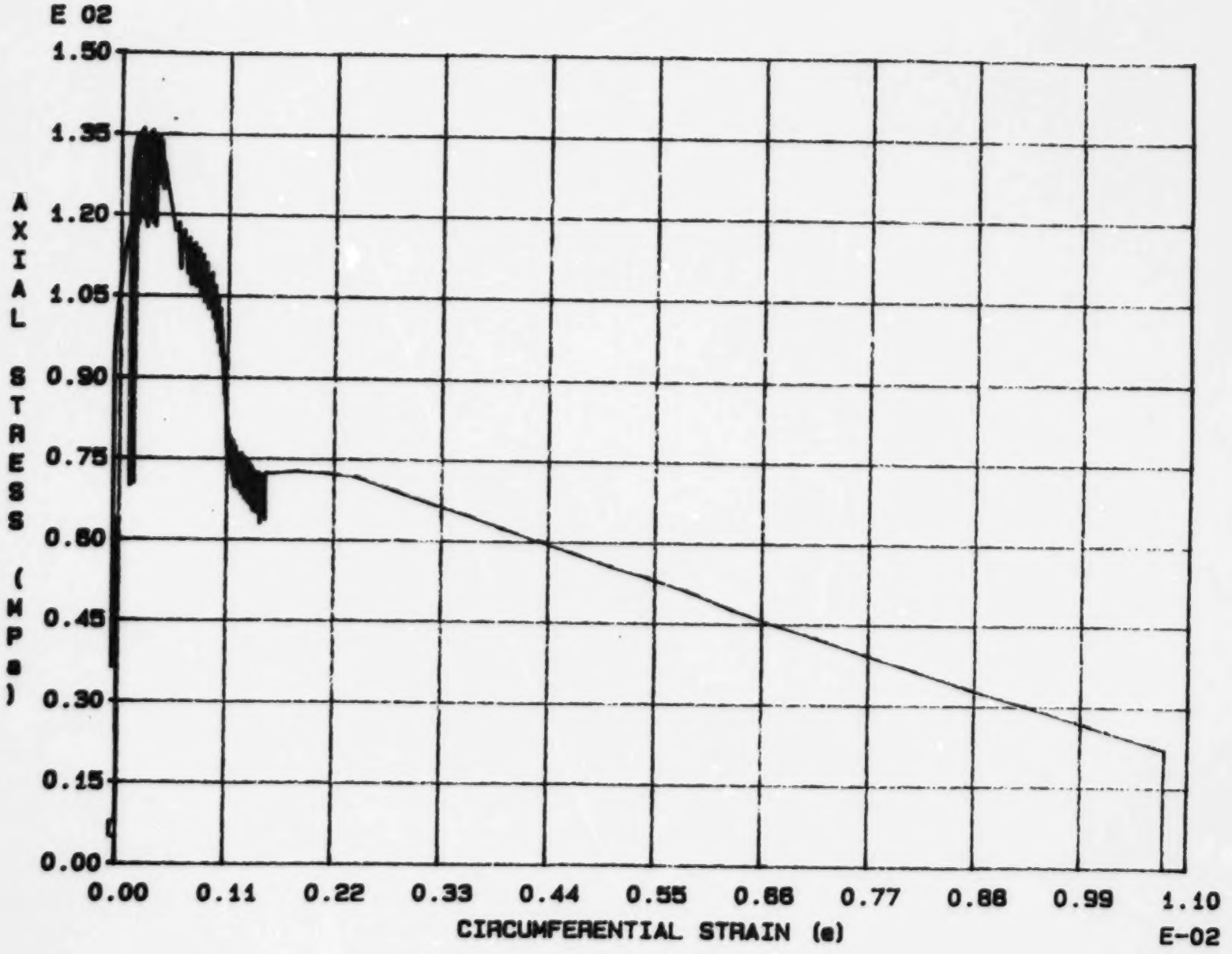

FIG. D-11 SPECIMEN 9522

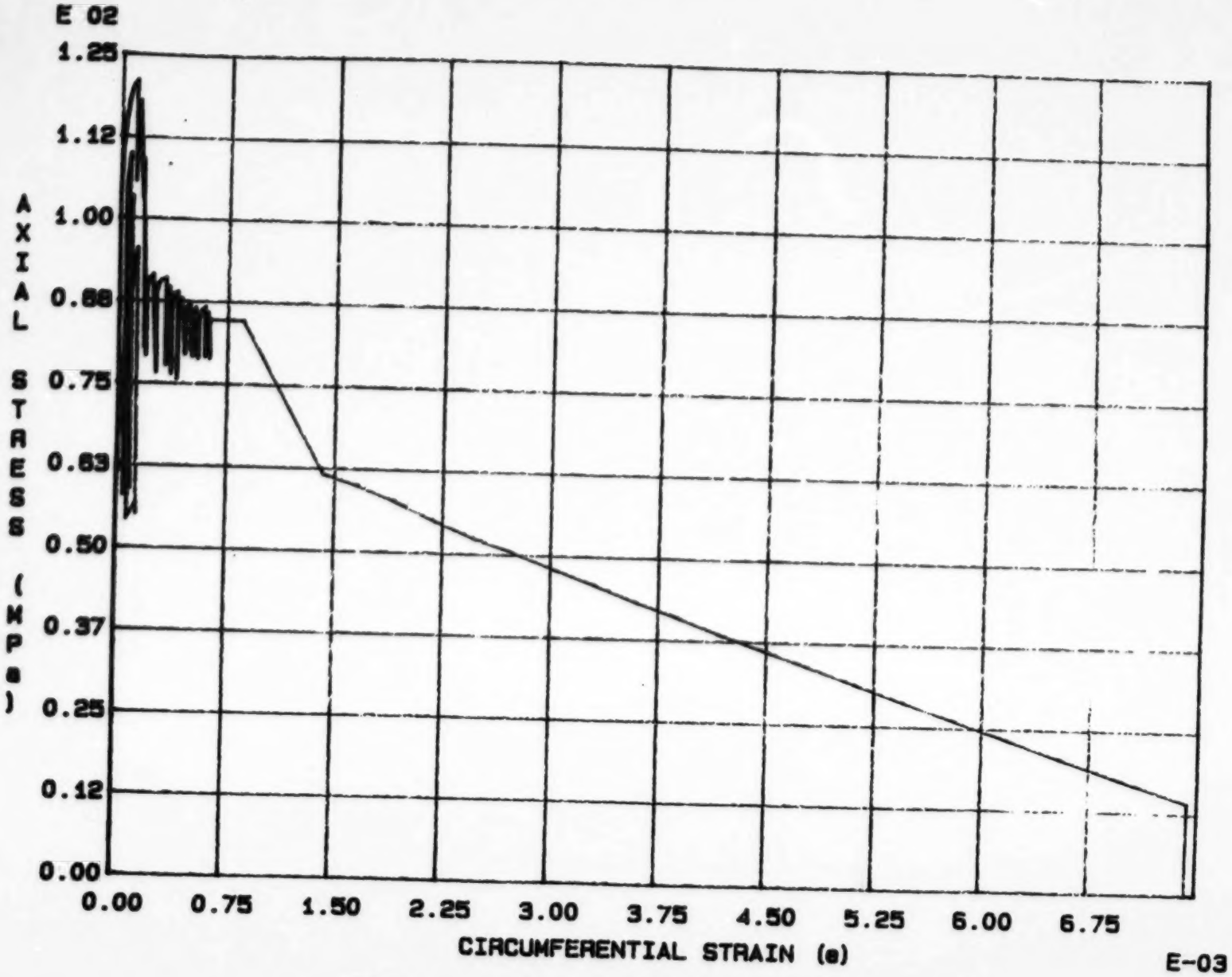

FIG. D-12 SPECIMEN 9524

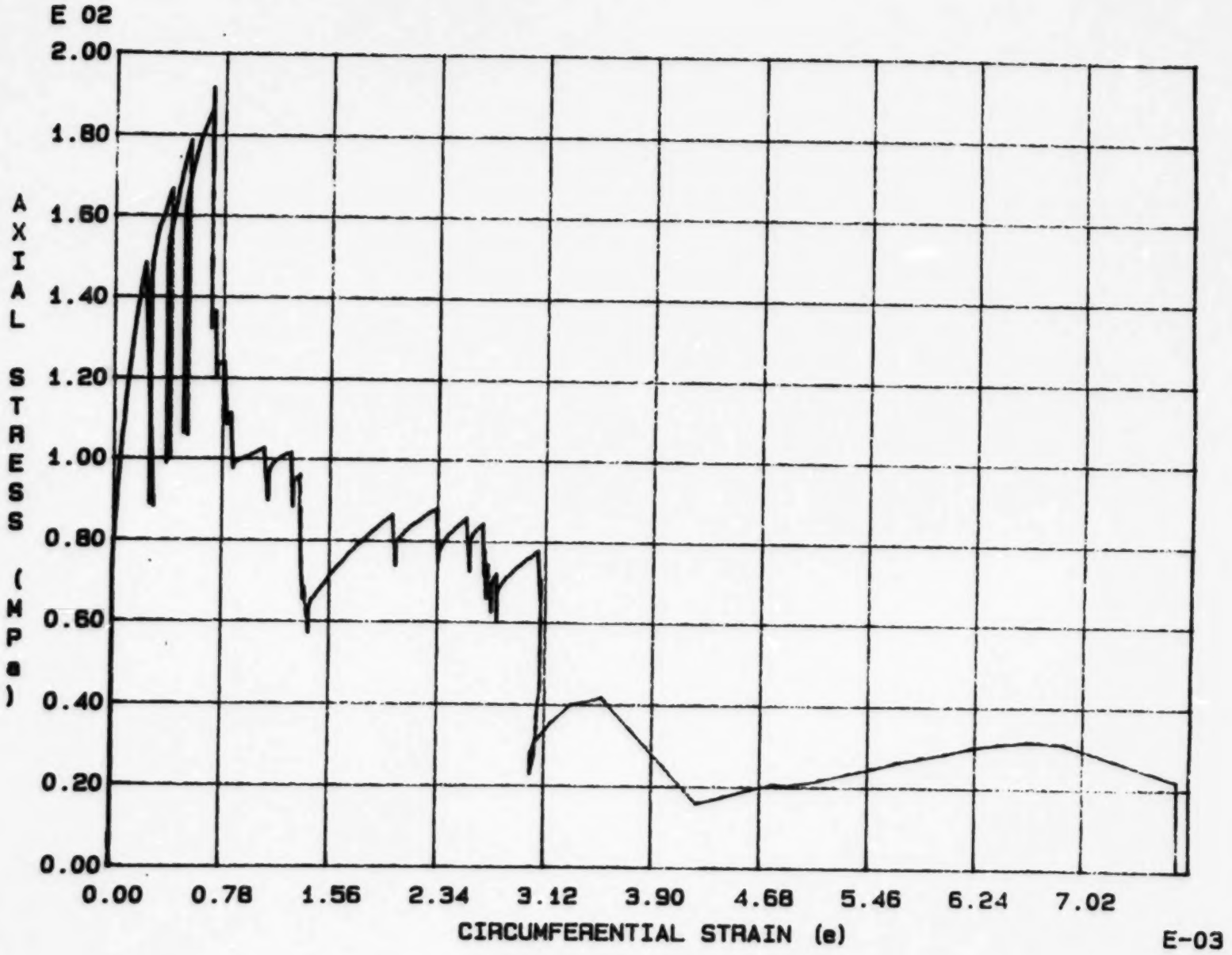

FIG. D-13 SPECIMEN 9532

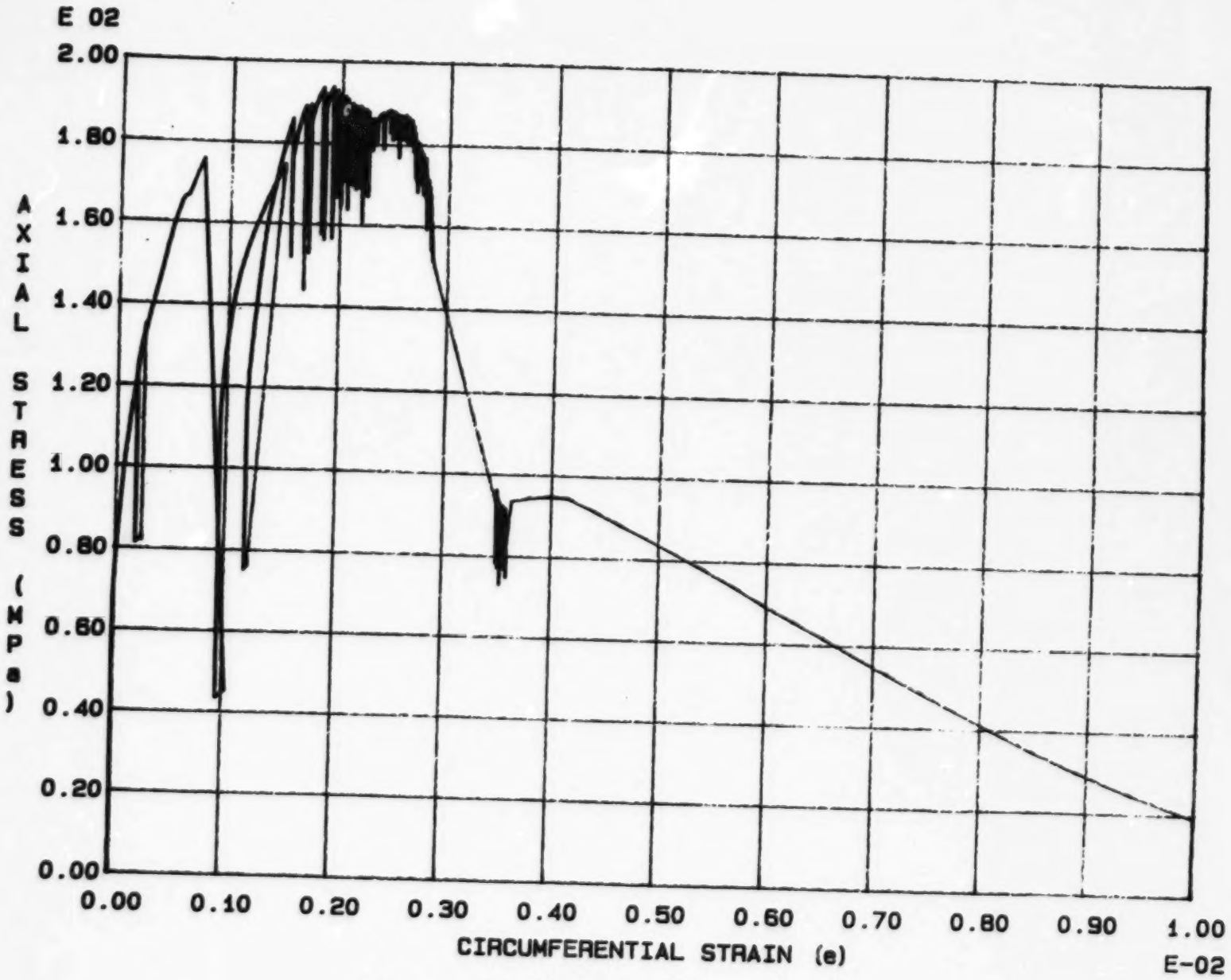

FIG. D-14 SPECIMEN 9534

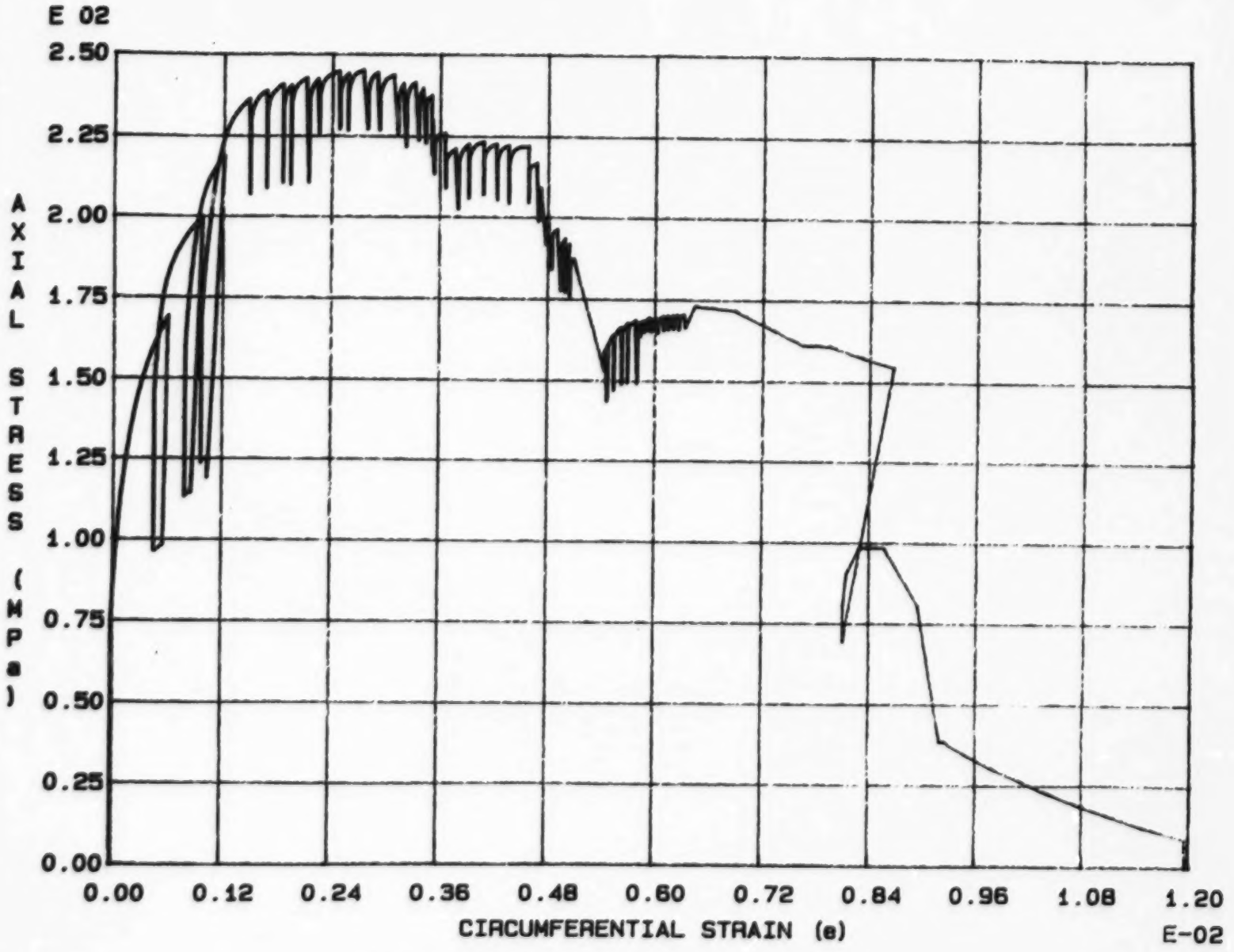

FIG. D-15 SPECIMEN 9536

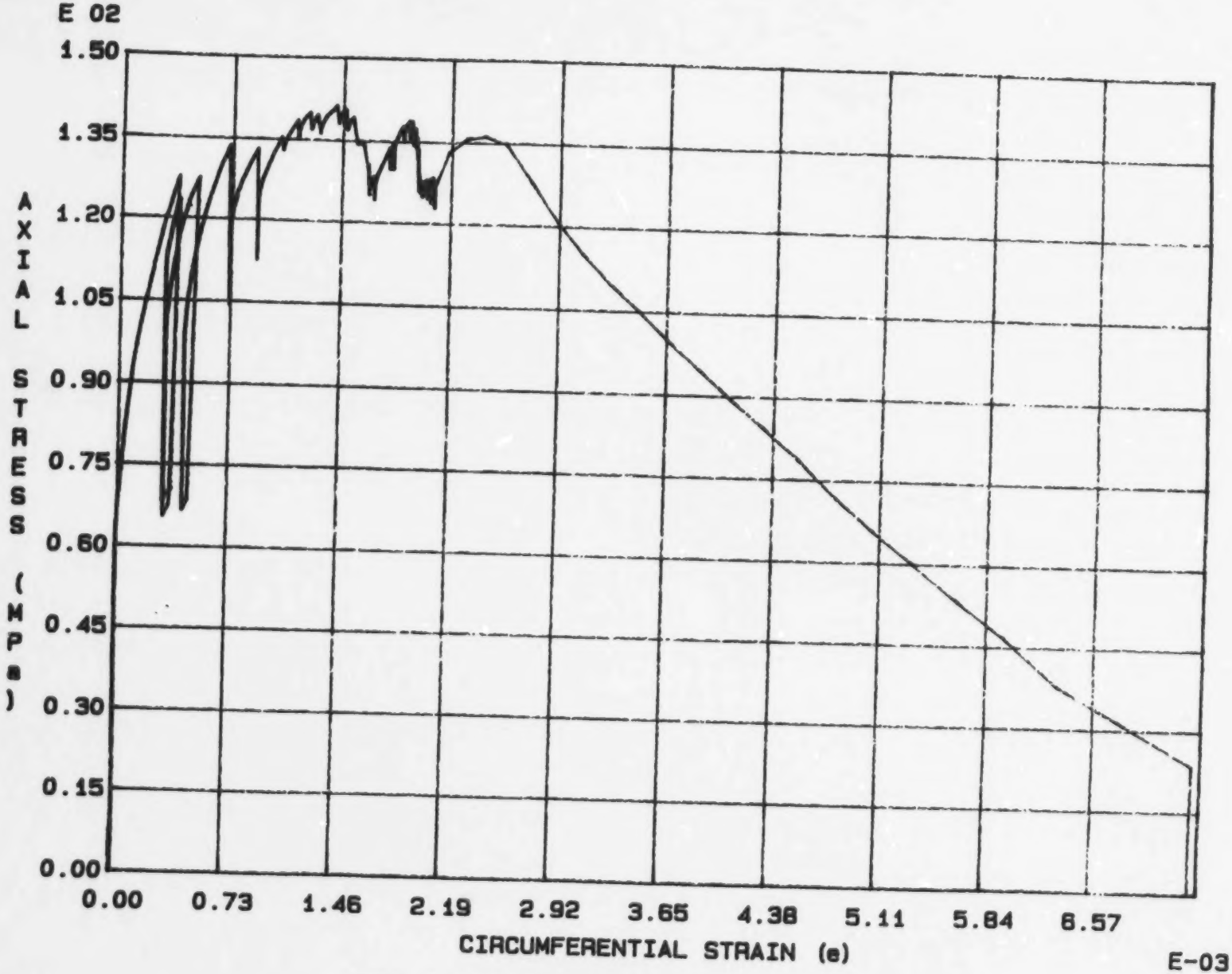

FIG. D-16 SPECIMEN 4012

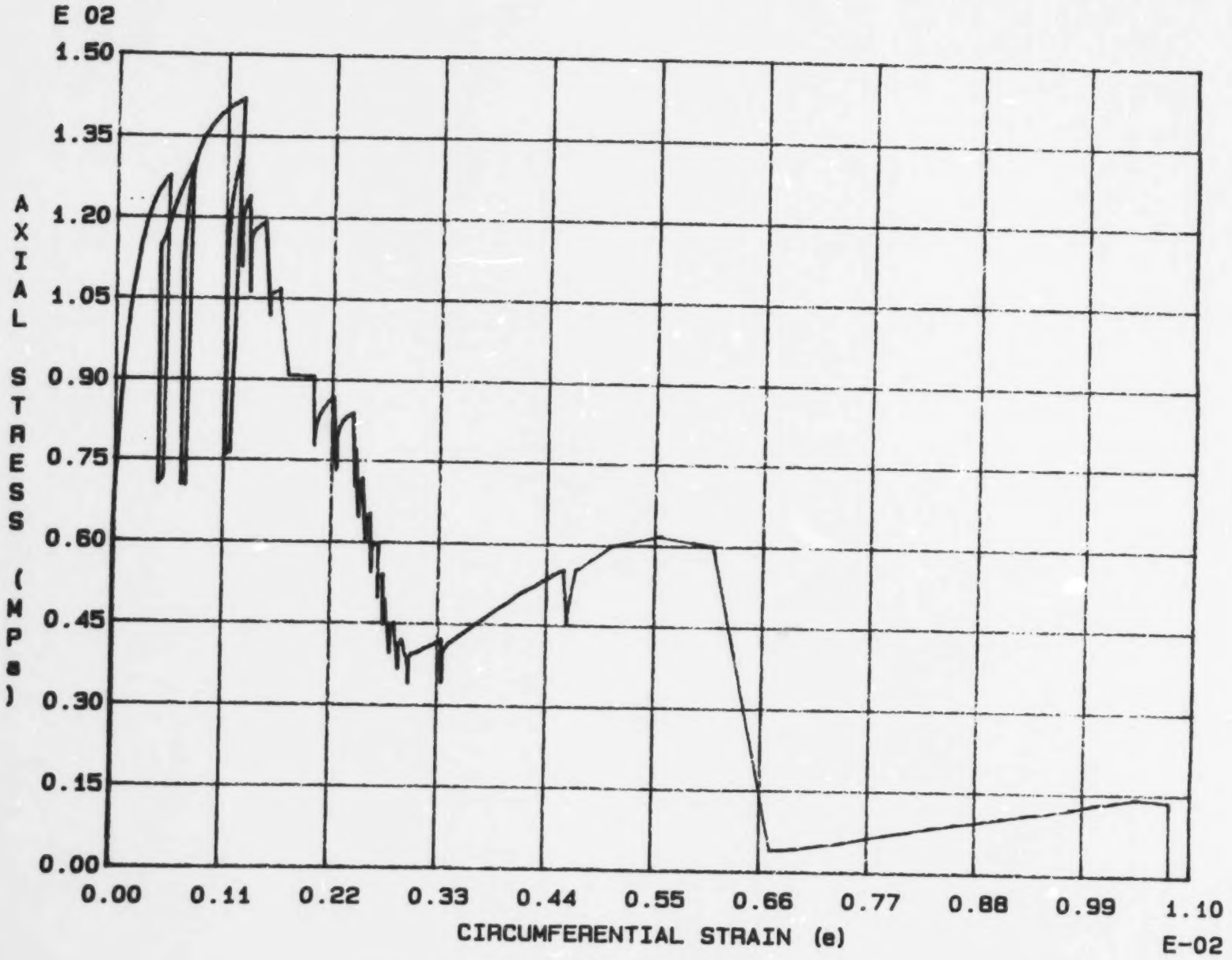

FIG. D-17 SPECIMEN 4014

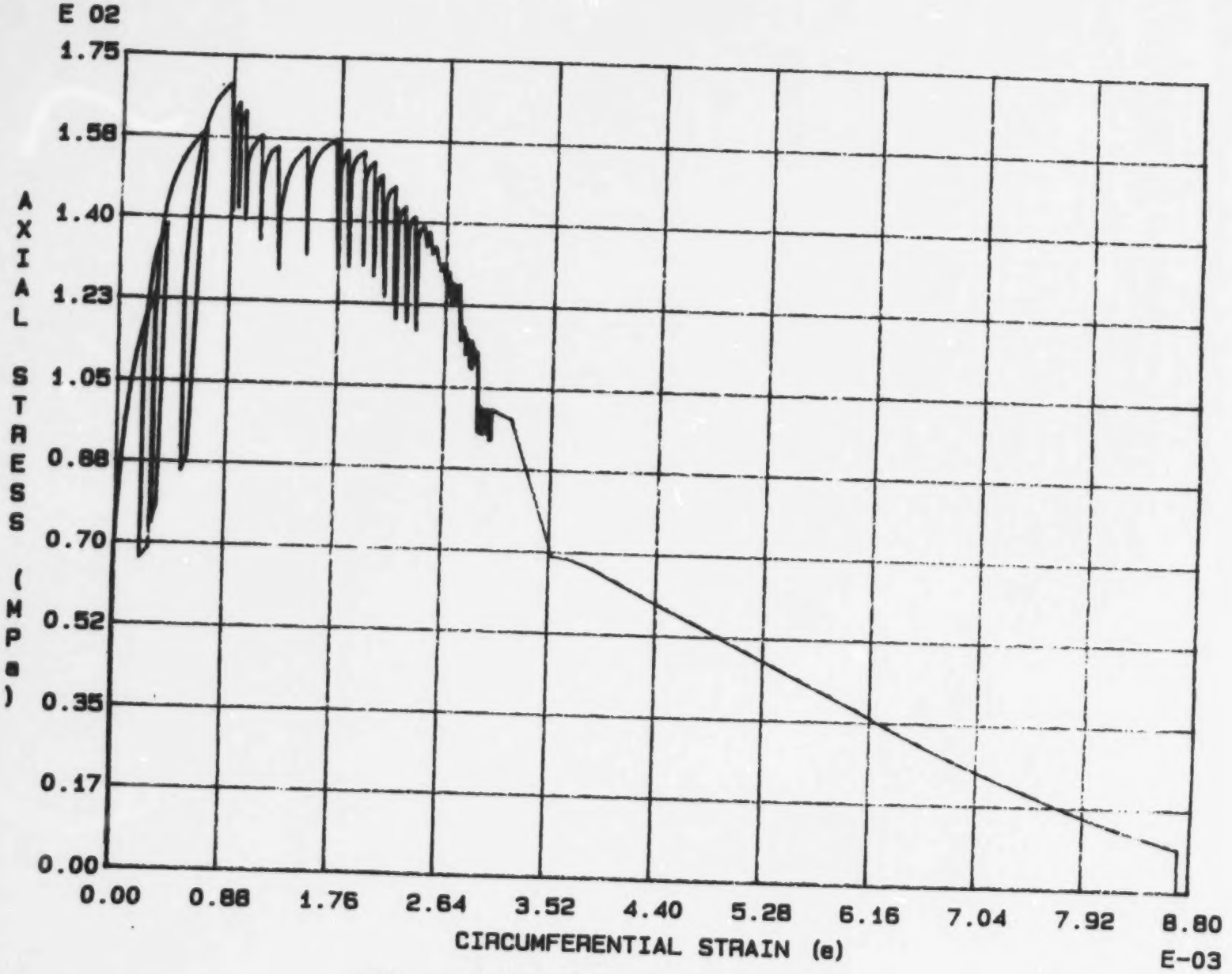

FIG. D-18 SPECIMEN 4016

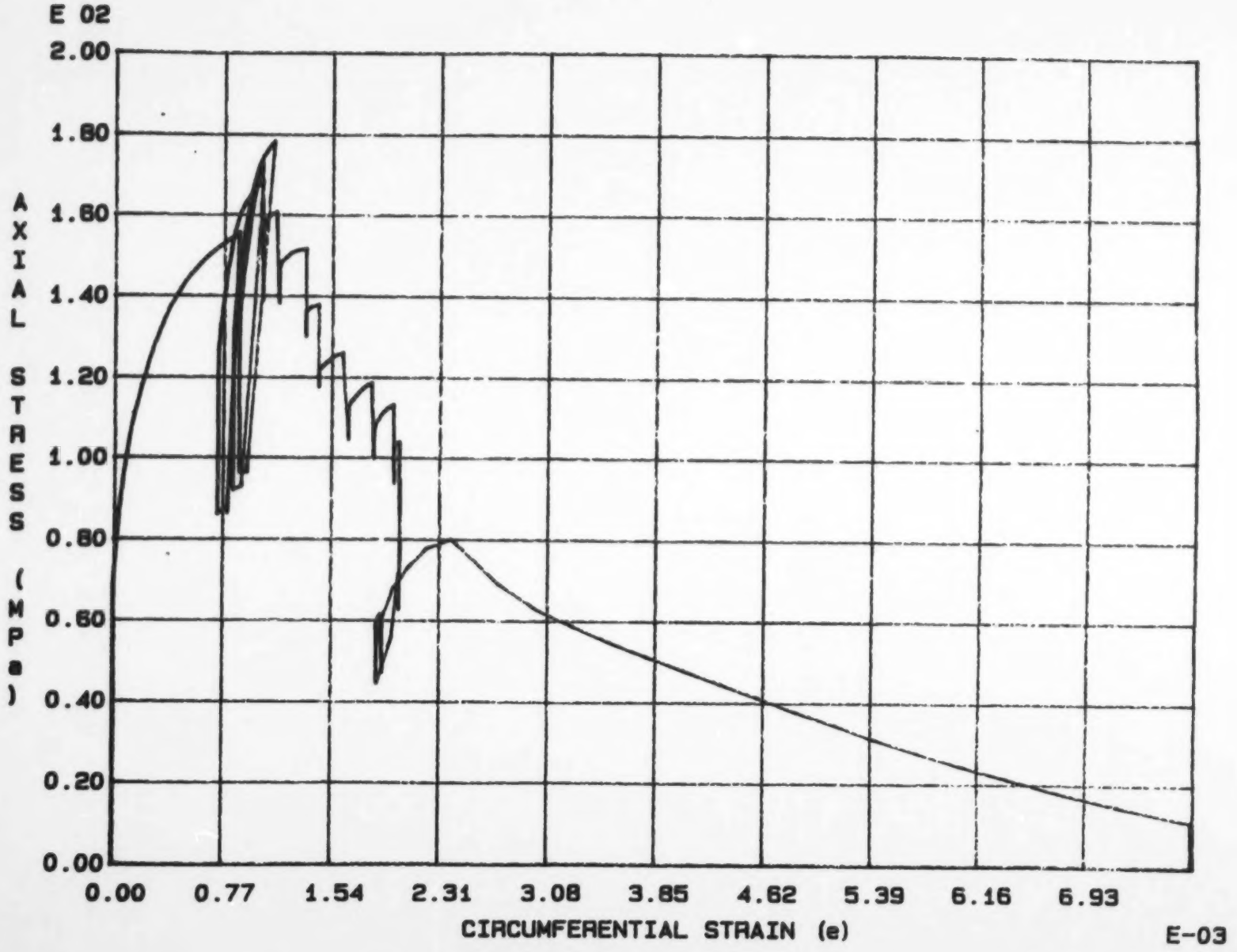

FIG. D-19 SPECIMEN 4018

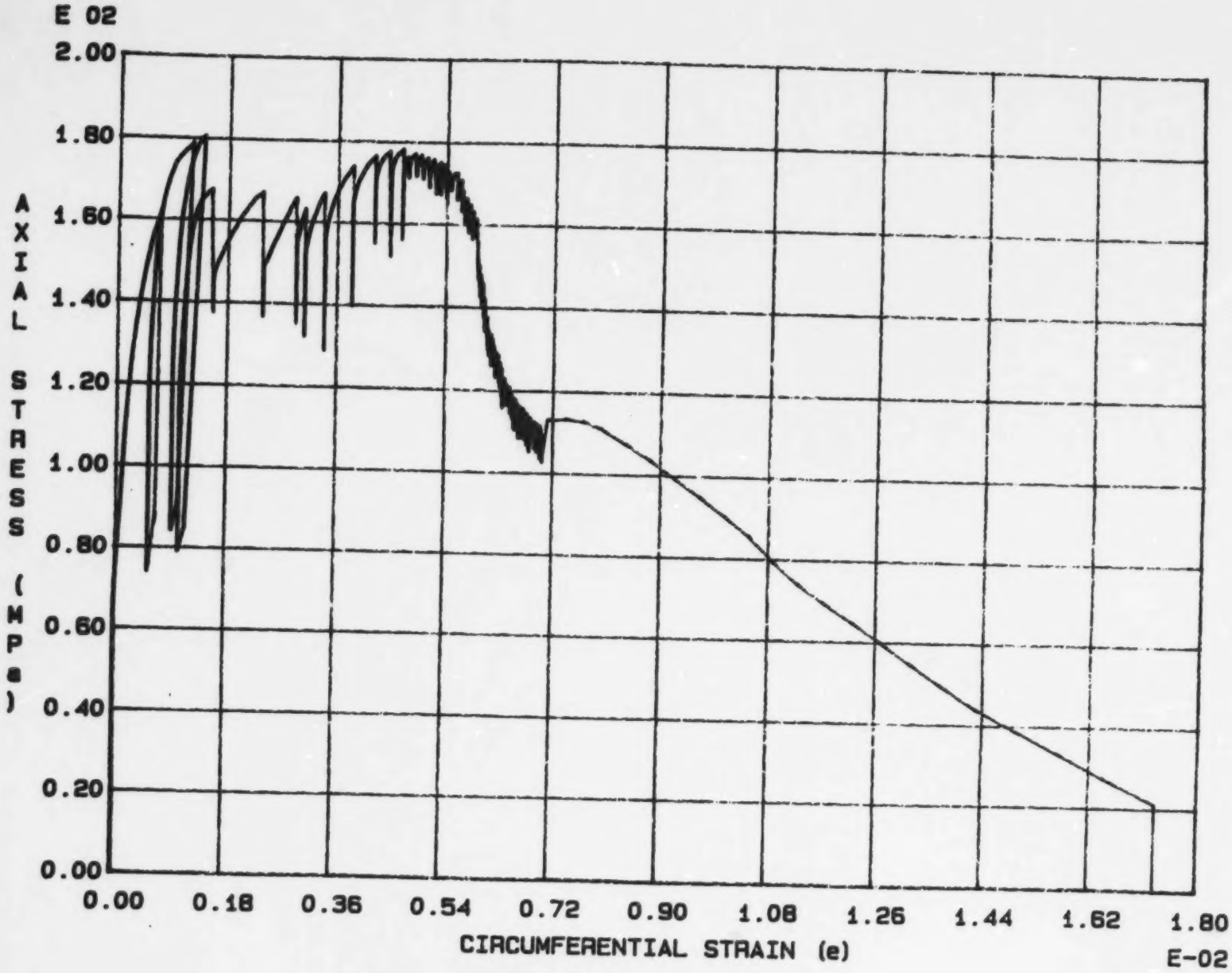

FIG. D-20 SPECIMEN 4022

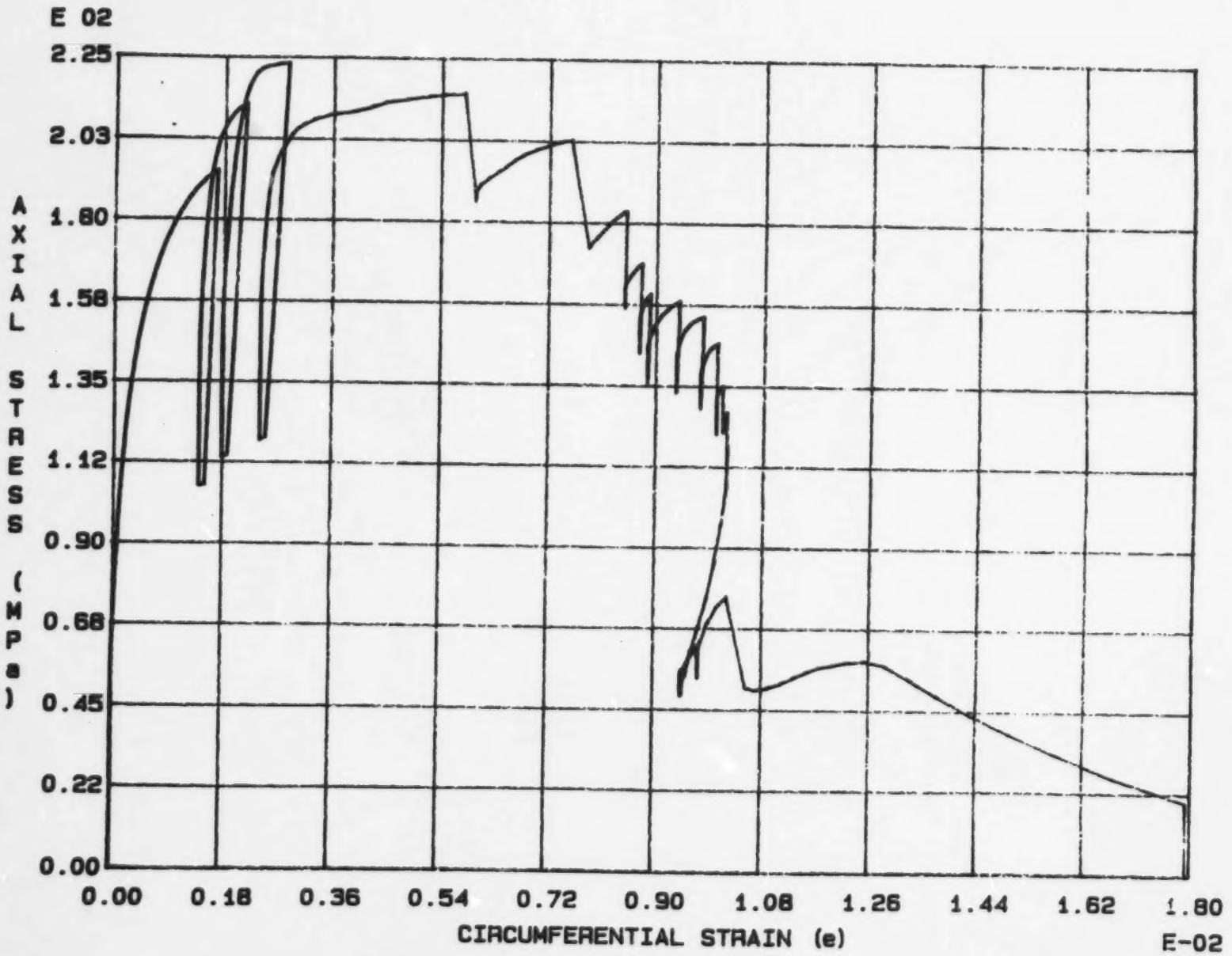

FIG. D-21 SPECIMEN 4024

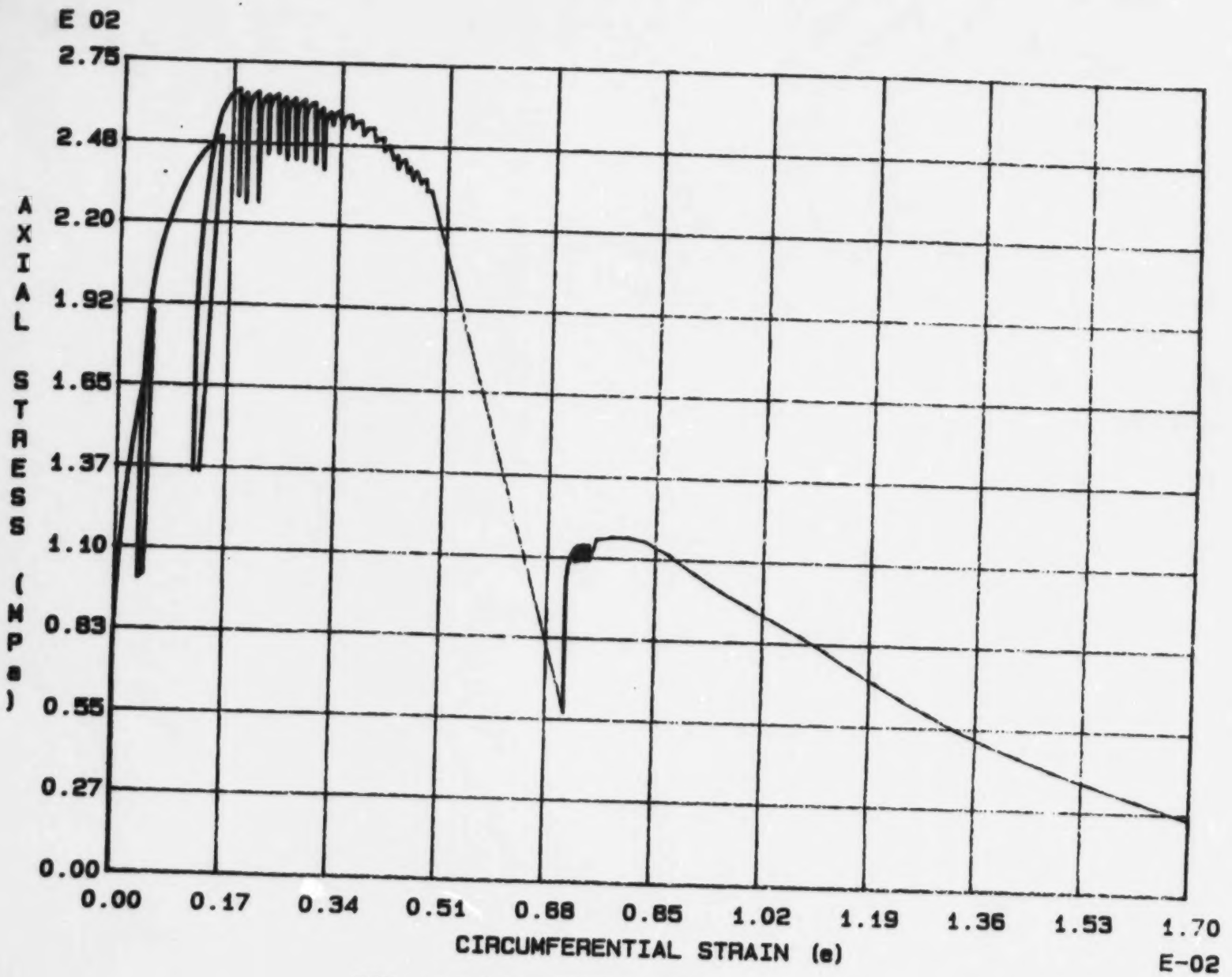

FIG. D-22 SPECIMEN 4032

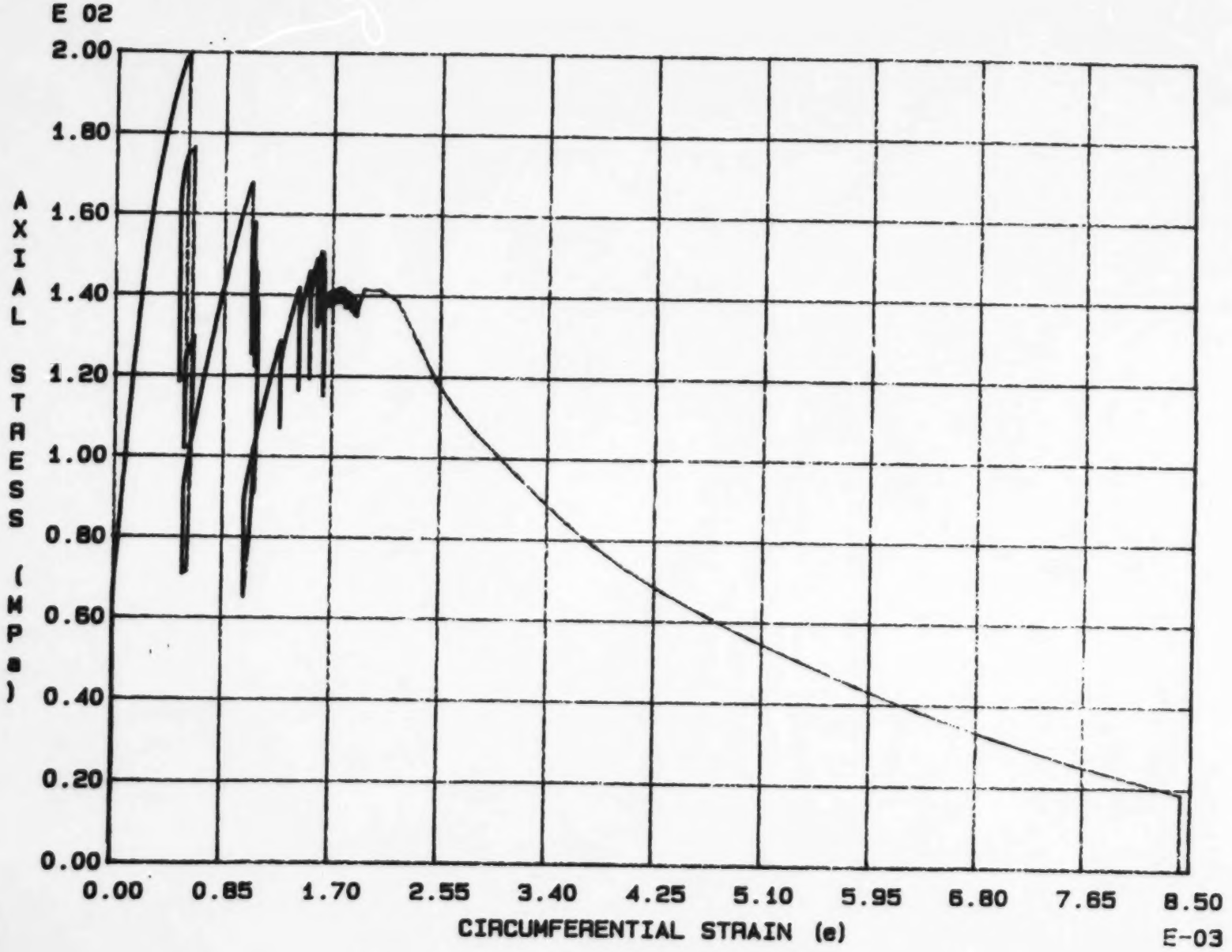

FIG. D-23 SPECIMEN 4034